THE UNIVERSITY OF CHICAGO

INTEGRATIVE GENOMIC ANALYSIS UNCOVERS UNIQUE DIFFUSE LARGE B CELL (DLBCL) IMMUNE ENVIRONMENTS AND IDENTIFIES ASSOCIATIONS WITH SPECIFIC ONCOGENIC ALTERATIONS

A DISSERTATION SUBMITTED TO
THE FACULTY OF THE DIVISION OF THE BIOLOGICAL SCIENCES
AND THE PRITZKER SCHOOL OF MEDICINE
IN CANDIDACY FOR THE DEGREE OF
DOCTOR OF PHILOSOPHY

COMMITTEE ON CANCER BIOLOGY

BY
SRAVYA TUMULURU

CHICAGO, ILLINOIS
JUNE 2023

To my family for always believing in me and my friends for always supporting me. Thank you for all you've done for me along the way.

Table of Contents

List of Figures

List of Tables

Acknowledgements

First, I would like to thank my mentor, Justin Kline. Justin has been a wonderful and supportive mentor throughout my time in graduate school. He has encouraged creativity, intellectual curiosity, and the importance of asking thoughtful questions. He has also exemplified diligence, drive, and commitment to science and has set the standard to which I aspire. I would not have made it to this point without his guidance and support.

I would like to thank the other members of the lab, from whom I have learned so much. Jovian Yu and Alan Cooper were instrumental in this project, and I could not have finished this undertaking without their hard work and dedication. Xiufen Chen and Lishi Xie have been an invaluable resource, and I am fortunate to have them in the lab to help me troubleshoot or discuss experiments. Brendan MacNabb has taught me so much about subjects that were unrelated to my thesis project and expanded my horizons. Finally, I would like to thank James Godfrey, who I was fortunate enough to sit next to when I joined the lab. He has celebrated the triumphs, commiserated with the failures, stayed up late brainstorming new ideas, and pushed me to become a better scientist and better person. This project was only possible because of his guidance and input, and he continues to inspire me with his passion and enthusiasm.

I would also like to thank members of my committee, Megan McNerney, Marisa Alegre, and Fotini Gounari for their invaluable guidance and input during my graduate career. In addition, I would like to thank the all the members Committee on Cancer Biology, Committee on Immunology, BSD and University of Chicago community for guidance, feedback, and support during my time in graduate school. I would like to thank all the staff in the core facilities, without whom none of these experiments would have been possible. Finally, I would like to thank the administrative staff who are critical for keeping the department running.

I would also like to thank all of our collaborators. We received cell lines from Joshua Brody, spleens from Ari Melnick, data, cell lines, and reagents from Christian Steidl. I appreciate your willingness to freely share your resources, and your generousity has greatly benefitted this project.

The best part of graduate school has been the friendships that I've made. I would sincerely like to thank Katrina Hawley from the bottom of my heart for always being in my corner, supporting me through the darkest times, and filling my days with laughter. I could not have made it through without her support. I look forward to more adventures, more laughter, and the continuation of a lifelong friendship. I would also like to thank my other friends who have been instrumental in making sure that I take time to relax and have fun.

Finally, I am most grateful to my family. My mother, father and sister are not biologists but they have made every effort to understand and support my dreams. I appreciate all of the sacrifices they have made for me, including moving halfway around the world to give me more opportunities. Their unconditional love and encouragement have meant so much to me.

Abstract

Non-Hodgkin lymphoma (NHL) is a diverse category of hematological malignancies, and is the 5th most commonly diagnosed malignancy in the United States, with over 70,000 newly diagnosed cases every year[1]. The most common histological subtype of NHL is diffuse large B cell lymphoma (DLBCL), which comprises around 40% of all NHLs[2]. DLBCL is an extremely aggressive subtype of lymphoma, characterized by large sheets of malignant B cells that efface normal lymph node architecture. The standard of care treatment for DLBCL is R-CHOP (rituximab, cyclophosphamide, doxorubicin, vincristine, and prednisone), a chemoimmunotherapy regimen that is curative in the majority of patients (~60%)[4]. However, the remaining 40% of patients with relapsed or refractory (r/r) DLBCL will eventually succumb to their disease.

A significant hurdle in finding more effective treatments for DLBCL is the morphological, transcriptional, and genetic heterogeneity of the disease. However, recent advances in next-generation sequencing (NGS) technologies has enabled a more refined classification of DLBCL, and identified several novel therapeutic targets. In addition to targeted therapies, several immunotherapies – CAR T-cell therapy, bispecific antibodies (bsAbs), checkpoint blockade (CBT) – have also shown efficacy in subsets of patients with DLBCL[5–12]. A deeper understanding of the immune environment of DLBCL, and the molecular and cellular factors that regulate the immune environment, may expand the subset of patients with r/r DLBCL that will benefit from immunotherapies.

Here, we show that DLBCLs are characterized by a spectrum of immune environments. These "hot" and "cold" environments are recurrently associated with several oncogenic alterations that may play a role in orchestrating the immune environment. For example, loss of function (LoF) mutations in *SOCS1* – a negative regulator of IFNγ-driven JAK/STAT signaling – are recurrently

associated with “hot” DLBCLs. In solid cancers, tumor cell-intrinsic sensitivity to IFNγ – a critical T cell derived effector cytokine- is a key determinant of response to immunotherapy. Therefore, *SOCS1* mutant DLBCLs may represent a subset of “inflamed” DLBCLs that may be sensitive to T cell-based immunotherapies. Confirmatory studies *in vitro* and *in vivo*, using *Socs1*-deficient B cells and *Socs1*-deficient melanoma cells, show that genetic ablation of *Socs1* may render cells more sensitive to IFNγ.

Overall, understanding the immune environment of DLBCL and how it affects the response to immunotherapies can aid in identifying patients who could benefit from such treatments. Moreover, uncovering intrinsic factors of lymphoma cells that regulate the immune environment could reveal new therapeutic targets that may complement immunotherapies and expand the pool of individuals who could benefit from them.

1. Introduction

1.1 Germinal center origin of B cell lymphomas

B cell neoplasms often arise from oncogenic transformation of mature B cells that have undergone the germinal center (GC) reaction **(Figure 1)**[13]. During a normal humoral immune response, naive B cells encounter antigen via the B cell receptor (BCR) in the periphery[13–15]. Following antigen recognition, activated B cells migrate to specialized structures in the lymph nodes known as germinal centers, where they cycle between two distinct zones in order to generate high affinity antibodies, termed affinity maturation[14–16]. The dark zone (DZ) is mostly composed of highly proliferative B cell "centroblasts" that are undergoing somatic hypermutation (SHM) of the variable region of the BCR to generate high affinity antibodies. Following proliferation, centroblasts traffic to the light zone (LZ) where they compete to capture antigen from the surface of follicular dendritic cells (fDCs) and internalize the BCR-antigen complex for presentation on MHC-II to cognate CD4+ T follicular helper (T_{fh}) cells. T_{fh} cells deliver help to LZ "centrocytes" with the highest affinity BCR through CD40-CD40L interactions and secretion of IL-4/IL-13 and IL-21, which support B cell proliferation and survival. Positively selected B cells continue to cycle between the DZ and LZ until they receive cues to exit the germinal center and become memory B cells or antibody-secreting plasma cells[14–16].

Affinity maturation relies on the expression of activation induced cytidine deaminase (AID), which converts cytosine to deoxy-uracil (U) in the immunoglobulin locus. Following this U substitution, the cellular DNA damage response then initiates base substitution at the initial lesion, leading to SHM. AID-mediated double stranded DNA breaks can also occur in the switch

region of the immunoglobulin locus, leading to class switch recombination (CSR), to change the isotype of the BCR from IgM/IgD to IgG, IgE, or IgA depending on the nature of the pathogen.

Sequencing of the variable region of the BCR demonstrated SHM and/or CSR in several NHLs, including follicular lymphoma (FL)[17], Burkitt lymphoma (BL)[18,19], multiple myeloma (MM)[20,21], Hodgkin lymphoma (HL)[22,23], and DLBCL[24–26], suggesting the cell of origin is a germinal center or post-germinal center B cell[13,27].

While the germinal center reaction is usually tightly regulated, germinal center B cells rely on pathways that make them vulnerable to oncogenic transformation **(Figure 1)**[15,27–29]. First, dark zone centroblasts undergo proliferative bursts, which are supported by altered metabolic requirements of proliferating cells, downregulation of pathways leading to apoptosis, and inactivation of cell cycle checkpoints, which are all defining features of tumor cells. Second, as B cells iteratively traffic between the LZ and DZ, they may use epigenetic regulation to maintain phenotypic plasticity, and this "dedifferentiated" state is another hallmark of neoplastic cells. Finally, a key feature of the germinal center reaction is the process of creating double-stranded DNA (dsDNA) breaks that are subsequently repaired. Therefore, germinal center B cells may be specialized to withstand genotoxic stress caused by dsDNA breaks. Moreover, the imperfect fidelity of the DNA repair process could lead to off-target AID-mediated mutations in key oncogenes or tumor suppressor genes that can ultimately lead to development of lymphoma.

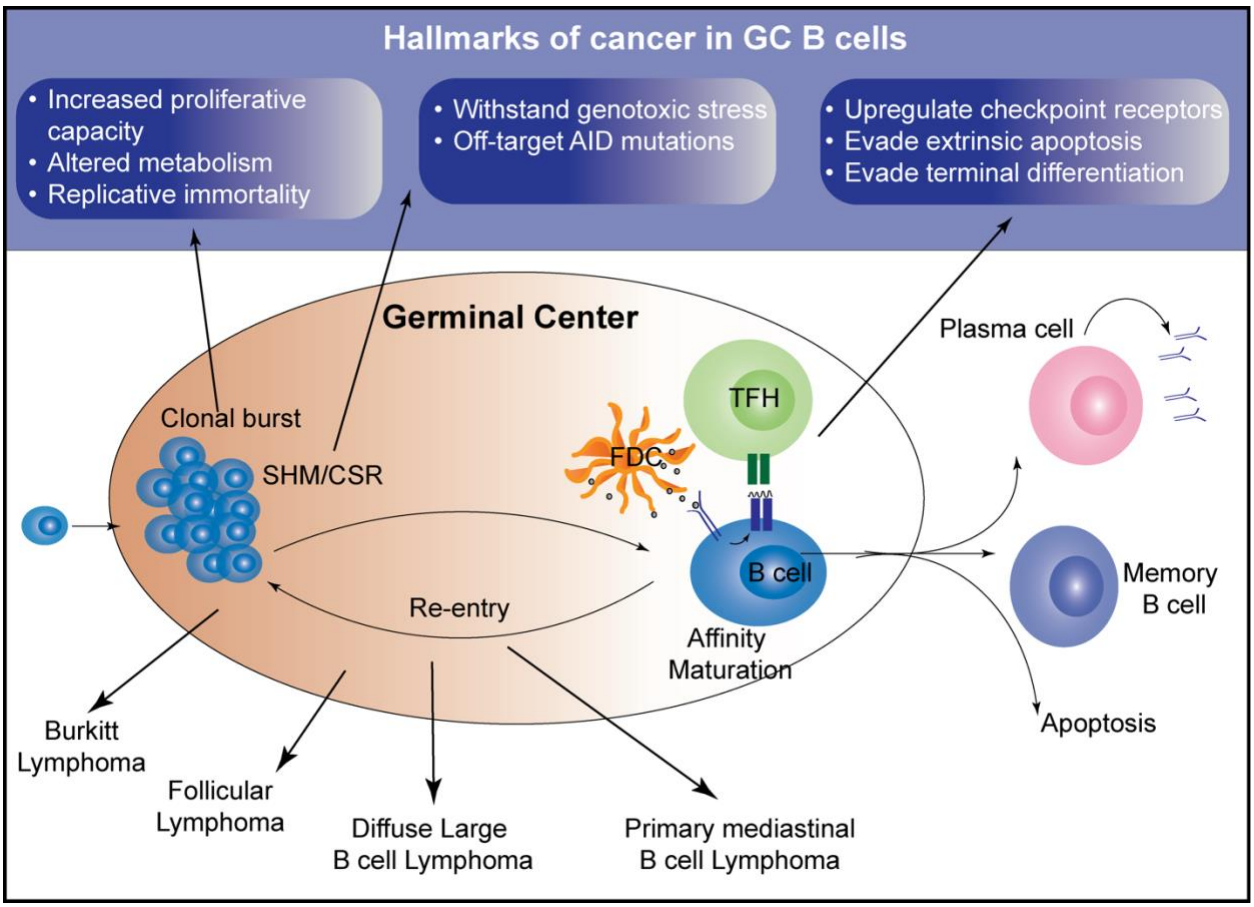

Figure 1. Germinal center origin of B cell lymphomas. Naïve B cells in the periphery encounter antigens and traffic to the germinal center, where they undergo successive rounds of proliferation, followed by somatic hypermuatation (SHM) and class switch recombination (CSR) to generate high affinity antibodies. In order to undergo successful affinity maturation, germinal center B cells rely on pathways at different stages of the germinal center reaction that render them vulnerable to oncogenic transformation. B cells at distinct stages of the germinal center reaction may acquire unique alterations that lead to the formation of distinct lymphomas.

1.2 Diffuse large B cell lymphoma (DLBCL)

Acquisition of genetic lesions during the germinal center reaction can lead to the development of several types of non-Hodgkin lymphoma, the most common subtype of which is DLBCL NOS, an extremely aggressive malignancy that accounts for ~40% of all NHLs[2]. Most DLBCLs arise in lymph nodes. However, approximately 30-40% of DLBCLs can originate in extranodal sites such as the gastrointestinal tract, central nervous system (CNS), breast, and bone[3]. In addition, DLBCLs can also spread from the primary site to other organs, complicating the identification of the site of origin. DLBCL is usually diagnosed after a biopsy of the lymph node or extranodal tumor where malignant B cells grow in a diffuse pattern that leads to effacement of the normal architecture of the organ.

The standard of care for DLBCL is a combination regimen, R-CHOP – 1) Rituximab, an anti-CD20 targeting monoclonal antibody, 2) Cyclophosphamide, an alkylating agent, 3) doxorubicin hydrochloride, a DNA intercalating agent, 4) vincristine (Oncovin), a microtubule inhibitor, and 5) Prednisone, a corticosteroid. R-CHOP cures the majority of patients with DLBCL (~60%), even in the advanced stage[4,30]. However, for the remaining 40% with relapsed or refractory (r/r) disease, outcomes remain poor even in the era of immunotherapy.

Though DLBCL is treated uniformly in the clinic, it is characterized by striking molecular heterogeneity. Therefore, efforts in the last two decades have focused on identifying subsets of DLBCLs with shared biological features that may benefit from novel therapeutic strategies. The development of new technologies has enabled a deeper understanding DLBCL biology and led to the development of classification systems to identify subsets of DLBCL patients that may benefit from novel therapies. Currently, several classification methods exist to group DLBCLs based on shared histology, transcriptional features, or mutational profiles.

1.2.1 Histological classification of DLBCL

Historically, DLBCLs were classified based on morphological features of the cells and nuclei into three broad categories: centroblastic, immunoblastic, and anaplastic[31–33]. The most common variant, centroblastic, consists of diffuse sheets of medium to large blasts with multiple nucleoli and a narrow rim of cytoplasm. Immunoblastic DLBCLs have large cells with single nuclei and abundant cytoplasm. Anaplastic variants are extremely rare, with large cells containing pleomorphic nuclei. Several approaches have tried to define a unifying histological classification system for DLBCL, but this has proved to be challenging due to: 1) the heterogeneity of the disease, 2) poor inter-observer and intra-observer reproducibility, 3) no meaningful clinical or prognostic significance associated with morphological subtypes. The advent of new high throughput sequencing technologies has enabled more meaningful classification of DLBCLs based on molecular features.

1.2.2 Molecular classification of DLBCL

***Cell of Origin*.** DLBCL can be divided into two transcriptionally-defined subsets – activated B cell (ABC) DLBCL and germinal center B cell (GCB) DLBCL **(Figure 2)**[34]. In a landmark study, hierarchical clustering of the transcriptomes of mature B cell neoplasms (DLBCL, FL, CLL), purified populations of non-malignant B from peripheral blood and tonsil, purified populations of T cells from peripheral blood and fetal thymus, and DLBCL cell lines was performed[34]. This comparative analysis found that DLBCLs had a distinct transcriptional profile compared to FL and CLL. Moreover, there was significant heterogeneity within DLBCL, and some DLBCLs shared significant transcriptional overlap with non-malignant germinal center B cells from tonsils (GCB-

like DLBCLs, or GCB DLBCLs) while others had a transcriptional program that was shared with B cells from peripheral blood that are activated *in vitro* with mitogens (ABC-like DLBCLs, or ABC DLBCLs). Several unique genes that are characteristic of germinal center B cells were also expressed in GCB DLBCLs, including *BCL6*, a master regulator of germinal center responses. ABC DLBCLs showed marked upregulation of *IRF4*, which is induced during B cell activation. A third subgroup, unclassified DLBCLs, was later described that does not share transcriptional features with either ABC or GCB DLBCLs. In general, the transcriptomes of ABC and GCB-DLBCLs are non-overlapping, suggesting differences in underlying oncogenic drivers.

Importantly, COO classification is clinically meaningful. ABC DLBCLs are consistently associated with poor outcomes compared to GCB DLBCLs in several independent datasets. Additionally, the association of COO with outcomes remains even after controlling for other clinical variables such as IPI (international prognostic indicator), suggesting that COO is an independent prognostic factor. Therefore, several IHC based surrogates for determining COO were developed. The most widely accepted algorithm, developed by Hans et al., uses a combination of IHC markers (CD10, BCL6, MUM1), to assign DLBCLs into either a GCB DLBCL group or non-GCB DLBCL group. Overall, the concordance between IHC and GEP-based classifiers is around ~70-80%, and the association of IHC-classified GCB DLBCLs with improved survival remains[35].

COO classification has also provided important biological and therapeutic insights in DLBCL[36]. For example, ABC DLBCLs are dependent on constitutive NFκB signaling downstream of oncogenic activation of the BCR, indicating a therapeutic vulnerability to agents that target this pathway**(Figure 3)**[37,38]. Pre-clinical studies in DLBCL cell lines and xenograft models showed that ABC-DLBCLs with activating mutations leading to BCR dependent NFκB signaling, were uniquely sensitive to ibrutinib, a Bruton's tyrosine kinase (BTK) inhibitor[39–43].

Similarly, ABC-DLBCLs were also shown to be sensitive to lenalidomide, an immunomodulatory drug that is thought to target NFκB[39,40,42,44,45]. Finally, bortezomib, a proteasome inhibitor, has also shown activity in pre-clinical models of ABC-DLBCLs[46,47]. However, these therapies have not been translated to the clinic successfully, and patients with ABC-DLBCL continue to have diverse outcomes, suggesting COO is not fully capturing the heterogeneity present in DLBCL.

GCB DLBCLs are characterized by mutations in chromatin modifiers and PI3K signaling molecules **(Figure 3)**. Gain-of-function mutations in *EZH2,* a histone methyltransferase that is part of polycomb repressive complex 2 (PRC2) is frequently mutated in GCB DLBCLs and follicular lymphoma (FL), an indolent NHL[48–50]. In addition, inactivating mutations in *CREBBP* and *EP300*, which both belong to the KAT3 family of acetyltransferases, are common in GCB DLBCL. As these DLBCLs are reliant of epigenetic modification, the addition of EZH2 and/or HDAC inhibitors to the R-CHOP backbone are currently being clinically investigated.

COO classification has been an important advance in the biological understanding of DLBCL. However, it is important to note that while it has been shown that DLBCLs arise from germinal center B cells, cell of origin may be a misnomer as ABC and GCB DLBCLs may not arise from distinct populations of cells in the germinal center. A comparative analysis of the transcriptomes of BL, FL, and DLBCL with germinal center derived centroblasts or centrocytes showed that FLs and DLBCLs are most similar to light zone resident centrocytes[51]. Furthermore, genes contained the in the ABC or GCB signatures were identified in both centroblasts and centrocytes suggesting that COO-related gene signatures contain features that are distinct from those that define centroblasts and centrocytes.

***Consensus clustering*.** Another microarray-based classifier described alternative clusters of DLBCL, independent of COO[52]. Monti et al. used three different clustering algorithms to perform consensus clustering (CC) on a cohort of DLBCLs and identified three distinct subgroups: 1) BCR/proliferation, characterized by expression of genes related to BCR signaling and proliferation, 2) OxPhos, defined by upregulation of genes involved in oxidative phosphorylation, and 3) host response (HR), which had abundant expression of genes related to the immune environment, including T cell and dendritic cell (DC) related genes, which may indicate the presence of an ongoing immune response. These clusters do not correlate with clinical outcomes with R-CHOP; however, further studies have shown that distinct pathways in OxPhos- and BCR-DLBCLs clusters can be sensitive to targeted therapies. For example, OxPhos-DLBCLs are sensitive to perturbations in fatty acid oxidation and glutathione synthesis, as shown by the use of inhibitors that target these metabolic pathways in pre-clinical models[53]. Similarly, BCR-DLBCLs, were shown to be sensitive to genetic and pharmacological inhibition of SYK, a key downstream mediator of BCR signaling[54]. No therapeutic interventions have been suggested for HR-DLBCLs, however, as they are characterized by a robust T cell infiltrate, they might be sensitive to recently developed immunotherapies. Ultimately, these consensus clusters show little overlap with COO, suggesting both methods are capturing different aspects of DLBCL biology.

***Genetic clustering algorithms*.** Recently developed genetic clustering algorithms have extended our understanding of DLBCL biology beyond COO and CC methods **(Figure 2)**. One approach from the Staudt lab used probabilistic clustering to group DLBCLs into seven genetic clusters based on co-occurring mutations and copy number alterations (CNA)[55]. These LymphGen clusters share some overlap with COO. ABC DLBCLs are largely subdivided into four clusters : 1) MCD

DLBCLs, defined by co-occurring gain-of-function mutations in *CD79B* and *MYD88*, leading to constitutive BCR-dependent NFκB signaling, 2) N1 DLBCLs, characterized by gain of function mutations that activate *NOTCH1* signaling, 3) A53 DLBCLs that have loss of *TP53* and large chromosomal aberrations, and 4) BN2 DLBCLs that are driven by *BCL6* translocations and *NOTCH2* mutations. GCB-DLBCLs are grouped into 3 clusters: 1) EZB DLBCLs are characterized by gain of function mutations in *EZH2* and *BCL2* amplifications and be further bifurcated into 2 classes based on MYC activity – EZB-MYC^{+} DLBCLs and EZB-MYC^{-} DLBCLs, 2) ST2 DLBCLs, which are characterized by mutations in *SGK1* and *TET2*. Some GCB DLBCLs also fall into the BN2 cluster, suggesting that DLBCL heterogeneity is not fully captured by either genetic or transcriptional clustering methods, but may be better resolved using an integrative approach that considers multiple variables.

Another approach from the Shipp lab similarly clustered DLBCLs based on genetic lesions into five distinct clusters[56]. Cluster 1 (C1) is similar to the BN2 cluster and consists of DLBCLs that harbor *BCL6* translocations and *NOTCH2* pathway mutations. However, unlike BN2 which contains almost equivalent numbers of GCB DLBCLs, ABC DLBCLs, and unclassified DLBCLs, C1 DLBCLs are almost all ABC COO. Cluster 2 (C2) shares significant overlap with A53, and DLBCLs in this cluster are characterized by *TP53* inactivation and chromosomal instability. C2 is comprised of both GCB and ABC DLBCLs, and therefore, does not fully recapitulate the phenotype of A53 DLBCLs. Cluster 3 (C3) and cluster 4 (C4) are mostly comprised of GCB DLBCLs, with C3 harboring *BCL2* translocations and mutations in epigenetic modifiers such as *EZH2*, similar to the EZB cluster described by Staudt and colleagues. C4 DLBCLs contained mutations in *SGK1* and mutations in immune-related signaling molecules such as *CD83* and *CD58*. C4 DLBCLs share some features of ST2 DLBCL, but lack the *TET2* mutations. Finally, cluster 5

(C5) DLBCLs are mostly ABC DLBCLs with *MYD88* and *CD79B* mutations, and therefore overlap with the LymphGen-defined MCD cluster.

Both approaches of classifying DLBCLs based on oncogenic alterations are reproducible and concordant. One key difference is that LymphGen employs more stringent threshold and therefore does not classify nearly ~40% of DLBCLs, which are grouped into a heterogenous "Other" category. Nonetheless, both classification systems have prognostic significance, and show that genetic classification can further stratify DLBCLs over COO alone. C4/ST2 DLBCLs are associated with favorable outcomes, while MCD/C5 and A53/C2 are associated with dismal outcomes. While these genetic classifications have furthered the understanding of DLBCL biology, the clinical impact of these genetic clusters remains to be determined.

Conclusion. NGS technologies have furthered our understanding of biological features of DLBCL and identified new subgroups that may benefit from novel treatment strategies. Recently, immunotherapies have changed the treatment landscape of cancer, leading to a confluence of data supporting the role of the immune environment in anti-tumor immunity and response to checkpoint blockade (CBT) in solid cancers (detailed in Section 1.3). Moreover, several cancer cell-intrinsic mechanisms that shape the immune environment and response to immunotherapy have been identified in solid cancers. In contrast, while several types of immunotherapy have shown clinical activity in DLBCL, little is known about the immune environment and the lymphoma cell-intrinsic factors that may be regulating the immune environment and response to immunotherapies in DLBCL. Characterizing the immune landscape of DLBCL and identifying features that may be orchestrating the immune environment may 1) identify populations that benefit from

immunotherapies and 2) identify novel lymphoma cell-intrinsic pathways that could be targeted therapeutically to synergize with immunotherapies.

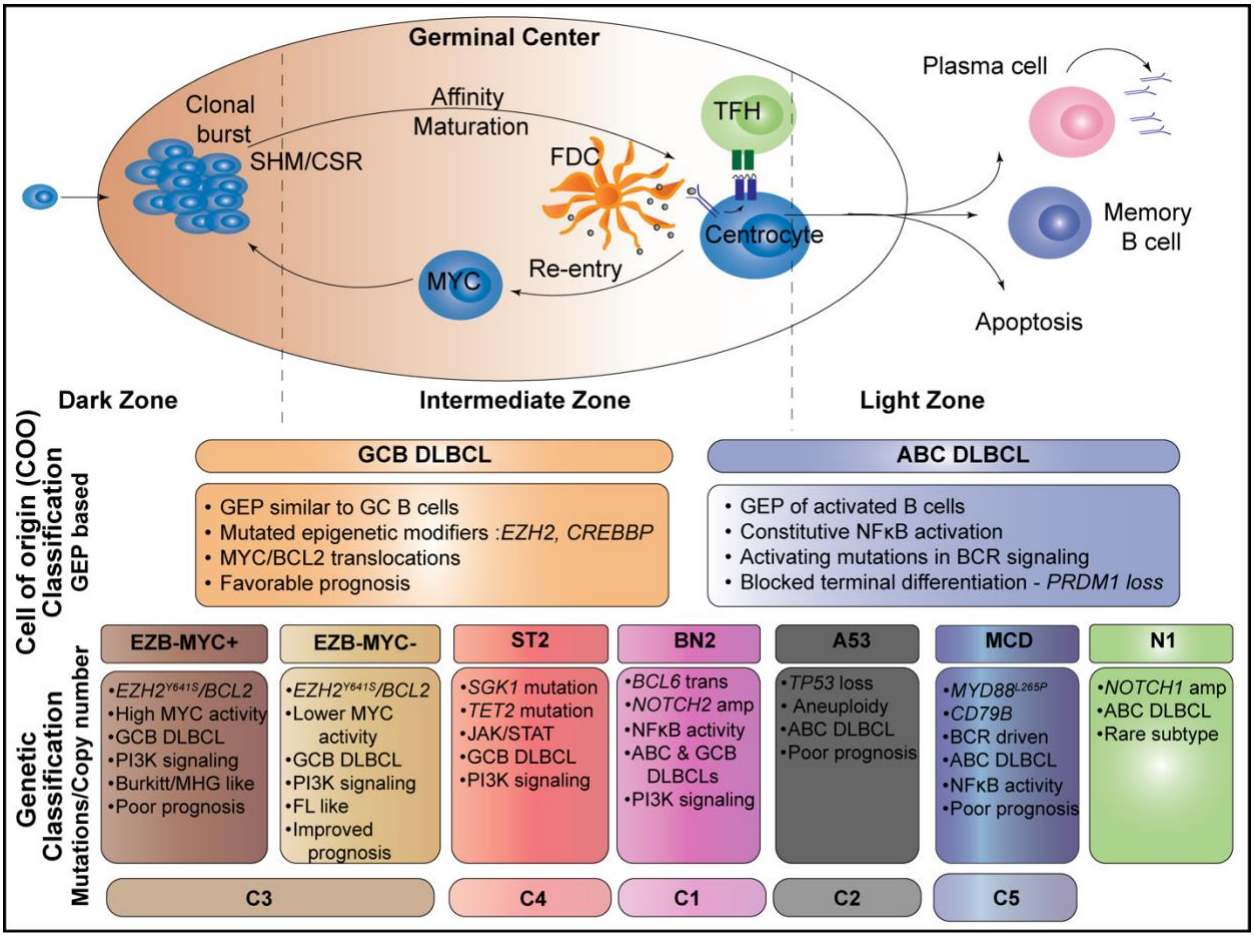

Figure 2. Molecular classification in DLBCL. Cell of origin (COO) groups DLBCLs based on transcriptional similarity to germinal center B cell (GCB DLBCL) or activated B cells (ABC DLBCLs). Newer taxonomic systems (NCI : EZB, ST2, BN2, A53, MCD, N1; Harvard : C1-C5) cluster DLBCLs based on co-occurrence of mutations or copy number alterations.

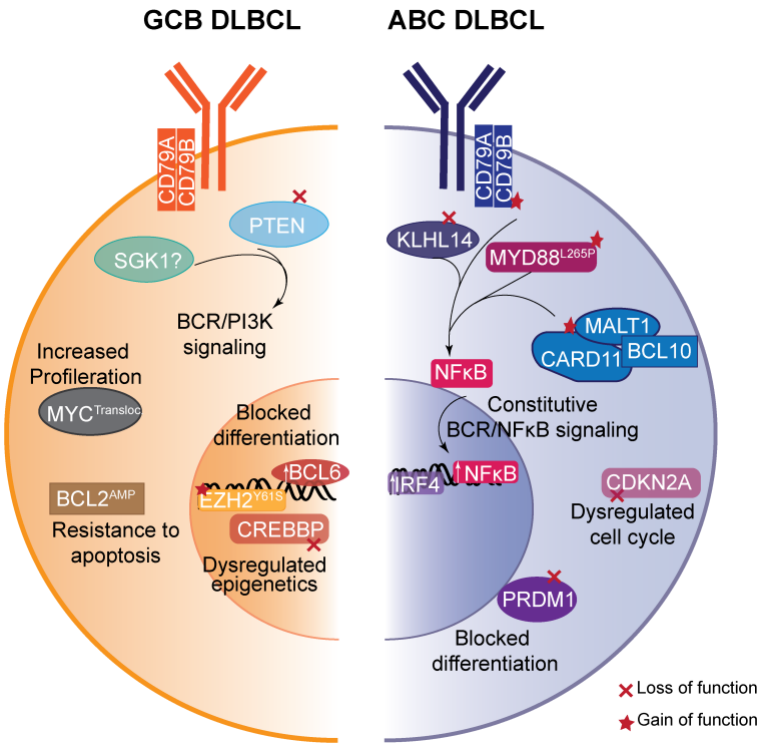

Figure 3. Genetic alterations commonly found in GCB and ABC DLBCLs. GCB DLBCLs are characterized by alterations in epigenetic modifiers and activation of PI3K signaling. ABC DLBCLs often acquire mutations that lead to constitutive NF κB signaling.

1.3 Immune system and Cancer

The role of the immune system in defending against foreign pathogens such as viruses and bacteria is well established. However, the function of the immune system in recognizing and controlling tumor growth has been widely debated. The last few decades have seen major breakthroughs in our understanding of the role of the immune system in cancer, and it is now accepted that immune cells in the tumor microenvironment (TME) can function as potent tumor suppressors.

Anecdotal evidence for the power of the immune system to eradicate cancer has long been recorded by physicians, including cases in which the development of erysipelas – a skin infection caused by *Streptococcus pyogenes*– causes spontaneous regression of tumors[57,58]. The first systematic study was conducted in the late 19th century by William Coley, who administered heat-inactivated extracts of *S. pyogenes* and *Serratia marcescens* to patients with soft-tissue and bone sarcomas and observed long-term remission of in approximately 30-40% of the patients[59–61]. Though this trial lacked appropriate controls by modern day standards, "Coley's toxins," referring to the bacterial extracts, were the precursor to modern immunotherapy and provided initial evidence that the immune system can eradicate cancer.

Despite the success of Coley's toxins in improving survival of sarcoma patients, the mechanism by which this therapy functioned was unknown until several decades later. The initial hypothesis that the immune system protects against the development of cancer by recognizing and destroying neoplastic cells was proposed in 1909 by Paul Ehrlich [62]. The first supportive evidence was based on experiments using 3-methylcholanthrene (MCA) to induce sarcomas in an inbred mouse strain, C3H. Mice in which MCA-induced tumors spontaneously regressed were significantly more resistant to re-inoculation with the same MCA-induced sarcoma cells,

suggesting the presence of a host anti-tumor immune response [63]. Other key studies found that re-inoculation of mice with MCA-induced sarcomas from the same inbred strain produced an immune response, but re-inoculation of mice with spontaneously occurring sarcomas or MCA-induced sarcomas from different tissue sites did not lead to an anti-tumor immune response[64,65]. Taken together, these data suggest that an immune response may be developed against tumors and that the immune response is specific to tumor antigens. These experiments and clinical observations that organ transplant patients on immunosuppressive therapy had a higher risk of developing cancer led to the development of the "immune surveillance" hypothesis [66–70]. This framework posits that the adaptive immune system can recognize transformed neoplastic cells and eliminate them, reducing the risk of developing cancer. However, enthusiasm for immune surveillance hypothesis dimmed when subsequent experiments demonstrated that athymic nude mice showed no difference in incidence or latency of spontaneous and carcinogen-induced sarcomas compared to immunocompetent mice [71,72].

The advent of more sophisticated immunodeficient mouse models on pure genetic backgrounds spurred a resurgence in research investigating the role of the immune system in controlling cancer. Key experiments showed that mice that lack IFNγ signaling, through genetic ablation of *Ifnγr* or *Stat1*, were more likely to develop cancer upon administration of carcinogens[73,74]. Similarly, the incidence of spontaneous and carcinogen-induced tumors was significantly higher in *Rag2*$^{-/-}$ mice, which lack an adaptive immune system[75]. Moreover, when MCA- induced sarcomas from *Rag2*$^{-/-}$ mice were inoculated in WT mice, the tumors were spontaneously rejected, suggesting that the immune system may be shaping tumor immunogenicity. These data led to the development of the cancer immunoediting hypothesis.

1.3.1 Cancer immunoediting

Cancer immunoediting is thought to occur in three phases: elimination, equilibrium, and escape **(Figure 4)**.

Elimination. Normal cells that have undergone malignant transformation can be detected and eliminated through the coordinated actions of several immune cell subsets. The initiation of a spontaneous anti-tumor immune response can be understood through the framework of a step-wise, iterative process known as the "cancer-immunity cycle" [76]. First, tumor cell-specific antigens –neoantigens that are created through genetic lesions – are acquired by antigen-presenting cells (APC) such as macrophages and dendritic cells (DCs) in the environment. Several subsets of DCs and other myeloid cells can acquire tumor cell-associated antigens (TAA) that are processed and cross-presented on major histocompatibility complex (MHC) I and MHC-II on the cell surface. Simultaneously, DCs also traffic to the draining lymph node and undergo a process of maturation that leads to the expression of costimulatory molecules (CD80/CD86) on the cell surface. In the draining lymph nodes, activated DCs present TAAs (Signal 1) along with co-stimulatory molecules (Signal 2) and soluble factors (Signal 3) to $CD4^+$ and $CD8^+$ T cells to prime and activate antigen-specific T cells. Activated T cells then traffic to the tumor site and exert their effector function upon recognition of cognate peptide: MHC complexes displayed on cancer cells or APCs.

While the elimination phase has not been directly visualized in mice or humans, several mouse models have been employed to show that lacking several components of the immune system, including T cells[73,77,78], IFNγ pathway signaling components[73,74,79,80], perforin[81,82], TRAIL[83], FAS/FASL[84], can lead to increased susceptibility to cancer in carcinogen-induced, spontaneous, and genetically engineered mouse models[85,86]. Under ideal conditions, this process

continues cyclically until the cancer is eradicated; however, some rare tumor cell clones may escape elimination and move to the next phase: equilibrium.

Equilibrium. In the equilibrium phase, the immune system exerts pressure on the tumor cells to maintain a state of dormancy. Experimental evidence for the equilibrium phase was initially shown when transplantable cell lines were inoculated in immunized, syngeneic hosts. These mice eventually developed tumors after a period of time, suggesting the immune system is playing a role in establishing a dormant state[87,88]. Similarly, Koebel et al. found that mice treated with low doses of MCA harbored occult cancer cells, though the mice did not have detectable tumors at that time. When monoclonal antibodies (mAbs) were used to deplete CD4 and CD8+ T cells or to neutralize IFNγ, MCA-treated WT mice developed tumors. Moreover, in mice that did not have detectable tumors, further examination found that the cells that were present were transformed as inoculation of syngeneic mice with these occult tumor cells led to the development of cancer[89]. Taken together, these results suggest the immune system is maintaining tumors in an equilibrium phase that is distinct from elimination and the next phase, escape[89].

Escape. Equilibrium and elimination may represent terminal endpoints for cancer immunoediting; however, failure at either stage leads to escape of the tumor from immune surveillance, leading to the clinical manifestation of cancer. Mechanisms of escape result from 1) tumor cell-extrinsic or 2) tumor cell-intrinsic mechanisms that may result in either an immunosuppressive or immune-ignorant state.

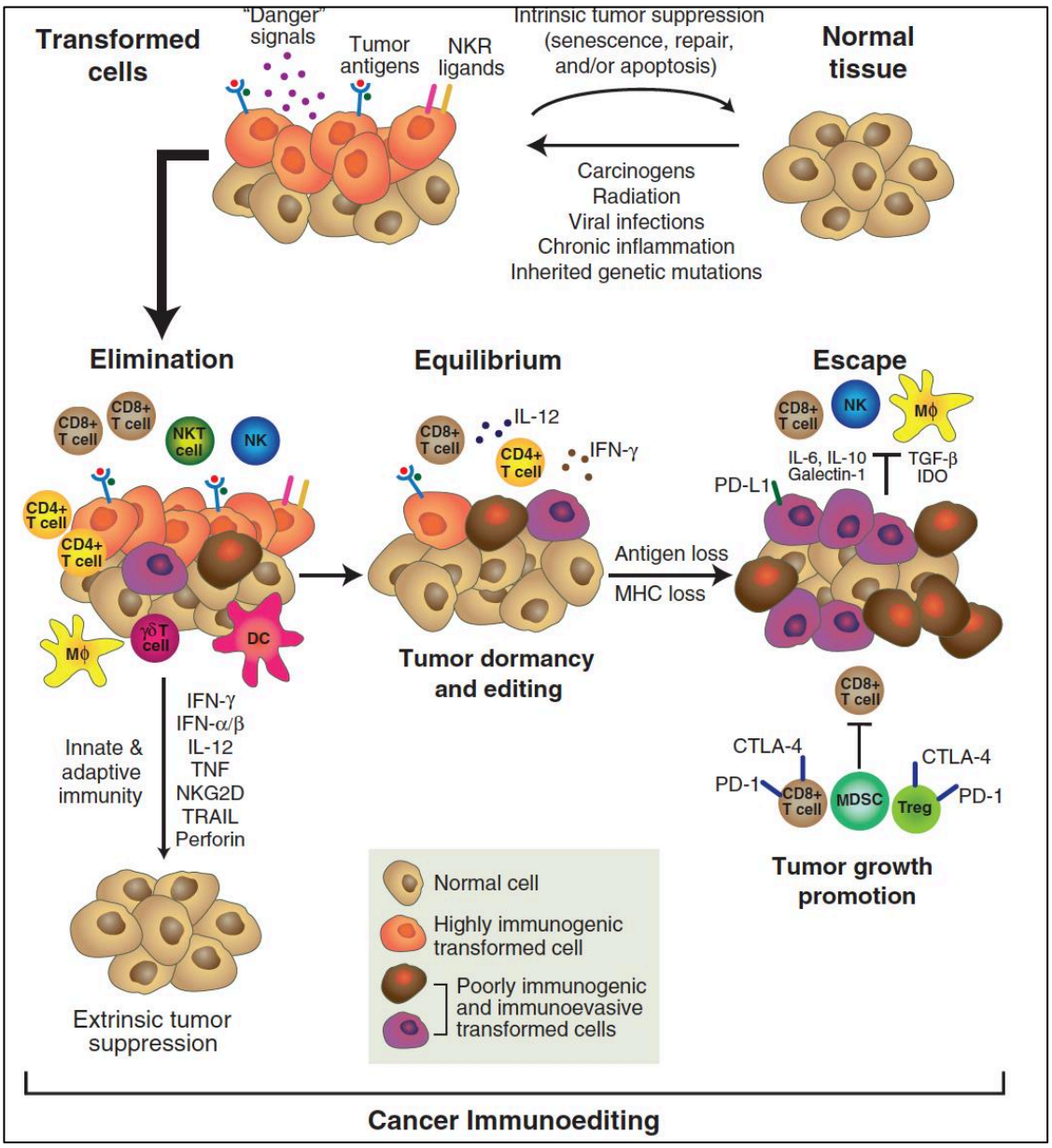

Figure 4. Three steps of cancer immunoediting: elimination, equilibrium, and escape. Transformed cells are recognized and eliminated by innate and adaptive immune cells. If elimination fails, cancer cells may exist in equilibrium indefinitely or until stochastic mutations allow cancer cells to escape immune surveillance. (Source : Schreiber et al., *Science* 2011[90]).

1.3.2 Mechanisms of immune escape

Mechanisms of escape result from 1) tumor cell-extrinsic or 2) tumor cell-intrinsic mechanisms that may result in either an immunosuppressive or immune-ignorant state **(Figure 5)**.

Tumor cell-extrinsic mechanisms of immune escape. The acquisition of antigens is critical to initiate an immune response and relies on DCs, an extremely heterogenous population that can adopt different cell states and subset specific functions depending on the site and inflammatory context of the tissue[91–94]. The critical mediators of anti-tumor immunity – a result of superior ability to prime $CD8^+$ T effector cells – are BATF3-lineage DCs (cDC1s). Within this subset migratory,$CD103^+$ cDC1s are required to acquire TAAs and traffic to the lymph node[91,92,94,95]. The importance of DCs for effective priming of T cells in the lymph node is well appreciated; however, some recent evidence suggests DCs may also play a role in recruitment and *in situ* expansion of T cells within the tumor[95]. DC accumulation and localization within the TME is dependent on one or more chemokines (CCL4, CCL5, and XCL1) and other growth factors (Fms-related tyrosine kinase 3 ligand, FLT3-L), which may be impacted by several mechanisms[94,96,97]. Oncogenic activation of WNT/β-Catenin in the tumor cells has been shown to decrease expression of CCL4 and negatively impact recruitment of DCs to the tumor[94]. In addition, DCs need to be appropriately activated and licensed for effective T cell priming, and an immunosuppressive TME may reduce DC stimulatory potential. For example, IL-10 production from cancer cells and regulatory T cells (T_{reg}) has been shown to antagonize IL-12 production by DCs. Finally, DCs may adopt an immunoregulatory cell state by upregulating inhibitory receptors such as PD-L1, which may restrict anti-tumor immunity[98]. Finally, the antigenome of DCs – the antigens presented on MHC-I and MHC-II – may also impact T cell activation. Somatic mutations in tumor cells may lead to

the presentation of neoantigens and a tumor-specific T cell response. Studies have shown that tumor mutation burden is correlated with T cell infiltration, cytolytic activity, and response to checkpoint blockade therapy in some cancers[99–105]. However, intra-tumoral heterogeneity and inter-patient heterogeneity, as well as several other factors including HLA haplotype and immunoediting, may affect the number and quality of neoantigens presented by DCs and lead to suboptimal anti-tumor T cell responses[106].

T cells in the tumor environment play complex and opposing roles in anti-tumor immunity. The abundance and activation state, specifically the presence of an IFNγ signature, of $CD8^+$ T cells in the tumor environment has been shown to be a biomarker of response to anti-PD1 therapy in solid cancers [107–109]. However, T cells in the tumor environment can lack effector function for several reasons. In addition to lack of effective priming by DCs, T cells can also fail to appropriately traffic to the tumor site. Recent work has suggested that a CXCL9/CXCL10 chemokine gradient are important for $CXCR3^+$ T cell chemotaxis and localization in the tumor site[110–113], and the expression of CXCL9/10 is correlated with T cell abundance in melanoma and lung cancer[114]. Moreover, other immune cell subsets, including regulatory T cells (T_{reg}) and macrophages, may interfere with the function of cytotoxic $CD8^+$ T cells by orchestrating an immunosuppressive tumor environment.

T_{reg} cells can suppress host anti-tumor immune responses through antigen-dependent and antigen-independent mechanisms. For example, T_{reg} cells, which constitutively express high levels of the high affinity IL2R α chain (CD25), can suppress the activation and expansion of conventional T cells (T_{cons}) by sequestering IL-2 in the environment. Other cell surface receptors, such as ectoenzymes CD39 and CD73 that convert ATP to adenosine, can alter the availability of metabolites to dampen the activity of effector T cells and DCs[115]. Treg cells can also secrete

immunosuppressive cytokines (TGF-β or IL-10), or perforin and granzyme B to dampen the anti-tumor immune response. T_{reg} cells may also directly lyse target cells through the secretion of perforin and granzyme B. Finally, T_{reg} cells constitutively express high levels of CTLA-4 – an inhibitory receptor that competes with CD28 for binding to costimulatory molecules CD80 and CD86– which has been shown to capture its ligands through trans-endocytosis and decrease the level of T cell activation[116].

Finally, the magnitude and duration of an anti-tumor immune response can be regulated through the balance of co-stimulatory and inhibitory receptors on the surface of T cells. Following activation, T cells transiently upregulate a number of inhibitory checkpoint receptors (eg., CTLA-4, PD-1, TIGIT) which can engage with their cognate ligands (eg., CD80/86, PD-L1/PD-L2, CD155/PVR) that are expressed on tumor cells or other cells in the TME to dampen effector T cell responses. However, chronic TCR stimulation leads to CD8+ T cell exhaustion, a distinct differentiation stage characterized by poor proliferative and cytolytic capabilities, dysregulated cytokine production, and constitutively high levels of expression of checkpoint inhibitors. T cell exhaustion was first characterized using chronic LCMV infection in mice [117], and studies have confirmed the presence of exhausted cells in human and mouse viral infections as well as cancer[118–120]. Key experiments subsequently demonstrated that genetic ablation of *Pdcd1*[121] or monoclonal antibodies targeting PD-1 or PD-L1 could lead to partial reversal of CD8+ T cell exhaustion and increased viral clearance and tumor regression in several mouse models[122–126]. This pivotal discovery, along with the discovery of CTLA-4 as another negative regulator of T cell function, laid the groundwork for checkpoint blockade as a pillar of cancer therapy.

Tumor cell intrinsic mechanisms of immune escape. Mechanisms to escape immune surveillance may occur at the level of the tumor cells, through the acquisition of alterations or activation of pathways that are required for innate and adaptive immune recognition[99,127,128].

Resistance to innate immunity. Tumor cell growth requires avoiding recognition by macrophages and other myeloid cell subsets. Macrophages phagocytose apoptotic or pathogenic cells while sparing healthy cells through recognition of "eat me" and "don't eat me" signals on the surface of target cells. For example, CD47 – a pentaspanin protein that is widely expressed on the cell surface of normal cells – was discovered as marker of self when red blood cells from *Cd47*$^{-/-}$ mice were rapidly cleared upon transfusion into wildtype hosts[129] and bone marrow from *Cd47-/-* mice was unable to rescue lethally irradiated immunodeficient hosts[130]. Mechanistically, ligation of CD47 with SIRPα on the surface of macrophages and DCs recruits phosphatases to SIRPα ITIM domains and triggers an inhibitory signal that prevents function of myosin-II in phagocytosis [131–136]. Tumor cells can evade phagocytic clearance through upregulation of CD47, which is overexpressed in several cancer types, including lymphomas, acute myeloid leukemia (AML), and breast cancer[137–140]. Little is known about the molecular regulation of CD47 overexpression in cancer cells; however, several oncogenic pathways have been suggested to play a role in CD47 regulation including NFκB[140–142], MYC[143], and STAT3[144] and are currently being investigated. Nevertheless, antibodies that disrupt CD47/ SIRPα interaction, as well as other "don't eat me" signals such as CD24/SIGLEC-10[145], have shown efficacy *in vitro* and *in vivo* in promoting increased clearance of several cancer cell types, including NHL, and are currently under clinical investigation[135,139,140,146,147].

Cancer cells may also activate other pathways that regulate the infiltration of innate immune cells in the tumor microenvironment. One study investigating mechanisms of immune evasion in malignant melanoma found that activation of WNT/β-catenin was associated with a T cell non-inflamed environment in patients[94]. Using an autochthonous melanoma model (*TyrCre-ER* , $Braf^{V600}$, $Pten^{fl/fl}$, $R26\text{-}^{LSL\text{-}CNNTB1}$), Spranger et al. demonstrated that conditional WNT/β-catenin activation in melanocytes led to lower DC infiltration in the tumor and decreased T cell priming in the lymph node, leading to a "cold" environment and decreased response to PD-L1/CTLA-4 checkpoint blockade therapy[94]. Moreover, adoptive transfer of tumor antigen-specific T cells to mice with WNT/β-catenin activation did not restore an "inflamed" environment or sensitivity to CBT. Deeper mechanistic studies found that endogenous and adoptively transferred T cells are dependent on DC-derived CXCL10 for trafficking and localization to tumor sites[95]. Interestingly, WNT/β-catenin activation does not appear to play an oncogenic role in melanoma, and tumor growth is similar between mice with and without WNT/β-catenin activation, suggesting that tumor cells activate this pathway to evade immune recognition[94,95].

Other tumor cell-intrinsic mechanisms that may impact the infiltration, localization, or function of innate immune cells in the tumor environment have also been investigated. A recent study found that melanoma cell-derived prostaglandin E2 (PGE2) inhibited the accumulation and activation of CD103+ DCs in the tumor[148]. Genetic ablation or pharmacological inhibition of cyclooxegnases (COX) – enzymes that catalyze prostaglandin precursors – restored CD103+ DC infiltration and sensitivity of melanomas to CBT[148]. Others have found that *NOTCH* activation[149], *MYC* amplification [150,151], and other oncogenic pathways can impact the innate immune response to various cancers[126–128]. The role of oncogenic pathways or alterations in promoting sensitivity or

resistance to innate immune recognition or activation, as well as mechanisms to target innate immune cells, continues to be an active area of investigation.

Resistance to adaptive immunity. Cancer cells may also acquire alterations that promote resistance to adaptive immunity, through evading recognition by $CD8^+$ T cells or modulating resistance to T cell-mediated killing. In order to exert effector functions, CD8+ and CD4+ T cells require recognition of their cognate peptide presented on MHC-I or MHC-II molecules, respectively. Cancer cells can downregulate or modify the antigens presented on MHC-I or MHC-II through "irreversible" or "reversible" changes. For example, point mutations, deletions, or loss of heterozygosity in HLA-A,B,C or in B2M– a critical component of MHC-I complex – are found in melanoma, MSI-H colorectal cancer, NSCLC, and cHL[99,152–155]. MHC-I and II expression on the cell surface can be induced by IFNγ, a key effector cytokine secreted by activated CD8+ and CD4+ T cells, through regulation of MHC-I and MHC-II transactivators *NLRC5* and *CIITA,* respectively. Several pre-clinical models, genome wide CRISPR screens, and clinical data have shown that loss of function mutations in IFNγ sensing, through JAK/STAT mutation or IFNγR mutations, can lead to resistance to T cell-mediated control of tumors[99,152,156–160,160–163]. Conversely, mutations in negative regulations of IFNγ signaling can sensitize tumor cells to T cell-mediated killing[157,160,162]. Finally, mutations in epigenetic regulators such as *ARID2* and *EZH2* have been posited to downregulate MHC-I and MHC-II as well as several components of the IFNγ signaling pathways, leading to "reversible" alterations that may be targeted to restore anti-tumor immunity in some pre-clinical models of melanoma, prostate cancer, and lymphoma[158,164–167]. It is important to note that the role of IFNγ is not limited to the antigen presentation machinery. Therefore, mutations targeting this pathway could lead to increased T cell-mediated tumor control through other

complementary mechanisms, such as modulating key chemokines (*CXCL9/10*) that are important for T cell trafficking[158,164].

In addition to downregulating pathways necessary for recognition by the immune system, cancer cells may also upregulate inhibitory receptors that contribute to immune evasion. IFNγ – dependent upregulation of *PD-L1* on cancer cells has now been established as a main mechanism of resistance to adaptively immunity[168–170]. Interestingly, *PD-L1* may also be constitutively expressed as a result of stabilizing mutations in the 3' UTR region or genetic alterations in 9p24.1 – the chromosomal region containing *PD-L1* and *PD-L2*. Genetic mechanisms of increasing *PD-L1* expression are uncommon in solid tumors, but are prevalent in several types of lymphomas including cHL (~90%), PMBL (~40-50%), and DLBCL (10-15%)[171–176]. While PD-L1 expression is sometimes correlated with response to CBT in some types of solid cancers, *PD-L1* gene alterations may enrich for responders to CBT in cHL and DLBCL, suggesting that this genetic alteration may be a predictive biomarker of inflamed, immunotherapy-sensitive cancers.

Finally, cancer cells may modulate pathways that increase cell-intrinsic fitness. For example, cancer cells may mutate pathways downstream of growth factor signaling components such as EGFR (epidermal growth factor receptor) or HER2, leading to sustained proliferative capacity. In addition to increased growth capacity, overexpression of anti-apoptotic molecules, such as BCL-2, is a common mechanism by which cancer cells may resist cell death. Other genetic lesions may lead to evasion of growth suppressors, such as mutations in *TP53* or *RB1*[177]. Taken together, alterations that increase the fitness of cancer cells – either through increased growth or decreased apoptosis - may make them more resistant to immune cell-mediated killing.

Several mechanisms of immune escape have been shown to be active in solid cancers, and the composition and activation state of the immune environment has been shown to impact

response to CBT in solid cancer. Moreover, the role of cancer cell-intrinsic alterations in regulating the immune environment has been demonstrated in several solid cancer models. Whether similar mechanisms are also active in DLBCL, and the bidirectional interactions between lymphoma cell-intrinsic alterations and the immune landscape, have not yet been thoroughly investigated.

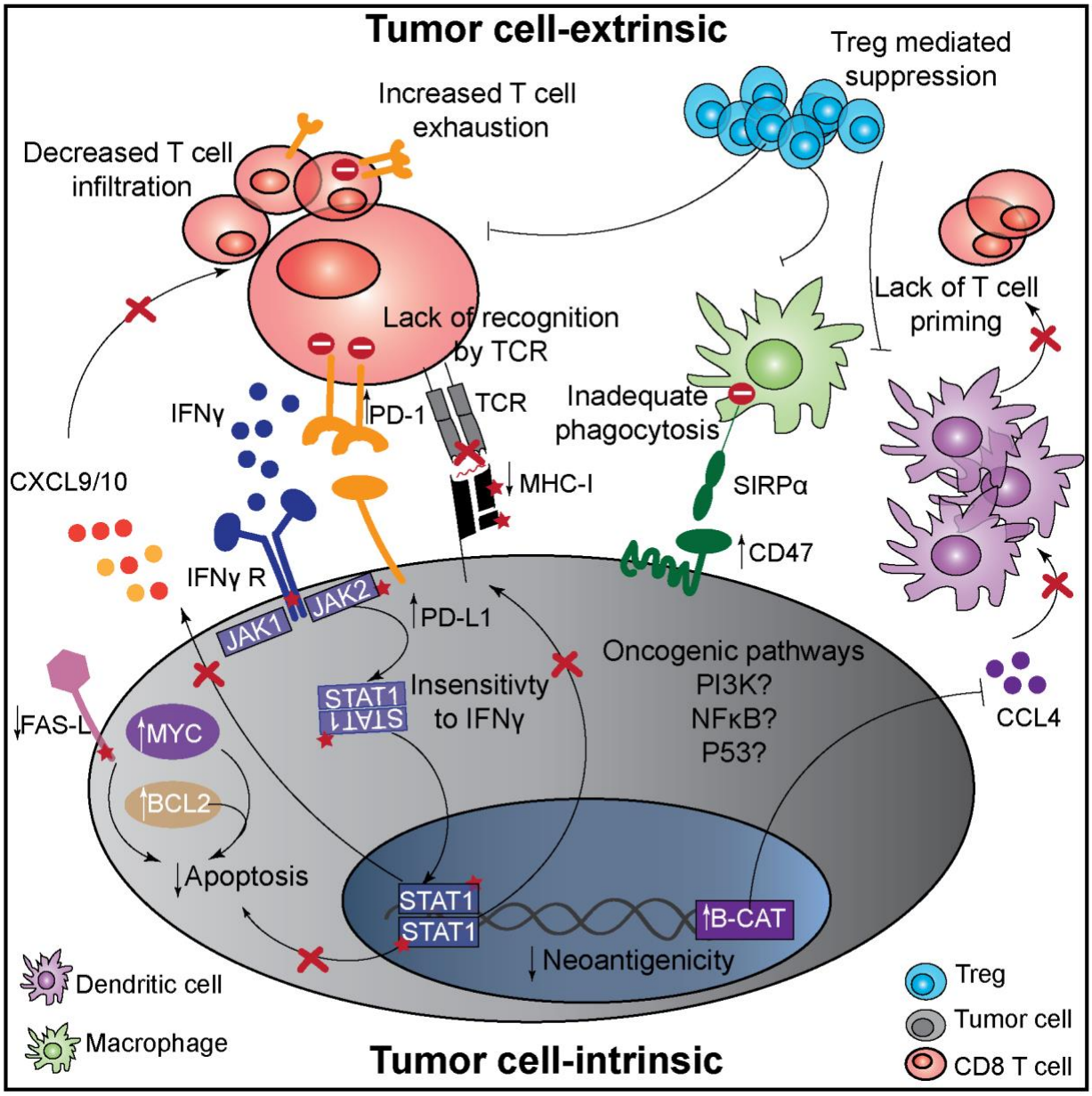

Figure 5. Mechanisms of immune escape in cancer. Tumor cell-extrinsic factors (infiltration and activation of immune cell subsets) and tumor cell-intrinsic factors (oncogenic alterations, upregulation of checkpoint receptors, and sensitivity to T cell derived effector cytokines) contribute to cancer cell escape from immune surveillance. *(Mutations/alterations – red star)*.

1.4 Immunotherapies in DLBCL

Standard of care treatment in DLBCL consists of a chemoimmunotherapy regimen, R-CHOP, that leads to durable remission in approximately 60% of patients[4]. However, remaining 40% of patients with relapsed or refractory disease will eventually succumb to their disease. For the last few decades, new treatment strategies for DLBCL focused on understanding lymphoma biology, leading to the development of several targeted therapies that have been met with varying levels of clinical success. More recently, the rapid advances in the field of cancer immunotherapy have led to new therapeutic modalities for the management of DLBCL. Several new immunotherapies that target components of innate and adaptive immunity in DLBCL have been investigated clinically, detailed below **(Figure 6).**

CD47 antibody. Innate immune cells play an important role in controlling tumor growth through phagocytosis. Immunotherapies targeting functions of innate immune cells have shown activity in lymphoma. Cancer cells can evade phagocytosis through upregulation of "don't eat me" signals, such as CD47 or CD24, on the cell surface[129,131,137,145,178]. Ligation of CD47 with SIRPα on the surface of macrophages triggers an inhibitory signal that prevents phagocytosis, which can be reversed with a monoclonal antibody[131,146,178–181]. Anti-CD47 antibodies have shown remarkable efficacy as single agents *in vitro* and in xenograft mouse models of NHL[179,182,183]. Moreover, anti-CD47 antibodies synergize with Rituximab in promoting macrophage-mediated phagocytosis, as a result of simultaneously blocking an inhibitory signal and delivering a FcR stimulating signal[179]. A phase I clinical trial evaluating the combination of magrolimab (an anti-CD47 antibody) and rituximab in NHL has shown promising results, with an ORR of 36% in patients with r/r

DLBCL[182]. However, the remaining fraction of patients failed to response or relapse. Therefore, alternative strategies to improve the function of CD47/ SIRPα targeting antibodies are required.

Recent efforts to improve CD47 blockade have focused on altering the balance of pro-phagocytic and anti-phagocytic signals on the surface of cancer cells. One strategy is to identify and block other innate immune checkpoints, including CD24 binding to SIGLEC-10 and B2M interactions with LILRB1[145,184]. However, the role of these "don't eat me" signals and the co-blockade with anti-CD47 antibodies has not been investigated in DLBCL. Other groups have focused on increasing the expression of pro-phagocytic signals on the surface of cancer cells. For example, Ennishi et al identified that LoF mutations or deletions in *TMEM30A* – a flippase responsible for the asymmetric distribution of phosphatidylserine (PS), a potent "eat me" signal, on the cell surface – leads to aberrant exposure of PS on lymphoma cells. Moreover, *TMEM30A* mutant DLBCLs are characterized by increased macrophage infiltration and sensitivity to anti-CD47 antibodies[185].

While anti-CD47 and anti-SIRPα targeting antibodies lead to increased tumor control through macrophage-mediated phagocytosis, the clearance of malignant cells may be an "immunologically silent" mechanism that suppresses anti-tumor immunity. One key study found that PI3Kγ signaling in macrophages modulates macrophage polarization, and genetic ablation or pharmacological inhibition of PI3Kγ can reprogram macrophages from immunosuppressive (M2 macrophage) to immunostimulatory (M1 macrophage)[186]. PI3Kγ inhibition in macrophages resulted in improved CD8+ T cell activation in tumors and synergized with CBT. Therefore, we hypothesized that PI3Kγ inhibition may synergize with a-CD47 therapy to promote phagocytosis and repolarize M2 macrophages to M1 macrophages. Treatment of macrophages with duvelisib, a PI3Kγ/δ inhibitor, promotes phagocytosis of lymphoma cells *in vitro* and in xenograft mouse

models alone and in combination with anti-CD47 antibody *(manuscript under review)*. However, whether this combination also improves anti-tumor T cell responses and synergizes with T-cell based immunotherapies remains unknown.

Checkpoint blockade therapy. A major breakthrough in the field of cancer immunotherapy was the discovery that cytotoxic T-cell antigen 4 (CTLA-4), which prevents T cell activation by outcompeting CD28 for binding to CD80/CD86[187–191], could be therapeutically targeted to improve the effector function of T cells[192]. Humanized CTLA-4 blocking antibodies were subsequently shown to induce durable remissions in ~10-20% of patients with metastatic melanoma[193–196]. The success of CTLA-4 blockade renewed interest in other immune checkpoint molecules, including programmed death-1 (PD-1). Genetic ablation of *Pdcd1* led to heterogenous autoimmune pathologies in mice, demonstrating the role of PD-1 in restraining T cell activation[197–200]. Further studies showed that PD-1 is upregulated upon chronic T cell receptor (TCR) stimulation and when PD-1 engages its ligand, programmed death-ligand 1(PD-L1), it can induce a hypofunctional, "exhausted" T cell state[201,202]. Monoclonal antibodies that disrupt the PD-1/PD-L1 signaling axis have shown remarkable success in clinical trials as monotherapy and in combination with conventional chemotherapy in melanoma[203–206]. Additional successful clinical trials have expanded the use of anti-PD1 antibodies to several cancer types including Hodgkin lymphoma[207–209], primary mediastinal B cell lymphoma (PMBL)[210], urothelial carcinoma[211,212], head and neck squamous cell carcinoma (HNSCC)[213,214], non-small cell lung cancer (NSCLC)[215–219], and microsatellite instability high (MSI-high) colorectal cancer[220–222]. The success of anti-PD1 checkpoint blockade therapy (CBT) has spurred development of other antibodies that target co-inhibitory receptors (TIGIT [223,224], TIM3 [225,226], LAG3[227,228]) and co-stimulatory receptors (OX40

[229,230], 4-1BB[231,232] , ICOS [233,234]) that have shown varying degrees of clinical success in combination with anti-PD1 and/or anti-CTLA4 antibodies.

Though anti-PD1 therapy has resulted in substantial clinical benefit in cHL[207–209] and PMBL[210], it has only shown modest efficacy in unselected r/r DLBCL patients (~10% ORR)[10]. In cHL, the response to CBT correlates with *PD-L1* expression on the surface of the malignant Hodgkin Reed Sternberg (HRS) cell[209,235], which is often driven by genetic amplification of the *PD-L1* locus or Epistein Barr Virus (EBV) driven JAK/STAT activation. Moreover, the environment of cHL is characterized by a robust, but ineffective, T cell infiltrate that may be re-energized upon inactivation of inhibitory checkpoint receptors.

In contrast, copy number alterations (CNS) in 9p24.1 – the genetic locus containing *PD-L1, PD-L2,* and *JAK2* – is uncommon in DLBCL. We and others have shown that 10-15% of DLBCLs harbor *PD-L1* CNAs, which includes polysomy, low level copy gains, and amplifications[9,11,173]. Moreover, *PD-L1* gene-altered DLBCLs harbor an expanded, clonal CD8+ T cell infiltrate, suggesting *PD*-L1 gene alterations may identify a subset of "inflamed" DLBCLs that are sensitive to CBT. However, responses to CBT are not restricted to *PD-L1* amplified DLBCLs, and the immune landscape of DLBCL is extremely heterogenous, suggesting other mechanisms may be regulating the host immune response and immunotherapy sensitivity or resistance in DLBCL.

Chimeric antigen receptor (CAR) T cell therapy. CAR T-cell therapy represents a major breakthrough in the treatment of lymphoma. It is a modified version of adoptive cell therapy, where autologous T cells isolated from peripheral blood are engineered to express a chimeric antigen receptor (CAR) – an engineered molecule that contains 1) an antigen binding domain (scFv), 2) a

flexible linker/hinge region, and 3) intracellular signaling and co-stimulatory domains (CD3, CD28, 4-1BB)[236]. These CAR T-cells are then expanded *in vitro* and transfused back into the patient, leading to MHC-independent, T cell-mediated cytotoxicity. To date, CD19 CAR T-cell therapy has been approved for several B cell malignancies including B-ALL, DLBCL, transformed FL, and mantle cell lymphoma[236]. The success of CD19 CARs has paved the way for CAR T-cells directed against other tumor associated antigens expressed in hematological malignancies (CD22, BCMA).

CD19 CAR T-cell therapy has changed the treatment landscape of r/r DLBCL. However, despite its clinical success, the majority of patients (50-60%) relapse with CAR T-cell therapy, suggesting more work needs to be done to improve efficacy[5,6]. Several factors may impact the efficacy and outcome with CAR T-cell therapy including 1) CAR T-cell-intrinsic factors such as CAR design, composition of the CAR T-cell product, or fitness of peripheral blood lymphocytes, 2) lymphoma-related factors such as oncogenic alterations, tumor burden, or other clinical variable, and 3) the immune environment.

The role of the immune environment in mediating response to CBT has been investigated in solid cancers, and the activation of an anti-tumor immune response has been suggested as a predictive biomarker of response to CBT. However, a detailed understanding of the mechanisms by which the immune environment may be impacting response to CAR T-cell therapy is lacking.

One key study found that in patients treated with CD19 CAR T-cell therapy (ZUMA-1), a higher activated T cell infiltrate at baseline was associated with favorable outcomes to CD19 CAR T-cell therapy[237]. However, the interplay between the malignant lymphoma cells and the immune environment, which may be impacting response to CAR T-cell therapy, has not been thoroughly

investigated in DLBCL. Identifying features that determine response or resistance to CAR T-cell therapy will expand the subset of patients with DLBCL that derive clinical benefit.

Bispecific antibody therapy. CAR T-cell therapy has revolutionized the treatment landscape of DLBCL. However, the use of CAR T therapy in the clinic has been impeded due to the many logistical challenges including extended manufacturing time (3-6 weeks), cost, and limited access to most patients[236]. A new class of T cell-based immunotherapies– bispecific antibodies (BsAb) – may retain the features of CAR T-cell therapy with fewer logistic hurdles[238].

BsAbs are chimeric antibodies that co-target tumor associated antigens (CD19, CD20) and T cell antigens (CD3), and trigger T cell activation and cytotoxicity in an MHC-independent manner. Blinatumomab (CD19/CD3 bsAb) was a first-in-class bsAb that was approved for the treatment of B- acute lymphoblastic leukemia (B-ALL)[239,240]. However, clinical trials conducted in DLBCL demonstrated that the high doses of Blinatumomab required for clinical benefit led to severe adverse effects, leading to early termination of several clinical trials[241].

BsAbs targeting CD20/CD3 are currently under clinical investigation in NHL, and have shown efficacy as single agents in r/r DLBCL. Mosunetuzumab, a first-in-class CD20 /CD3 bsAb, was highly active in preclinical *in vitro* and *in vivo* models[242]; however, the ORR in aggressive NHL in phase I/II clinical trials was 35%, suggesting more work needs to be done to improve efficacy of bsAbs[7].

Several strategies to improve the efficacy of bsAbs are being investigated including 1) lack of a fragment crystallizable (Fc) domain, 2) affinity of the antibody binding fragment (Fab) regions, 3) number Fab arms to facilitate higher avidity, and 4) modifications in the linker regions. In one such example, Glofitamab, a CD20 x CD3 bsAb with a 2:1 ratio of CD20 Fab arms to CD3

and higher affinity CD20 Fab, has shown improved efficacy over mosunetuzumab (1:1 ratio of CD20:CD3 arms) in clinical trials (ORR ~47%)[8]. Further improvements to bsAb design are currently under pre-clinical or clinical investigation.

While strategies to improve the structure and function of bsAbs have -led to increased clinical efficacy, little is known about other mediators of response to bsAbs in DLBCL. Tumor lesions are comprised of many different immune cell subsets including: NK cells, T cells, macrophages, and DCs and the abundance of immune cells in the TME plays an important role in response to immunotherapy [107,243,244]. Indeed, the generation of a productive anti-tumor immune response has been shown to predict response to immunotherapies in many solid cancers. [107–109] The activity of bsAbs is dependent on T cells and the recruitment of T cells from circulation or the expansion and function of T cells within the tumor may be influenced by the baseline immune environment. Correlative studies in a phase II clinical trial of glofitamab showed a trend toward higher frequency of CD8+ T cells in complete responders (CR) vs all other patients[245]. However, the bsAb efficacy may be dependent on other immune cells in the environment (CD4+ T cells, T_{regs}, dendritic cells, macrophages) or lymphoma cell-intrinsic factors (CNAs, mutations, oncogenic pathways). Therefore, more work needs to be done to understand the cellular and molecular factors that are driving response or resistance to bsAbs.

Immunotherapies targeting both innate and adaptive immune cells have shown activity in DLBCL. However, a deeper understanding of the role of the DLBCL immune environment in mediating response to immunotherapy, as well as the underlying cellular and molecular factors that orchestrate the immune environment, is required to expand the population of patients that may benefit from these therapies.

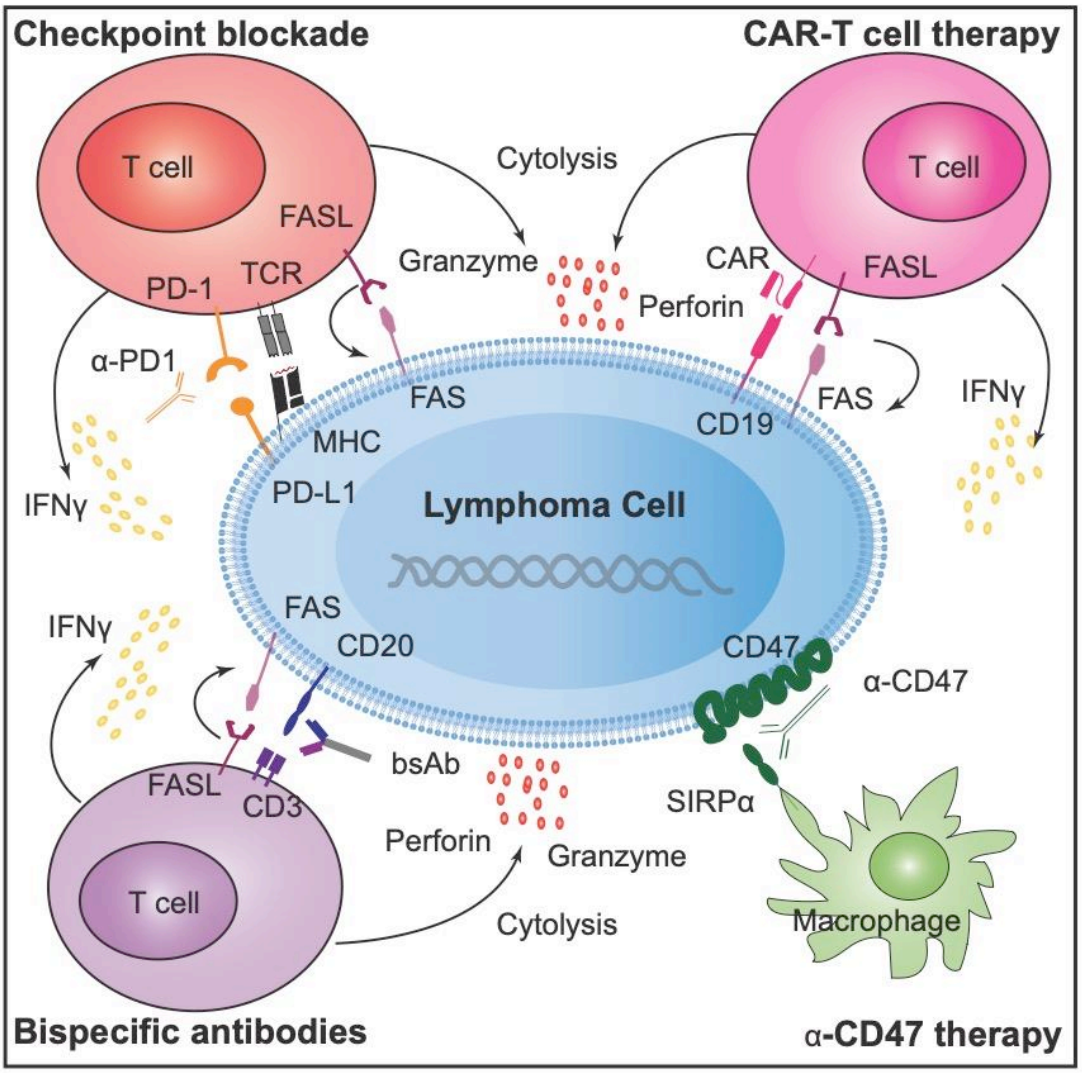

Figure 6. Summary of immunotherapies under investigation in DLBCL. Checkpoint blockade therapy targeting the PD-1/PD-L1 axis may re-activate lymphoma-specific T cells and lead to T cell-mediated cytotoxicity or killing via FAS/FASL interactions. CD19-directed CAR T-cells or bispecific antibodies (bsAbs) lead to MHC-independent T cell-mediated cytotoxicity or activation of extrinsic apoptosis via FAS/FASL interactions. Anti-CD47 antibodies block the interaction of CD47, a potent "don't eat me signal" with SIRPα on macrophages, leading to increased phagocytic clearance of lymphoma cells.

1.5 Immune environment in DLBCL

A major challenge in cancer immunotherapy is to determine the factors that influence response or resistance to immunotherapies to prospectively identify patients that may benefit from CBT, ACT, or other therapies and to identify other targetable cells or molecular pathways that may synergize with immunotherapies. Several factors have been proposed that may play a role in immunotherapy response including: 1) composition of the TME, 2) tumor cell-intrinsic alterations and oncogenic signaling **(Figure 7)**. Our understanding of the molecular factors that contribute to the pathogenesis of DLBCL has advanced considerably in the last few years. On the other hand, the interplay between the lymphoma cells and the immune environment has been less thoroughly investigated. Identifying DLBCLs that have been subjected to a host immune response is challenging. First, since most DLBCLs arise in the lymph node where non-lymphoma-specific immune cells reside, it may be challenging to identify "inflamed" lymphomas that have been surveilled by the immune system. Second, DLBCL is extremely heterogenous, with several distinct transcriptionally, genetically, and clinically defined subgroups. This heterogeneity may directly or indirectly impact the immune environment. Therefore, an integrative approach combining transcriptomic, genetic, and clinical variables may be required to identify features that are regulating the immune environment. Nevertheless, there has been some evidence of immune surveillance in DLBCL.

Lymph node signature. DLBCL COO classification was defined based on transcriptional similarity of DLBCLs to their normal germinal center B cell (GCB DLBCL) or activated B cell (ABC DLBCL) counterparts (*See COO section for more detail*)[34]. Hierarchical clustering performed on transcriptomes of DLBCLs, FLs, CLLs, and purified non-malignant lymphocytes

found that some DLBCLs upregulated a lymph node gene expression program that was also highly expressed in normal tonsil and lymph node. The lymph node signature contained genes related to NK cells (*NK4*), monocytes/myeloid cells (*CD14, CSF-1, FCER1G*) Moreover, some DLBCLs also upregulated a T cell-related gene expression signature, which contains genes such as *CD3E*, *TCRB*, *CD2, PRKCD,* and *FYN*. Interestingly, germinal center B cells purified from normal tonsil and lymph node did not upregulate this gene expression module, suggesting this gene signature is reflective of non-malignant cells in the lymphoma environment. Taken together, these data suggest that there is heterogeneity in the DLBCL microenvironment and some DLBCLs may harbor an immune infiltrate. However, it is not known whether the environment is reflective of: 1) immunological noise, 2) requirement of immune cells for support and growth of the malignant cells, or 3) anti-lymphoma immune response.

Host response (HR) signature. A similar signature was also found in the consensus clustering (CC) approach used by the Shipp lab[52]. A comparative analysis of the transcriptomes of DLBCL identified three clusters: host response (HR), BCR/proliferation, and OxPhos *(See CC* section for more detail). HR DLBCLs were characterized by marked upregulation of T cell-related transcripts (*CD2, CD3D/E, CD28, PRF1*), monocyte/macrophage associated genes (*CD14, CD163, FGR1)*, interferon signaling pathway genes (*GILT, STAT1, IRF1, IRF7)*, and cytokine receptors (*IL2RG, IL6R, TGFBR*). HR DLBCLs were found to have increased numbers of $CD2^+$ and $CD3^+$ T cells compared to DLBCLs in the other two clusters. In addition, using GILT (gamma interferon inducible lysosomal thiol reductase; *IFI30*) to identify DCs, HR DLBCLs were found to have increased number of $GILT^+$ DCs compared to other DLBCLs. These data suggest that a subset of DLBCLs are infiltrated by T cells and DCs that may be required for a productive anti-lymphoma

immune response. However, the association of HR-DLBCLs with response to immunotherapies remains unknown.

Lymphoma microenvironment (LME) clusters. Next generation sequencing (NGS) techniques have enabled more comprehensive analyses of the immune environment of DLBCL. One such study clustered lymphomas based on the presence and activation states of several immune cell subsets in the lymphoma microenvironment[246]. Briefly, 25 functional gene expression scores (F^{GES}) were developed using transcriptomic profiles of purified cell populations. These gene sets included 1) immune cell subsets (Tregss, TIL, B cell, Macrophage), 2) non-immune cells (Extracellular matrix (ECM), cancer-associated fibroblasts (CAF)), 3) non-cellular mediators of immune responses (cytokines, T cell trafficking), and 4) cellular signaling pathways (NFκB, PI3K, cell proliferation). DLBCLs clustered into four LMEs based on F^{GES} for one or more gene sets: 1) germinal center- like, 2) mesenchymal (MS), 3) inflammatory (IN), and 4) depleted (DE). Germinal center-like DLBCLs (~15% of all DLBCLs) were characterized by increased expression of genes related to cellular constituents of the germinal center, including follicular dendritic cells (fDCs), T follicular helper cells (Tfh), and B cells. MS-DLBCLs (~33% of all DLBCLs) displayed marked upregulation of gene sets associated with vascular endothelial cells, CAF, and ECM components. LME-IN DLBCLs (25% of all DLBCLs) were characterized by increased FGES scores for CD8+ T cells, macrophage, NK cell, and other immune cell-related gene sets. Finally, LME-DE DLBCLs (27% of all DLBCLs) were characterized by increased expression of genes related to cellular proliferation and depleted for genes related to immune cell infiltration.

LME classification may have some prognostic significance, as LME-IN and LME-DP DLBCLs have worse overall survival with R-CHOP compared with LME-GC and LME-MS.

However, the association of LMEs with response to immunotherapies has not been shown. Interestingly, LMEs also show little overlap with consensus clustering, as BCR, OxPhos, and HR DLBCLs are equally represented among LME-IN DLBCLs, suggesting these methods are identifying unique aspects of lymphoma biology.

***PD-L1* gene alterations.** Upregulation of PD-L1 on the surface of cancer cells is usually driven by IFNγ secreted by T cells or NK cells in the tumor microenvironment and is a well-characterized mechanism of immune escape in solid cancers. In contrast, unique genetic mechanisms often increase PD-L1 expression in lymphoma. Copy number alterations (CNAs) in chromosome 9p24.1, the locus that contains *PD-L1*, *PD-L2*, and *JAK2* are frequently found in cHL and PMBL[172,235,247,248]. A recent study using fluorescence in situ hybridization (FISH) identified that cHLs harbor a spectrum of *PD-L1* gene alterations – chromosome 9 polysomy, 9p24.1 copy gain or 9p24.1 amplification[172]. Moreover, the level of *PD-L1* gene alteration correlated with PD-L1 protein expression and response to CBT. In contrast, *PD-L1* CNAs are infrequent in DLBCL. We and others have identified that *PD-L1* gene alterations are found in 15-25% of DLBCLs, and are enriched in non-GCB DLBCLs[173,249]. DLBCLs with *PD-L1* gene amplifications (defined as 5 or more copies) were characterized by an increased, clonal CD8+ T cell infiltrate and sensitivity to CBT compared to *PD-L1* non-amplified DLBCLs. Therefore, *PD-L1* gene alterations may serve as a predictive biomarker of response to CBT. However, not all inflamed DLBCLs have *PD-L1* gene amplifications and clinical responses to CBT were not limited to patients with *PD-L1* gene alterations. Therefore, other mechanisms may be regulating the immune environment in DLBCL.

Taken together, these data suggest that a proportion of DLBCLs (25-33%) are characterized by a host immune response. However, the nature of the immune response, the

molecular mechanisms that may impact the immune response, and the association of these "inflamed" DLBCLs with immunotherapy has not been investigated.

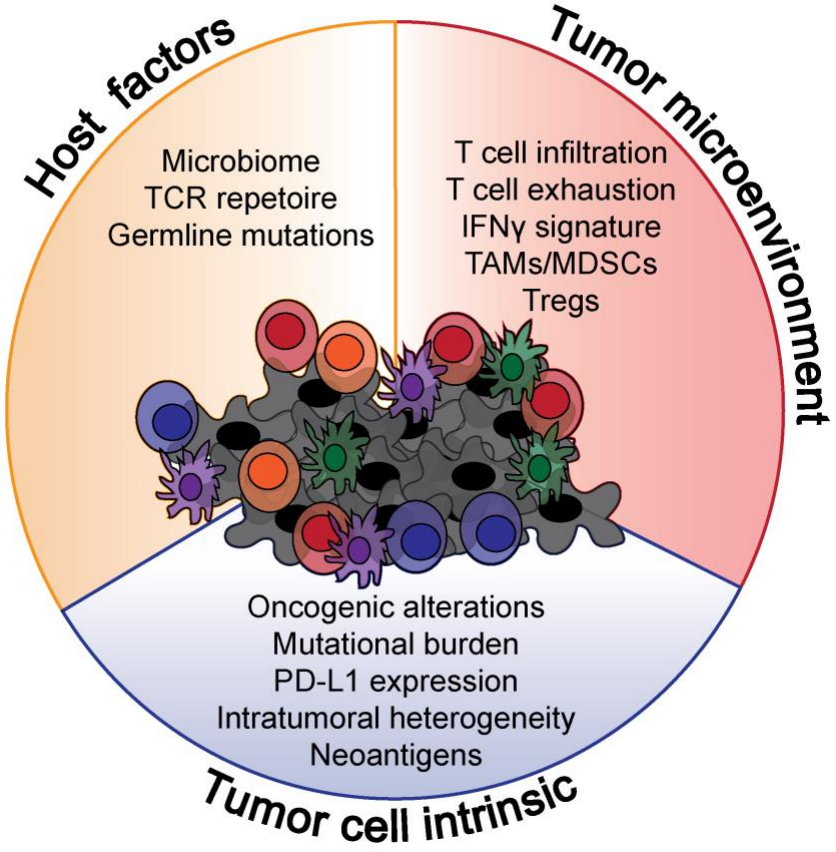

Figure 7. Summary of factors that have been proposed to play a role in response of resistance to immunotherapy in solid cancers.

2. Methods

Data sets

NCI cohort: Contains RNA-sequencing and whole exome sequencing (WES) performed on 481 treatment-naive DLBCL biopsies. Contains annotations for molecular COO, LymphGen classification, DHIT0-signature, 5-year EFS and OS, other clinical information

UCMC cohort: Contains RNA-sequencing and whole exome sequencing (WES) performed on 96 DLBCL (84 treatment-naïve, 12- relapsed/refractory) biopsies

BCCA cohort: Contains RNA-sequencing and whole exome sequencing (WES) performed on 285 treatment-naive DLBCL biopsies. Contains annotations for molecular COO, LymphGen classification, DHIT-signature, 5-year EFS and OS, other clinical information.

HMRN cohort: Contains 1310 patients with Illumina microarray (1042 DLBCL: 487 *de novo*; 41 transformed; 514 unknowns; 45 PMBL: 19 *de novo*; 2 transformed; 24 unknown; 40 cHL; 21 GZL; 83 BL; 31 THRLBCL: 16 *de novo*; 1 transformed; 14 unknown; 26 PBL; 5 PCNSL; 15 Plasmacytoma; 1 MGUS; 1 LPD-NOS) and 496 with targeted exome sequencing.

Gene set compilation

Gene sets were manually curated following an extensive literature search and focused on genes related to 1) immune cell infiltration and activation, 2) cell-of-origin gene sets and 3) gene sets related to key transcription factors related to cell-of-origin.

Immune-related gene sets: Twelve immune-related gene sets were included, known to be associated with immune activity in other cancer types. Gene sets were excluded if they had fewer than 3 or more than 200 genes. Gene sets were related to activation state of T cells (t.cell.activation[99], t.cell.exhaustion[99], IFNγ_ayers[108]), non-cellular mediators of immune

responses (ifn1_rooney[99], cytolytic.score[250]), and presence of immune cell subsets (tfh_charoentong[251], th1_charoentong[252], th2_charoentong[251], treg_rooney[99], cd8t_charoentong[251], macrophage_rooney[99], dc_xcell_total[253]). In general, immune-related gene sets had less than 15% overlap.

***Cell of origin gene sets*:** A total of four COO gene sets - 2 ABC DLBCL (ABCDLBC-1, ABCDLBCL-2) specific gene sets and 2 GCB DLBCL specific gene sets (GCBDLBCL-1, GCBDLBCL-2) - were included. Gene sets are derived from the seminal gene expression classifier[254], found in SignatureDB. (https://lymphochip.nih.gov/signaturedb/index.html) .

Transcription factor gene sets: Three transcription factor related gene sets, found in SignatureDB, were included. Two gene sets related to genes regulated by IRF4 (IRF4Up-7, IRF4dn-1). Signatures were derived from gene expression profiling following IRF4 knockdown in 3 ABC DLBCL cell lines (OCI-LY10, HBL1, TMD-8)[39]. Gene set related to BCL6 targets (BCL6Dn-1), from SigDB, derived from consensus BCL6 targets from multiple studies[255–260].

Immune signature clustering model

Gene set variation analysis (GSVA) using 19 immune-related and COO-related gene sets was performed as previously described on bulk transcriptomes from 2 genomic datasets (NCI[55,261], n = 581; UCMC, n = 108)[244,262].

Resulting GSVA enrichment scores were resolved using principal component analysis (PCA). Unsupervised k-means clustering was utilized to assign samples into unique clusters. Subsequent

analyses using the third independent BCCA dataset as well as the 3-dataset combination were performed in the same structured steps to yield equivalent clustering.

Identification of recurrent genetic alterations associated with immune clusters

Only driver genes from Reddy et al[263]. and Chapuy[264] et al. were considered including mutations and copy number changes (~300 genes). For each comparison, genes are filtered out if they are mutated in less than 10% of any group in the comparison. Genes not altered in at least 10 cases for either cluster (or 10% of cases, if this is smaller) are excluded from the comparison. Statistical significance of categorical variables was performed with a Fisher's exact test for two group comparisons and a multi-way Fisher's exact test followed by post-hoc individual pairwise testing for three or more groups. Alpha was set to a p-value of 0.05. All p-value adjustments were performed using the Benjamini-Hochberg method, unless indicated otherwise.

Generation of *MYC* expression groups

GSVA using MycUp4 signature (from sigDB) was performed on all DLBCLs in UCMC, NCI, and BCCA datasets. DLBCLs were then split into ABC and GCB groups and a 25-75 percentile split within each COO was used to assign DLBCLs to "MYC-High" and "MYC-Low" groups.

Multispectral immunofluorescence

Multi-spectral immunofluorescence (mIF) microscopy was performed on 54 DLBCLs (UCMC) for which paired RNAseq and GSVA data were available. mIF analysis was performed after staining with fluorescence-labeled antibodies against a T cell panel and myeloid cell panel *(see mIF antibody section*). Each slide was scanned using the Vectra Polaris (Akoya Biosciences)

imaging platform and the Phenochart software (PerkinElmer). Through Phenochart, at least 5 representative regions of interest per tissue section were acquired as multispectral images at 40x magnification. Watershed segmentation was used to identify nuclei using DAPI staining and cell borders of individual cells in each ROI. The supervised machine-learning algorithm in the inForm software (v. 3.3) was used to classify each cell into specific phenotypes.

1. Slides were divided by panel and by specific features determined during the initial watershed segmentation, including cell border detection, average cell size, autofluorescence, and DAPI strength.
2. Samples were divided into 4 separate groups for each panel. 2 ROIs were chosen per sample to train the machine-learning algorithm in inForm to identify the following phenotypes with the associated markers:
    1. **T cells** : CD8+ T cell, CD4+ T cell, PAX5+ DLBCL cell
    2. **Myeloid cells**: CD68+ Macrophage, CD11c+ dendritic cell
3. Once the initial training groups were processed, all ROIs in each group of samples were classified using the matching training cohort.
4. Results of per-slide frequencies of each phenotype were tabulated in R using exported values from inForm using the `phenoptr` package and the representative mIF images were also exported through inForm. Given heterogeneity of tumor and microenvironment composition in each ROI, comparisons were made between total number of each TME cell population/phenotype normalized against the number of DLBCL cells present across all ROIs per slide.

Table 1. Antibodies for multispectral immunofluorescence (mIF) – myeloid panel

Panel 1 - -Myeloid	Location	Opal	Primary Ab Info	Clone	Ag retrieval	Primary Ab Diluent
HLA class I	membrane	520	Abcam	EMR8-5	AR6	1:50
HLA-DR	membranous	690	DAKO, M07401-8	TAL 1B5	AR9	1:100
PAX5	nucleus	620	BioCare Medical,CM 207	BC/24, mouse mAb	AR9	1:50 in Da Vinci Green
PD-L1	membranous & cytoplasmic	650	Cell Signaling, 13684S	E1L3N, rabbit mAb	AR9	1:2500
CD68	membrane+cytoplasma	570	BioCare Medical, CM033A	KP1, mouse mAb	AR9	1:50 in Da Vinci Green
CC11c	membrane+cytoplasma	540	BioCare Medical, ACI3122A	5D11, mouse mAB	AR9	1:100 in Renoir Red

Table 2. Antibodies for multispectral immunofluorescence (mIF) – T cell panel

Panel 2 – T cell	Location	Opal	Primary Ab Info	Clone	Ag retrieval	Primary Ab Diluent
FoxP3	nucleus	650	BioCare Medical, API 3164 AA	236A/E7, mouse mAb	AR9	ready-to-use
CD4	membrane	520	BioCare Medical, ACI3148A	4B12, mouse mAb	AR9	1:50 in Van Gogh Yellow
PAX5	nucleus	620	BioCare Medical,CM 207	BC/24, mouse mAb	AR9	1:50 in Da Vinci Green
PD-1	membrane	570	Abcam	EPR4877, rabbit mAb	AR9	1:300, increase to 1:150
CD8	membrane	690	R&D, NBP232836B	C8/144B, mouse mAb	AR9	1:50
CXCR5	membranous	540	R&D Systems, MAB190-SP	51505, mAb	AR9	1:200 (1mg stock, 5ug/ml working)

Statistical methods

Alpha was set to a p-value of 0.05 unless otherwise noted. All p-value adjustments were performed using the Benjamini-Hochberg method, unless indicated otherwise. Statistical significance of categorical variables was performed with a Fisher's exact test for two group comparisons and a multi-way Fisher's exact test followed by post-hoc individual pairwise testing for three or more groups. Statistical significance of continuous variables was performed with a Mann-Whitney U test for two group comparisons and a Kruskal-Wallis test followed by a post-hoc Dunn's test for three or more groups.

Generation of *Socs1* sgRNA containing plasmid

1 ug of Lenti-sgRNA blasticidin plasmid (104993) was digested with *Bsm*BI at 55C for 60 mins, followed by gel extraction of ~8kb band. *Bsm*BI digestion liberates ~2kb stuffer fragment that should not be gel extracted. 100 uM of Forward and 100 uM reverse complimentary sgRNA oligos were annealed using touchdown PCR (95C for 5 mins, followed by ramp down to 25C at -5C/min). Annealed oligos (25 nM) and digested gel-purified plasmid (50ng) were ligated overnight at 16C using T4 DNA ligase (NEB, M0202S). DH5a bacteria were transformed with ligated plasmid, following manufacturer's protocol. Single colonies were selected and expanded following colony PCR and Sanger sequencing to confirm successful incorporation of sgRNA oligos. Plasmids were extracted following manufacturer's protocol (Qiagen Miniprep).

Cell lines

Parental A20 cells were obtained from ATCC and maintained in RPMI-1640 supplemented with 10% FBS. B16 and HEK293(F)T cells were maintained in DMEM supplemented with 10% FBS.

A20$^{Socs1-/-}$ cell line. A20-Cas9 cells were obtained from Joshua Brody and maintained in RPMI-1640 supplemented with 10% FBS and maintained in 2 ug/mL puromycin. A20$^{Socs1-/-}$ cells were generated through lentiviral transduction. Briefly, single guide RNAs (sgRNA) targeting *Socs1* were synthesized and cloned into lenti-sgRNA blasticidin vector using a previously published protocol from Feng Zhang.

Socs1 sgRNAs:

1. TGGTGCGCGACAGTCGCCAA
2. TGATGCGCCGGTAATCGGAG
3. TCTCGCGGCTGCCGTCCAAG
4. AGCCGACAATGCGATCTCCC
5. GCGTGCACGGGGCGCACGAG

Lentivirus was generated by transfection of HEK293(F)T cells with packaging plasmid (psPax2, Addgene #12260), VSV-G envelope plasmid (pMD2.G, Addgene#12259), and *Socs1*-sgRNA plasmid (lenti-sgRNA blast, Addgene #104993) using calcium phosphate transfection (Sigma, K278001). Plasmids were delivered at 1.5 (psPax2) : 1 (pMD2.G) : 2 (lenti-sgRNA blast) ratio. sgRNA control cells were generated using empty lenti-sgRNA blast vector (A20Cas9^{EV}).

Virus was collected 48 hours after transfection. A20-Cas9 cells were maintained in puromycin containing media for the duration of transduction procedure. A20-Cas9 cells were transduced with viral supernatant using spinoculation (900g, 2 hours, 33C) and cells were incubated overnight in viral-supernatant. Medium was replaced after 24 hours. Cells were transduced with virus 2 more

times (for a total of 3 times) following the same protocol. Following transductions, A20Cas9$^{Socs1-/-}$ cells, A20Cas9^{EV}, A20-Cas9 parental were grown in fresh media for 3 days and then blasticidin (10ug/mL) was added to the media to select for cells that contained empty vector or *Socs1* sgRNA. When 100% of parental A20-Cas9 cells were dead under blasticidin selection (~ 6 days), A20Cas9$^{Socs1-/-}$ cells and A20Cas9^{EV} were subjected to limiting dilution to select for monoclonal colonies. Briefly, cells were seeded in a 96 well plate at an average of 0.5 cells/ 100uL. Media was refreshed every 4-5 days, and cells were grown under constant puromycin and blasticidin selection pressure. Western blots were used to select a monocolonal population with Socs*1* deletion.

B16F10$^{Socs1-/-}$ and B16.SIY$^{Socs1-/-}$ *cell lines.* B16$^{Socs1-/-}$ cell lines were generated using lentiviral transduction, as above, with minor modifications. Briefly, single guides targeting *Socs1* were cloned into an all-in-one plasmid (lentiCRISPRv2-puro, Addgene #98290) containing Cas9 and a gRNA scaffold using a previously described protocol. Lentivirus was generated as described above and B16 parental cells were incubated in virus containing media for 24 hours. Media was replaced and B16 cells were allowed to grow for 72 hours. Monoclonal colonies were generated under puromycin (1ug/mL) selection. Knockouts were confirmed using western blots and sanger sequencing.

Isolation of B cells from splenocytes

Spleens from *CD19*$^{Cre/wt}$ and *CD19*$^{Cre/wt}$; *Socs1*$^{fl/fl}$ mice were obtained from Ari Melnick (Weill Cornell Medicine). Spleens were passed through a 70 µm cell strainer (Corning, 352350) and ground using the plunger of a syringe with 10 mL of PBS to yield single cell suspensions. Splenocytes were then washed twice in 10mL of PBS, followed by lysis of red blood cells in a

hypotonic solution, followed by three washes in 10 mL of PBS. Single cell suspensions were incubated with an anti-mouse CD19 biotinylated (Biolegend,115504) antibody to isolate B cells or anti-mouse CD3 biotinylated (Biolegend, 100244) antibody to isolate T cells. Labelled cells were then incubated with streptavidin microbeads (Miltenyi, 130-048-101) and CD19+ or CD3+ cells were isolated using magnetic activated cell sorting (MACS).

***In vitro IFN*γ stimulation**

5 x 10^4 cells from cell populations of interest (A20, B16, or spleen cells) were incubated with increasing concentrations of recombinant mouse IFNγ (0, 0.1, 1, 10, 100 ng/mL) for 48 hours (Peprotech, 315-05). Cells were then harvested and incubated with anti-mouse H-2 (Biolegend, 125506), anti-mouse I-A/I-E (Biolegend, 107619), and anti-mouse PD-L1 (Biolegend, 124311) antibodies and analyzed using flow cytometry. Cell counts were determined using counting beads (Spherotech, ACFP-50-5). Mean fluorescence intensity (MFI) and cell counts were normalized to media control in each experiment. Data shown are the average of at least 3 independent biological replicates.

Mouse models

B6 mice were obtained from Taconic labs and Balb/c mice and NSG mice were purchased from Jackson labs. All mice were maintained in a specific pathogen-free barrier facility and handled in accordance with protocols approved by the Institutional Animal Care and Use Committee.

***In vivo* tumor growth**

A20 or B16 cells were harvested and resuspended in PBS at a concentration of 50 x 10^6/mL or 10 x 10^6/ mL. Mice were subcutaneously inoculated in right flank with 5 x 10^6 A20 or 1 x 10^6 B16

WT or *Socs1*-deficient cells. Mice were monitored daily and tumor measurements were started 7 days post tumor injection. Mice were euthanized in accordance with IACUC protocols when an axis reached 20mm or when tumor volume reached 2000 mm^3. Tumor volume was calculated as (V = L x W x W/2)/2, with length(mm) as the longest axis and height was estimated as the width(mm)/2.

Quantitative real time PCR (qRT-PCR)

5 x 10^5 cells were incubated with increasing concentrations of IFNγ (0, 0.1, 1, 10, 100 ng/mL) for 18-24 hours. Total RNA was isolated from $A20^{WT}$ and $A20^{Socs1-/-}$ or ($B16^{WT}$ and $B16^{Socs1-/-}$) with TRIzol (Invitrogen, 15596026) following manufacturer's protocol. Total RNA (1ug) was used for cDNA synthesis (Fischer, High Capacity cDNA kit 4368814). 10ng of cDNA was used for real-time PCR using SYBR Green Master Mix (Bimake, B21703)

Cxcl9 : Fwd -CTGCCATGAAGTCCGCTGTT;

Rev - AGGGTTCCTCGAACTCCACAC

Cxcl10 : Fwd – CATCCTGCTGGGTCTGAGTG;

Rev - TCGTGGCAATGATCTCAACAC

CD274 : Fwd TGCGGACTACAAGCGAATCACG;

Rev – CTCAGCTTCTGGATAACCCTCG

Gapdh : Fwd – CATCACTGCCACCCAGAAGACTG;

Rev -ATGCCAGTGAGCTTCCCGTTCAG

Expression data were calculated from the cycle threshold (Ct) value. ΔΔCt method was used for quantification, and expression of *Gapdh* mRNA was used for normalization. Results were expressed as fold increase compared to control.

Western Blot

For phospho-Stat western blots, 1 x 10^6 cells were incubated with increasing concentrations of IFNγ (0, 0.1, 1, 10, 100 ng/mL) for 15 mins or 60 mins. Whole cell lysates were extracted using CellLytic M (Sigma, C2978), supplemented with HALT protease/phosphatase inhibitor cocktail (Fisher, 78446) following manufacturer's protocol. Protein concentration was determined using a Bradford Assay (Fisher, 23236). 20ug of total protein was resolved by sodium dodecyl-sulfate polyacrylamide gel electrophoresis (SDS-PAGE), transferred to PVDF membrane and incubated overnight at 4C with antibodies diluted in blocking buffer (5% BSA; TBST). Following overnight incubation, membranes were incubated with secondary HRP conjugated goat anti-rabbit antibody (Fisher, 31460) at 1:10000 dilution in blocking buffer. Following chemiluminescent development (Biorad, 1705062S), membranes were stripped using western blot stripping buffer (21059). Briefly, membranes were submerged in stripping buffer and incubated with shaking at room temperature for 10 mins. Membranes were incubated in blocking buffer for 60 mins at room temperature and incubated overnight at 4C with primary antibody.

Phospho-STAT1 (1: 500) – anti- pSTAT1 (Tyr701) (58D6) Rabbit mAb, CST #9167

STAT1 (1:1000) – anti-STAT1 Clone D1K9Y, Rabbit mAb, CST #14994

B-ACTIN (1:5000) – anti- B-ACTIN Clone 13E5, Rabbit mAb, CST #4970

SOCS1 (1:1000) – anti-SOCS1 Abcam, ab3691

Table 3. List of genes in gene sets.

Gene Set	Genes
T cell exhaustion	*LAG3 CTLA4 CD274 CD160 BTLA VSIR LAIR1 HAVCR2 CD244 TIGIT*
T cell activation	*ICOS CD28 CD27 TNFSF14 CD40LG TNFRSF9 TNFRSF4 TNFRSF25 TNFRSF18 TNFRSF8 SLAMF1 CD2 CD226*
Cytolytic score	*GZMA GZMH GZMM PRF1 GNLY*
Interferon gamma	*TIGIT CXCR6 CXCL9 CD27 CMKLR1 HLA-DQA1 CD8A NKG7 CD276 PDCD1LG2 CCL5 STAT1 LAG3 PSMB10 HLA-DRB1 CD274 IDO1 HLA-E*
IFN-1	*MX1 TNFSF10 RSAD2 IFIT1 IFIT3 IFIT2 IRF7 DDX4 MX2 ISG20*
CD8T	*ADRM1 AHSA1 C1GALT1C1 CCT6B CD37 CD3D CD3E CD3G CD69 CD8A CETN3 CSE1L GEMIN6 GNLY GPT2 GZMA GZMH GZMK IL2RB LCK MPZL1 NKG7 PIK3IP1 PTRH2 TIMM13 ZAP70*
Regulatory T cell	*FOXP3 LINC02694 IL5 CTLA4 IL32 GPR15 IL4*
TH2	*ASB2 CSRP2 DAPK1 DLC1 DNAJC12 DUSP6 GNAI1 LAMP3 NRP2 OSBPL1A PDE4B PHLDA1 PLA2G4A RAB27B RBMS3 RNF125 TMPRSS3 GATA3 BIRC5 CDC25C CDC7 CENPF CXCR6 DHFR EVI5 GSTA4 HELLS IL26 LAIR2*
TH1	*CD70 TBX21 ADAM8 AHCYL2 ALCAM B3GALNT1 BBS12 BST1 CD151 CD47 CD48 CD52 CD53 CD59 CD6 CD68 CD7 CD96 CFHR3 CHRM3 CLEC7A COL23A1 COL4A4 COL5A3 DAB1 DLEU7 DOC2B EMP1 F12 FURIN GAB3 GATM GFPT2 GPR25 GREM2 HAVCR1 HSD11B1 HUNK IGF2 RCSD1 RYR1 SAV1 SELE SELP SH3KBP1 SIT1 SLC35B3 SIGLEC10 SKAP1 THUMPD2 TIGIT ZEB2 ENC1 RETREG1 FBXO30 FCGR2C STAC LTC4S MAN1B1 MDH1 MMD RGS16 IL12A P2RX5 ADGRE5 ITGB4 ICAM3 METRNL TNFRSF1A IRF1 HTR2B CALD1 MOCOS TRAF3IP2 TLR8 TRAF1 DUSP14*

Table 3 (continued).

T follicular helper	*B3GAT1 CDK5R1 PDCD1 BCL6 CD200 CD83 CD84 FGF2 GPR18 CEBPA ADA2 CLEC10A CLEC4A CSF1R CTSS SYNM DPP4 LRRC32 MC5R MICA NCAM1 NCR2 NRP1 PDCD1LG2 PDCD6 PRDX1 RAE1 RAET1E SIGLEC7 SIGLEC9 TYRO3 CHST12 CLIC3 IVNS1ABP KIR2DL2 LGMN*
Macrophage	*FUCA1 MMP9 LGMN HS3ST2 TM4SF19 CLEC5A GPNMB KCNJ5-AS1 CD68 CYBB*
Dendritic cell	*CD1A CD1B CD1E CCL13 CCL17 ALDH1A2 CD209 ALOX15 HLA-DQA1 FPR3*
ABCDLBCL-1	*ACP1 BATF BCL2 CCND2 CSNK1E ENTPD1 FUT8 GOT2 IGHG1 IL16 IRF4 MARCKS PIM1 PIM2 PRKCB PTPN1 SLA SP140 SPIB TCF4*
ABCDLBCL-2	*BLNK BMF CCDC50 CCND2 ENTPD1 ETV6 FOXP1 FUT8 IGHM IL16 IRF4 PIM1 PTPN1 SH3BP5 TBC1D27P*
GCBDLBCL-1	*BCL6 CSTB FAM3C ITPKB LMO2 IRAG2 MME MYBL1 SPINK2 VCL*
GCBDLBCL-2	*BCL6 DENND3 ITPKB LMO2 IRAG2 MME MYBL1 NEK6 SAMD12 SERPINA9*
IRF4Up7	*ALAD ANKRD33B ARHGAP17 ARHGAP24 ARHGAP25 ARHGAP31 ARHGEF3 ARID3A ASPHD2 ATP1B1 AURKA BATF BCL2 BCL3 BLNK BMF BSPRY RHEX CABLES1 CARD11 CCDC113 CCDC88C CCL22 CCND2 CD47 CDKL1 CFLAR CLINT1 COL9A2 CORO1C CSNK1E CXXC5 CYB5R2 DCTD DGKG DHRS9 DNAJC25-GNG10 DOCK10 DUSP15 DUSP5 EHD1 EHD3 EIF2S2 ELL2 ELOVL7 ENTPD1 ERP29 ETV6 FA2H FCMR FCRL5 FKBP11 FOXP1 GAB2 GID4 GYG1 HCK HIVEP2 HSP90B1 IDH1 IL10 IL16 IQGAP2 IRF2 IRF2BP2 IVNS1ABP KLHDC9 KRAS LBH LDLR LYN MAP3K5 MAPKAPK2 MARS1 MLKL MOCOS MPEG1 MSRB1 MYOCD NCF2 NDRG1 NFKBIZ NRROS OAS1 PAK2 PARVB PDCD4 PDE4B PDLIM1 PHACTR2 PIAS2 PIGR PIM1 PNP POU2F2 PPFIBP2 PRDM2 PRPF40A PTPN1 RAC2 RAPGEF1 RARA RASGRP4 RHOQ RILPL2 RUBCNL S1PR1 SACS SCD SEC11C SERPINB8 SFTPB SH2D3C SH3BP1 SH3BP5 SIDT1 SKIL SLA SLC25A30 SLC33A1 SLC39A10 SLC4A5 SMARCA2 SNX9 SP140 SPIB SPTBN1 SSR3 ST3GAL1 ST6GALNAC4 STAMBPL1 STAT3 TCF4 TCTN3 TET2 TLE1 TMEM154 TNFAIP8 TOX2 TPM4 TRAM2 TREX1 UBALD2 UCK2 UNC93B1 VASH2 VAV2 VEGFA VOPP1 WNT10A WNT9A YARS1 ZBTB32 ZFAT ZNF432*

Table 3 (continued).

IRF4Dn1	*ADGRG5 AIM2 ALOX5AP ANK1 ANK3 ARHGAP44 ARL5B ATL2 BCAS4 BFSP2 BICD1 BORCS8-MEF2B BPTF SHLD1 CCDC126 CCDC69 CCND3 CD1A CD27 CD38 CD83 CD86 CDK14 CEP126 CFAP58 CLIC5 COA1 COTL1 CUX1 CYP39A1 DAAM1 DEF8 DHRS9 DIP2C DOK3 EBF1 EHD3 ELF1 EML6 ENPP3 EPSTI1 ERP44 FAM53B FANCA FCRL1 FCRLB GATAD2B GCNT1 GCSAM GPR160 HECW2 HGSNAT HSD17B12 HTR3A IGSF22 ILDR1 IQCD ITPKB IZUMO4 KCNN3 GARRE1 KIAA1549L KLF12 KLHL6 KRT13 LACC1 LCK LHPP LNPEP LPP IRAG2 LY9 LYL1 MAP3K7CL MAP4K4 MAST3 MBD4 MCTP2 MED12L MEF2C MET MILR1 MOB1A MOB3A MPZL3 MTF2 MYO1E NCALD NCOA7 NLRP2 NR3C1 OTULIN PACSIN1 PAG1 PALD1 PHLPP1 PIK3CG PIP4K2A PITPNC1 PLAG1 PLXNB2 POLD4 POLH PPIL2 PRAG1 PRKCD PRKRIP1 PTAFR PTK2B PTPN18 PTPRS PUDP PXK RCBTB2 RECQL5 REL RFTN1 RRM2B S1PR2 SEC14L1 SEMA4A SGPP1 SH2B2 SH3KBP1 SLC15A4 SLC25A27 SLC2A5 SLC6A16 SMARCA4 SMIM14 SOBP SOX5 SPRED2 STAG3 STX7 SWAP70 SYK SYNE2 SYT11 TBC1D4 TMEM123 TMEM131L TMEM229B TNFSF10 TOB2 TPCN1 TPCN2 UBE2J1 USP12 VGLL4 WIPI2 XKR6 XYLT1 ZFHX3 ZNF318 ZNF581 ZNF608*
BCL6Dn-1	*ATR CCL3 CCND2 CD44 CD69 CD80 CDKN1A CDKN1B CXCL10 CXCR4 GPR183 ID2 IFITM1 IFITM3 IRF9 NFKB1 PRDM1 STAT1 TP53*

3. Results[1]

3.1 Introduction

Diffuse large B cell lymphoma (DLBCL) is the most commonly diagnosed subtype of non-Hodgkin lymphoma (NHL). While a majority of people with DLBCL are cured with R-CHOP (rituximab, cyclophosphamide, doxorubicin, vincristine, and prednisone) chemoimmunotherapy, approximately 40% will develop relapsed or refractory (r/r) disease, which is often fatal[2,4,30,265,266]. Clearly, more effective therapies are needed to improve the survival of patients with r/r DLBCL.

Recently, immunotherapies have revolutionized the treatment landscape of r/r DLBCL. For example, CD19-directed chimeric antigen receptor T (CD19-CAR T) cell therapy induces durable responses in ~30-40% of people with r/r DLBCL[5,6]. Complete responses are also observed in up to 40% of patients who receive CD3-CD20 targeting bispecific antibodies (bsAbs)[7,8]. However, in many people with r/r DLBCL, bsAb therapy and CD19-CAR T-cell therapy either fail completely or confer fleeting responses. Finally, checkpoint blockade therapy (CBT) with anti-PD-1 antibodies can elicit responses in a small subset (10-15%) of r/r DLBCL patients, but are ineffective in the majority of unselected patients[9–11]. Collectively, these clinical observations indicate that while immunotherapies can be effective against DLBCL, additional research is needed to understand the cellular and molecular features that underlie immunotherapy responsiveness in order to expand the population of patients who might benefit from these therapies.

The role of the immune environment in mediating response to immunotherapy has been extensively explored in solid tumors. In particular, studies have demonstrated that a "T cell

[1] This chapter contains portions of a manuscript that is currently under preparation.

inflamed" environment identifies a subset of patients with a spontaneous anti-tumor immune response, and serves are a potential biomarker of response to checkpoint blockade therapy (CBT)[105,108,126,267,268]. Interestingly, subsets of DLBCL have been similarly characterized as exhibiting an inflamed tumor environment. For example, published work has identified DLBCL subsets that exhibited a transcriptional "host response" (HR) signature[52] or an inflamed microenvironmental signature (LME-IN)[246], which are enriched for expression of immune cell-related genes. While these data indicated that DLBCLs may possess unique immune environments, the vulnerability of HR DLBCLs or LME DLBCLs to immunotherapies remains unknown. In order to link the immune environment and response to immunotherapies in DLBCL, we have previously identified copy number alterations in chromosome 9p24.1 – a region that contains the *PD-L1* locus—as a biomarker of inflamed DLBCLs[249]. However, while *PD-L1* gene alterations can enrich for DLBCL patients that will benefit from CBT, responses to immunotherapies are not restricted to this relatively rare subset, indicating that other features of the DLBCL environment play a role in regulating immunotherapy sensitivity[9,10,12]. Therefore, a more comprehensive analysis of the factors regulating the immune environment and immunotherapy response in DLBCL is required.

3.2 Results

3.2.1 Gene set variation analysis (GSVA) in a large DLBCL cohort.

In solid cancers, a "T cell inflamed" gene signature identifies tumors against which a spontaneous anti-tumor immune response has been induced and enriches for a subset of cancers that are particularly vulnerable to immunotherapies, such as CBT[108,268,269]. Therefore, we first sought to transcriptionally cluster DLBCLs as "inflamed" or "non-inflamed" based on the immune cell composition of the environment. Our discovery cohort contained bulk transcriptomic data from diagnostic DLBCL biopsies from the NCI (n = 481) and an internal dataset from the University of Chicago Medical Center (UCMC, n = 108), for a total of 589 cases.

Gene set variation analysis (GSVA)[262] was used to calculate sample-wise relative enrichment scores based on the collective expression of genes comprising 19 gene sets that fell into 2 functional groups: 1) immune-related signatures 2) cell of origin (COO)-related signatures (*Table in Methods*). Immune-related signatures were manually curated following an extensive literature search and contained gene sets related to: IFNγ response[108], type I IFN response[99], cytolytic score[270], T helper 1 (T_H1) cells[251], T helper 2 (T_H2) cells[251], T follicular helper (T_{FH}) cells[251], T regulatory (T_{reg}) cells[99], $CD8^+$ T cells[251], T cell exhaustion and activation[99], macrophages[99], and dendritic cells (DCs)[253]. As COO classification segregates DLBCLs into germinal center B cell-like (GCB) and activated B cell-like (ABC) subtypes with distinct clinical, transcriptional, and genetic features, we hypothesized that immune environments associated with ABC and GCB DLBCLs might also differ significantly. To control for potential heterogeneity in DLBCL immune landscapes according to COO, the second category of gene sets selected contained canonical genes from a well-known gene expression-based classifier, as well as gene sets regulated by IRF4 and BCL6, two important transcription factors critical for COO

classification[254]. Altogether, 581 unique genes were included in the 19 gene sets selected for GSVA (<15% overlap between individual gene sets). The approach is summarized in **Figure 8.**

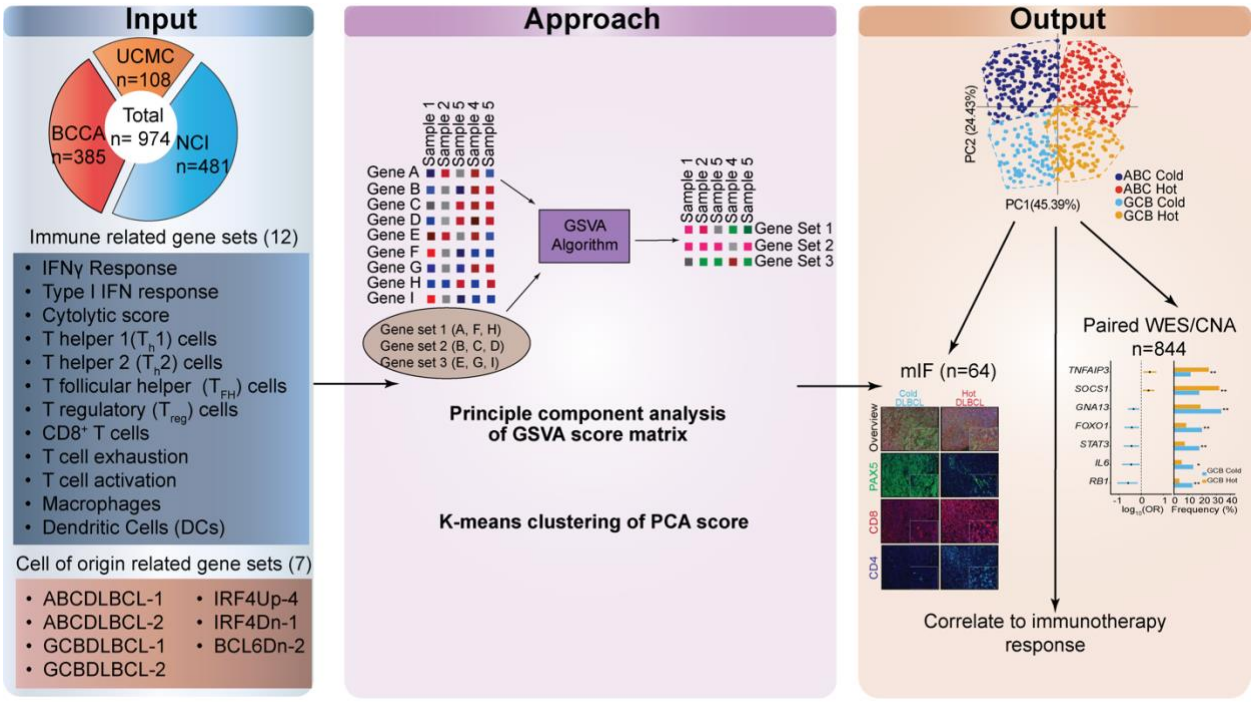

Figure 8. Gene set variation analysis (GSVA) in a large DLBCL cohort. Summary of approach to transcriptionally cluster DLBCLs based on the immune environment.

3.2.2 Transcriptomic analysis identifies four unique DLBCL immune environments.

GSVA scores were subjected to principal component analysis (PCA), which revealed that the majority (68.9%) of variance in gene expression score was explained by PC1 (45.4%) and PC2 (24.4%). Unsupervised k-means clustering was performed on the PCA-transformed dataset and the optimal number of clusters was determined to be four **(Figure 9A)**. DLBCLs in our discovery cohort were then assigned to one of four specific clusters (Cluster 1, 2,3, and 4). Samples from NCI and UCMC datasets were equally represented in each cluster, indicating any differences between clusters were not due to batch effects **(Figure 9B, 9C)**.

Our initial analysis showed that the immune-related gene sets were highly concordant **(Figure 2D)** and contributed exclusively to PC1 **(Figure 9E).** Conversely, COO-related gene sets offered the largest contribution to PC2, and did not contribute significantly to PC1 (**Figure 9F)**. ABC COO-related gene sets (ABCDLBCL-1, ABCDLBCL-2, IRF4Up-7) were highly concordant and positively associated with PC2, while GCB COO-related gene sets (GCBDLBCL-1, GCBDLBCL-2, IRF4Dn-1) were negatively associated with PC2 **(Figure 9D)**. Overall, DLBCLs can be effectively segregated into four unique clusters, each characterized by a distinct distribution of immune-related (PC1) and COO-related (PC2) scores.

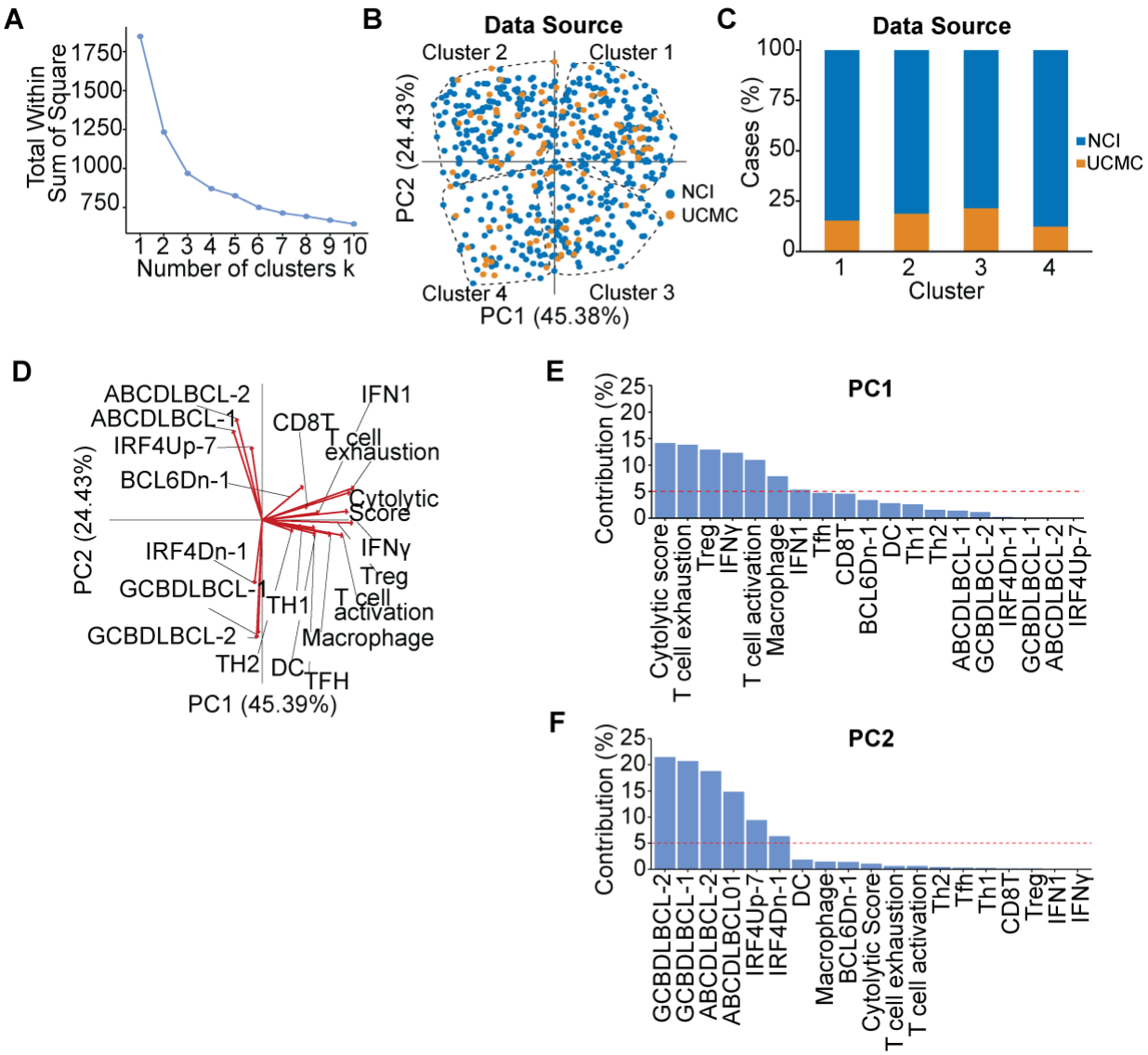

Figure 9. Transcriptomic analysis identifies four unique DLBCL clusters. A. Elbow plot showing optimal number of clusters in the data (k = 4). **B.** PCA plot showing distribution of DLBCLs from two independent data sources, indicating no batch effect (NCI – blue, UCMC-yellow). **C.** Bar plot quantifying distribution of cases from two independent data sources. **D.** Principal component analysis (PCA) biplot showing the contribution of immune-related gene sets and COO-related gene sets to PC1 and PC2, respectively. **E,F.** Bar plots showing contribution of 19 gene sets to PC1 **(E)** and PC2 **(F)**.

3.2.3 Principal component 2 (PC2) represents COO-related axis.

Principal component 2 represented 24.43% of the variance in our dataset. Moreover, COO-related gene sets contributed exclusively to PC2. ABC COO gene sets and GCB COO gene sets trended in opposite directions, suggesting ABC DLBCLs had a PC2 score >0 while GCB DLBCLs had a PC2 score < 0. Comparative analyses of the transcriptomes of putative ABC DLBCLs (PC2 >0) and GCB DLBCLs (PC2 <0) identified 291 differentially expressed genes. In line with previous reports, several genes (*BATF and IRF4)* known to be important for classification of ABC DLBCLs using molecular clustering methods were also upregulated in our GSVA-classified ABC DLBCLs. Differentially expressed genes in our GSVA-classified GCB DLBCLs (*MYBL1*, *SERPIN9A*, and *LMO2*) are also highly expressed in bona-fide GCB DLBCLs (**Figure 10A)**. As a separate, orthogonal validation of our COO-related PC2 axis, we compared the overlap between our GSVA-based COO calls with COO annotations using previously validated molecular classification methods. Molecular classifications and GSVA-based classifications were concordant over 95% of the time, suggesting GSVA can accurately cluster DLBCLs based on COO (**Figure 10B, 10C)**. Taken together, these data suggest that PC2 represents our COO-related axis.

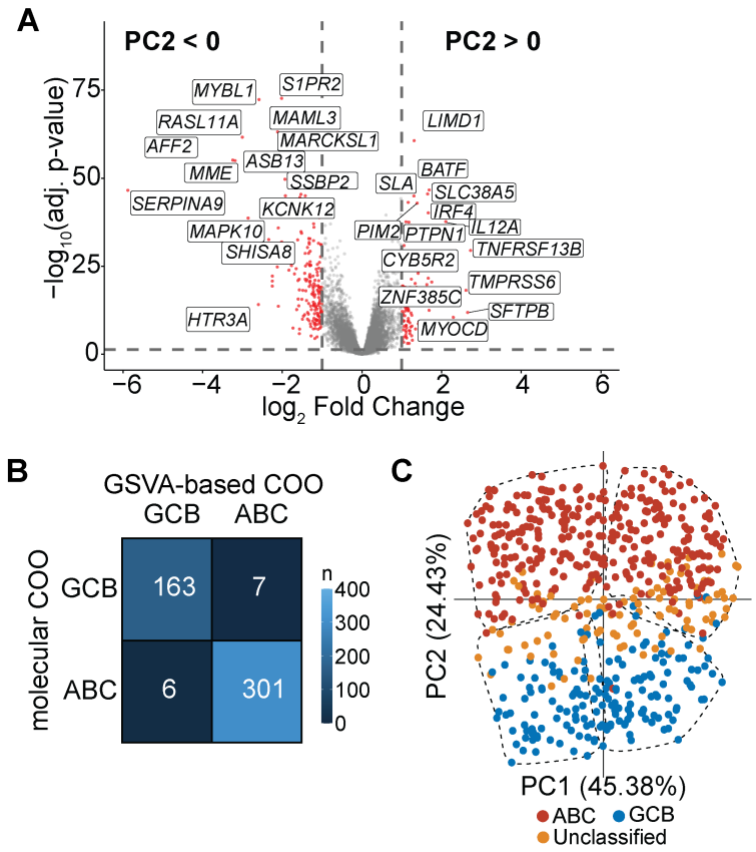

Figure 10. PC2 represents COO-related axis. A. Volcano plot showing differentially expressed genes ($log_2FC > 1.5$, adj p value < 0.05) between putative "ABC" DLBCLs (PC2> 0) and "GCB" DLBCLs (PC2 < 0). **B**. Confusion matrix showing the concordance between GSVA-based COO classification and molecularly-defined COO designations for all DLBCLs. **C.** PCA plot showing concordance between sample-wise GSVA COO scores and molecularly-defined COO calls for all DLBCLs in the discovery cohort (NCI/UCMC). Colors represent molecularly-defined COO, (GCB – blue, ABC – red, unclassified – orange). Clusters are defined by dashed-line.

3.2.4 Principal component 1 (PC1) identifies inflamed and non-inflamed DLBCLs.

The above analyses suggested that a subset of DLBCLs are characterized by increased expression of immune cell-related genes. Moreover, most immune-related gene sets contributed significantly to PC1. Therefore, differential gene expression (DGE) analysis was performed on putative "hot" (PC1 >0) and "cold" (PC1 <0) DLBCLs. This analysis revealed that "hot" DLBCLs were characterized by significant upregulation of canonical genes related to immune cell activation (e.g. *CD2, CD3D, CD3E, GZMK, IFNγ, CD8A, PRF1*) compared to "cold" DLBCLs **(Figure 11A)**. Based on these analyses, we determined that ABC DLBCLs could be transcriptionally defined as "ABC hot" (n = 182, PC1 >0, PC2 >0), characterized by high enrichment scores for immune-related gene sets, or "ABC cold" (n = 184, PC1 <0, PC2 >0). Similarly, GCB DLBCLs could be subdivided into "GCB hot" (n =122, PC1 >0, PC2 <0) and "GCB cold" (n = 89, PC1 <0, PC2 <0) clusters (**Figure 11B, 11C**). Collectively, these results indicate that DLBCLs can be assigned into four unique, transcriptionally defined, immune-related clusters **(Figure 11D)**.

Interestingly, we noted that ABC hot DLBCLs demonstrated increased expression of immune-related genes compared to GCB hot DLBCLs **(Figure 11D)**. These analyses utilized bulk transcriptomic data, and malignant lymphoma cells may share some overlap in gene expression with other immune cells in the lymphoma environment. Therefore, ABC hot DLBCLs may appear to be more inflamed transcriptionally. The quantity and nature of the immune environment of ABC hot DLBCLs, as well as their sensitivity to immunotherapy compared to GCB DLBCLs remains unknown. Moreover, there is striking heterogeneity in immune-related scores within each immune-related cluster suggesting a more granular analysis is required to understand the nature of the immune infiltrate in DLBCL and the role of the immune environment in immunotherapy response.

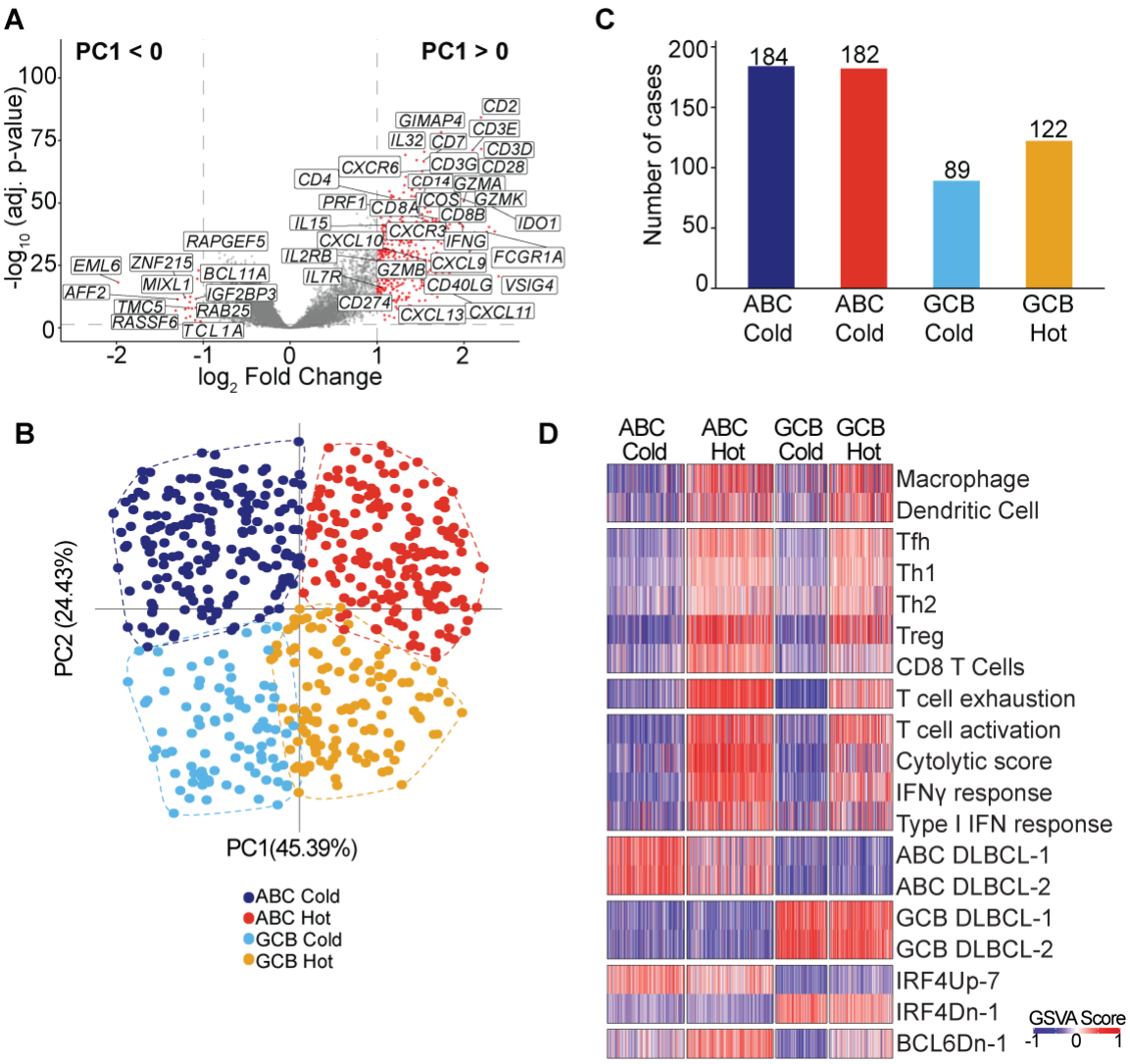

Figure 11. PC1 identifies inflamed and non-inflamed DLBCLs. A. Volcano plot showing differentially expressed genes ($log_2FC > 1.5$, adj p value < 0.05) between putative "hot" DLBCLs (PC1> 0) and "cold" DLBCLs (PC1 < 0). **B.** PCA plot showing sample wise GSVA enrichment scores for DLBCLs in the validation cohort (NCI/UCMC), labeled by cluster name (ABC Cold – dark blue, ABC Hot – red, GCB Cold – light blue, GCB Hot- yellow). **C.** Bar plot showing number of cases in each immune-related cluster. **D.** Heatmap showing sample wise GSVA enrichment scores for all gene sets for DLBCLs in each immune-related cluster.

3.2.5. Validation of GSVA-based clustering in an independent dataset.

To validate our clustering, we performed GSVA on an independent validation dataset (BCCA, n = 285), which revealed a similar clustering pattern **(Figure 12A)**, with immune-related gene sets contributing to PC1 and COO-related gene sets contributing to PC2 **(Figure 12B)**. Given the reproducibility of GSVA-based clustering across multiple data sources, we then combined datasets to power our analyses. GSVA clustering in the combined dataset showed that DLBCLs from different sources were equally distributed among the immune-related clusters, indicating no batch effect **(Figure 12C, 12D)**. Moreover, immune-related gene sets contributed to PC1 and COO- related gene sets contributed to PC2 **(Figure 12E)**, demonstrating the stability of GSVA-based clustering in identifying four unique DLBCL immune environments **(Figure 12F)**. Overall, the clusters retained the structure of a "four-leaf clover," with DLBCLs within each cluster residing along a spectrum of gene expression scores for COO and immune-related gene sets.

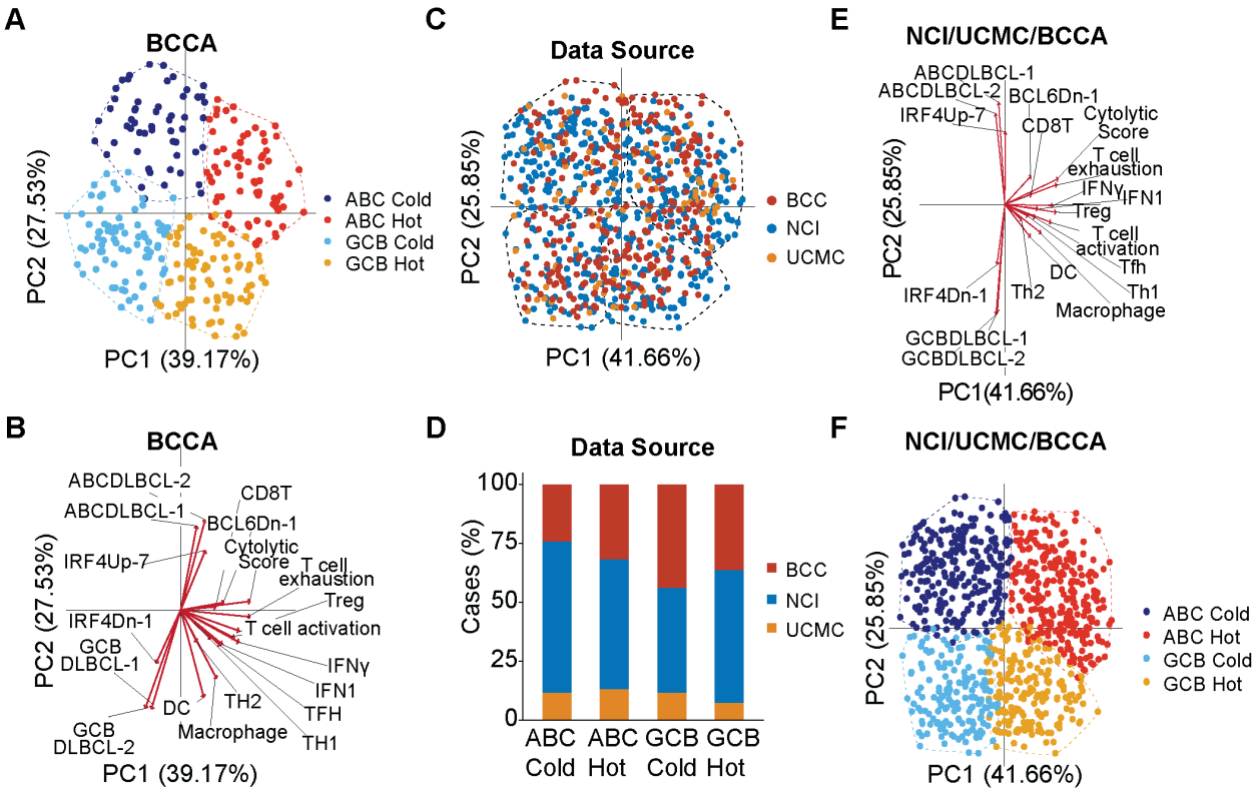

Figure 12. Validation of GSVA-based clustering in an independent dataset. A. PCA plot showing sample wise GSVA enrichment scores for DLBCLs in an independent dataset (BCCA). **B.** PCA biplot showing contribution of immune-related and COO-related gene sets to PC1 and PC2, respectively, in for DLBCLs from the BCCA dataset. **C**. PCA plot showing sample wise GSVA enrichment scores for DLBCLs from three datasets, colored by data source (NCI- blue, UCMC, - yellow, BCCA -red) . **D.** Bar plot showing distribution of cases from NCI, UCMC, and BCCA datasets within each GSVA-based immune cluster. **E**. PCA biplot showing contribution of immune-related and COO-related gene sets to PC1 and PC2 for DLBCLs in combined NCI/UCMC/BCCA dataset. **F**. PCA plot showing sample wise GSVA enrichment scores for combined NCI/UCMC/BCCA dataset.

3.2.6. Prognostic significance of immune-related clusters.

Having established that DLBCL is characterized by a spectrum of different immune environments, we then sought to determine whether immune environments can impact patient outcomes. As expected, patients with GCB-DLBCL showed improved progression-free survival (PFS) and overall survival (OS) compared to those with ABC-DLBCL. However, further stratifying within ABC or GCB DLBCL groups by immune-related clusters did not lead to improved outcomes with R-CHOP **(Figure 13A, 13B).** However, immune-related clusters may have prognostic significance in a cohort of patients treated with immunotherapy.

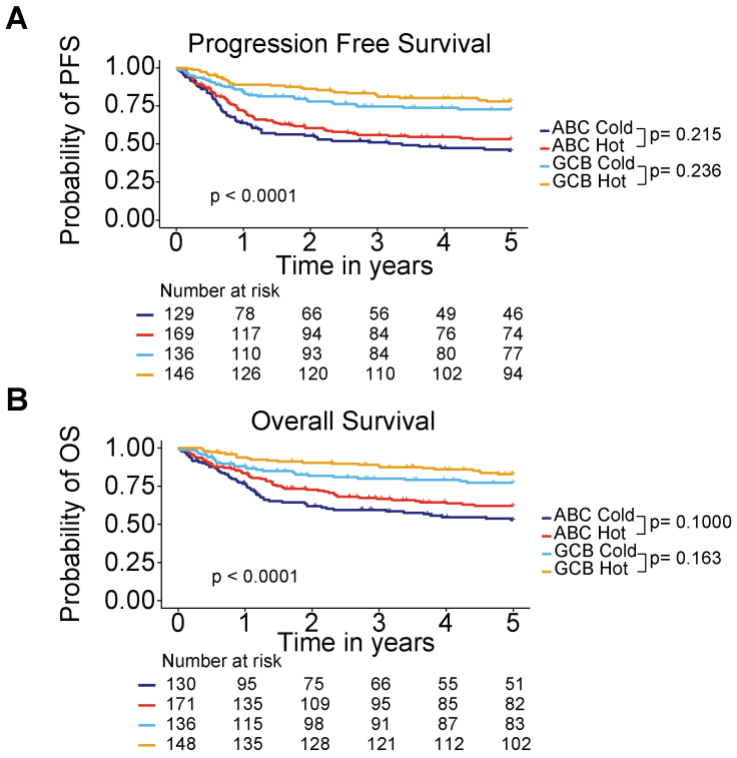

Figure 13. Prognostic significance of immune-related clusters. A,B . Five-year progression free survival (PFS) **(A)** and overall survival (OS) **(B)** of DLBCLs in immune-related clusters.

3.2.7 Transcriptional validation of immune-related DLBCL clusters.

Immune cell deconvolution analysis using CIBERSORTx was next performed on our transcriptomic data to determine the degree to which GSVA-based immune cluster assignment of DLBCL cases correlated with inferred proportions of various immune cell populations. As expected, higher estimated fractions of several immune cell subsets were observed among ABC and GCB hot DLBCLs **(Figure 14A)**. Specifically, GCB and ABC hot DLBCLs showed higher inferred proportions of $CD8^+$ T cells **(Figure 14B)**, $CD4^+$ T cells **(Figure 14C)**, $FOXP3^+$ regulatory T cells (T_{regs}) **(Figure 14D)**, macrophages **(Figure 14E)**, and dendritic cells (DCs) **(Figure 14F)**, when compared to GCB and ABC cold DLBCLs. Interestingly, most immune cell subsets are represented in ABC and GCB hot DLBCLs. However, more granular analyses may reveal the contribution of one or more immune cell subsets in coordinating an anti-tumor immune response.

Taken together, these data demonstrate that "hot" DLBCLs are characterized by higher infiltration of innate and adaptive immune cells, which is suggestive of the generation of an anti-lymphoma immune response. However, the majority of DLBCLs develop within lymph nodes, which are densely populated with immune cells. As a result, it is currently unclear whether an inflamed environment plays a role in facilitating a successful anti-tumor immune response and response to immunotherapy in DLBCL.

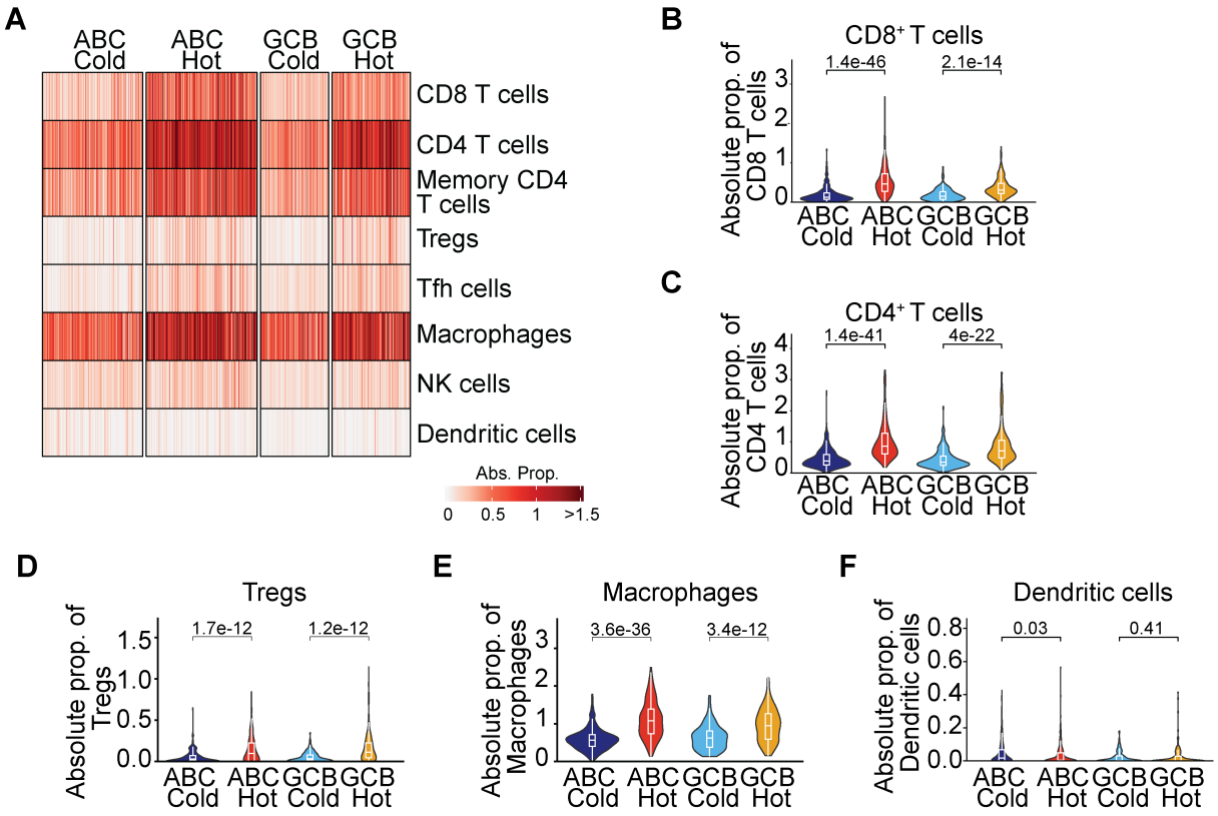

Figure 14. Validation of immune-related clusters. **A.** Heatmap showing sample-wise estimated fraction of each immune cell subtype in immune-related clusters for all DLBCLs. **B-F.** Violin plots showing estimated fractions of $CD8^+$ T cells **(B),** conventional $CD4^+$ T cells **(C)**, regulatory T cells **(D)**, macrophages **(E)**, and dendritic cells **(F)** in each immune-related cluster. Statistical analysis by Kruskal-Wallis test followed by a post-hoc Dunn's test with Benjamini-Hochberg (BH) adjusted p-values.

3.2.8 Validation of immune-related DLBCL clusters using multispectral immunofluorescence.

Next, to confirm that GSVA-based clustering of DLBCLs accurately reflected the immune cell composition of the lymphoma environment, multispectral immunofluorescence was performed on a subset of DLBCLs (n = 54, UCMC) for which paired RNA sequencing data were available. Slides were stained with fluorescently labeled antibodies against T cell markers (CD4, CD8, FOXP3, CXCR5, and PD1) and myeloid cell markers (CD68, CD11c, HLA-I, HLA-DR, and PD-L1). All cells were counterstained with DAPI and malignant B cells were labeled with an anti-PAX5 antibody in both T cell and myeloid cell panels (*List in methods*). $CD68^+$ macrophage: DLBCL ratios were not significantly enriched in any immune cluster **(Figure 15A)** and were not significantly correlated with a sample-wise PC1 score **(Figure 15B)**. Similarly, $CD11c^+$ DC: DLBCL ratios were not significantly different between clusters **(Figure 15C)** and were not significantly correlated with PC1 scores **(Figure 15D)**. Interestingly, immune cell deconvolution revealed increased inferred proportions of macrophages and DCs in ABC hot and GCB hot DLBCLs compared to ABC and GCB cold DLBCLs. However, it is possible that immune cell deconvolution – which relies on the identifying coordinate gene expression programs in immune cells – may be more sensitive than using expression of a single marker in identifying macrophages and DCs.

However, there were significant differences in T cell infiltration among the four immune-related clusters. Representative images are shown in **Figure 15E**. DLBCLs transcriptionally clustered by GSVA as ABC and GCB hot were characterized by significantly higher ratios of $CD8^+$ T cells to $PAX5^+$ DLBCL cells when compared to ABC and GCB cold counterparts **(Figure 15F)**. Furthermore, $CD8^+$ T cell to $PAX5^+$ DLBCL cell ratios were significantly correlated with

sample-wise hot/cold (PC1) axis scores **(Figure 15G)**. Similarly, the ratio of $CD4^+$ T cells to $PAX5^+$ DLBCL cells was significantly higher in ABC hot DLBCLs compared to ABC cold DLBCLs **(Figure 15H).** Finally, $CD4^+$ T cell to $PAX5^+$ DLBCL cell ratios were significantly correlated with sample-wise hot/cold (PC1) axis scores (**Figure 15I**). These data validate the accuracy of GSVA-based clustering method in classifying DLBCLs as harboring hot or cold immune environments.

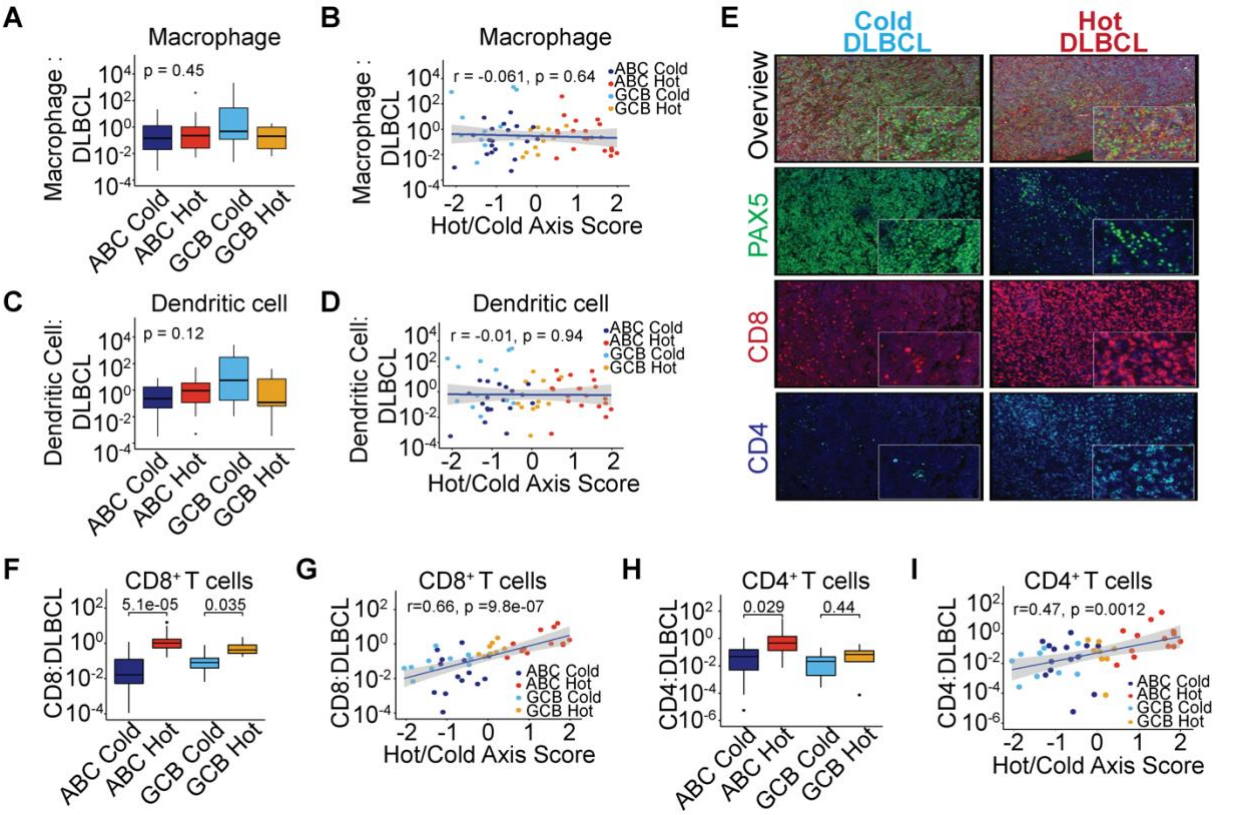

Figure 15. Validation of immune-related clusters. **A.** Box plot showing average $CD68^+$ macrophage :DLBCL ratios in immune-related clusters (n = 41). **B.** Scatter plot showing correlation of hot/cold axis score (PC1) and $CD68^+$ macrophage :DLBCL ratio (n = 41). **C.** Box plot showing average $CD11c^+$ dendritic cell:DLBCL ratios in immune-related clusters (n = 41). **D.** Scatter plot showing correlation of hot/cold axis score (PC1) and $CD11c^+$ dendritic cell:DLBCL ratio (n = 41). **E.** Representative multispectral immunofluorescence (mIF) images showing Pax5+ malignant lymphoma cells (green), CD8+ T cells (red), $CD4^+$ T cells (blue) for a cold (left) and hot (right) DLBCL. **F.** Box plot showing average $CD8^+$ T cell :DLBCL ratios in immune-related clusters (n = 41). **G.** Scatter plot showing correlation of hot/cold axis score (PC1) and

Figure 15 (continued). $CD8^+$ T cell:DLBCL ratio (n = 41). **H.** Box plot showing average $CD4^+$ T cell :DLBCL ratios in immune-related clusters (n = 41). **I.** Scatter plot showing correlation of hot/cold axis score (PC1) and $CD4^+$ T cell :DLBCL ratio (n = 41). Statistical analysis by Kruskal-Wallis test followed by a post-hoc Dunn's test with Benjamini-Hochberg (BH) adjusted p-value.

3.2.9 DLBCL subsets associated with different immune-related clusters.

Having established that DLBCLs can be segregated into four immune-related clusters, we were interested in examining the extent to which GSVA-based immune clustering reflected immune environmental features of previously defined DLBCL subtypes. For example, we previously demonstrated that *PD-L1* gene-altered DLBCLs (~10-15% of all DLBCLs) are enriched for a non-GCB COO and are associated with a T cell-inflamed environment[249]. Therefore, we sought to determine whether DLBCLs harboring *PD-L1* gene alterations would be enriched in the ABC hot cluster. Copy number gains/losses, deletions, and amplifications in the *PD-L1* locus were identified through analysis of paired whole exome sequencing (WES, UCMC and BCCA) or comparative genomic hybridization data (NCI). The analysis was restricted to *PD-L1* amplified DLBCLs to confidently identify DLBCLs that harbor alterations in this locus. *PD-L1* gene-amplified DLBCLs comprised 4.7% of the total population and were indeed enriched among ABC hot DLBCLs, verifying our previous results. However, given the relatively low incidence of *PD-L1* gene alterations, this result did not meet statistical significance **(Figure 16 A,16B)**.

Double hit signature-positive (DHIT-sig^+) lymphomas are a recently described DLBCL subset that shares significant transcriptional overlap with classical double hit lymphoma (high-grade B cell lymphoma with *MYC* and *BCL2* gene rearrangements), but lack *MYC*/*BCL2* translocations[271]. Like canonical double hit lymphomas, DHIT-sig^+ DLBCLs are highly skewed toward a GCB COO and are characterized by a paucity of infiltrating immune cells. When the

DHIT-sig was applied to our GSVA-defined DLBCL clusters, DHIT-sig^{+} DLBCLs were significantly enriched in the GCB cold cluster **(Figure 16C, 16D)**. Another subset of DLBCLs share features of primary mediastinal B cell lymphoma (PMBL) but lack mediastinal involvement (nm-PMBL-sig^{+})[272]. While the genetics of this subset have been described, little is known about the immune environment. We found that nm-PMBL-sig^{+} DLBCLs typically fell into the GCB hot cluster and may represent a distinct subset of DLBCLs that are sensitive to immunotherapy (**Figure 16E, 16F**).

Figure 16. DLBCL subsets associated with different immune-related clusters. A, B. PCA plot

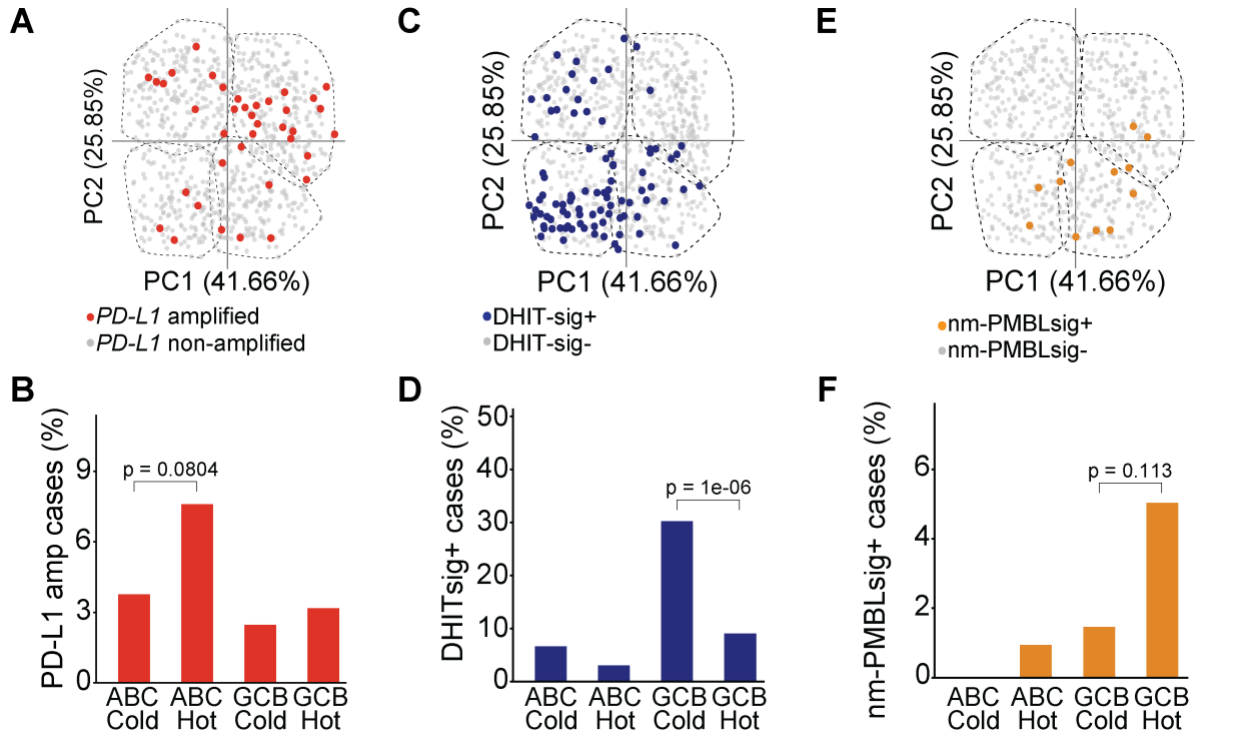

(A) and bar plot **(B)** showing frequency of *PD-L1* gene amplified DLBCLs are enriched in the ABC hot cluster. **C,D.** PCA plot **(C)** and bar plot **(D)** showing enrichment of DHIT-sig+ DLBCLs in the GCB cold cluster. **E,F.** PCA plot **(E)** and bar plot **(F)** showing overrepresentation of PMBLsig+ DLBCLs in the GCB hot cluster . Chi squared test, unadjusted p-values reported.

3.2.10. Association of immune-related clusters with previously defined DLBCL consensus clusters.

Monti et al. clustered DLBCLs into three transcriptionally defined clusters termed host response (HR), BCR/proliferation, and Oxidative phosphorylation (OxPhos). This analysis identified that ~33% of DLBCLs were characterized by upregulation of genes related to an anti-tumor immune response. Moreover, these host response (HR) DLBCLs showed increased infiltration of $CD3^+$ T cells and (gamma-inducible lysosomal thiol reductase) $GILT^+$ DCs. Therefore, we sought to determine whether HR, BCR, or Oxphos DLBCLs were enriched in our GSVA-based immune-related clusters. Compared to ABC and GCB hot DLBCLs, ABC cold and GCB cold DLBCLs had higher expression scores for genes in the OxPhos gene sets **(Figure 17A)**. Conversely, HR signature genes were highly expressed in ABC and GCB hot DLBCLs **(Figure 17B)**. Finally, ABC cold and GCB cold DLBCLs showed increased expression of genes related to BCR signaling and proliferation **(Figure 17C).** Overall, this analysis suggests that GSVA-based inflamed clusters may share overlap with HR-DLBCLs, indicating these two analyses may be identifying similar features of DLBCL biology. However, both ABC and GCB cold clusters displayed increased expression of genes associated with oxidative phosphorylation and BCR signaling, suggesting both signaling mechanisms maybe active in cold DLBCLs. Finally, the association of HR DLBCLs with immunotherapy response remains unknown.

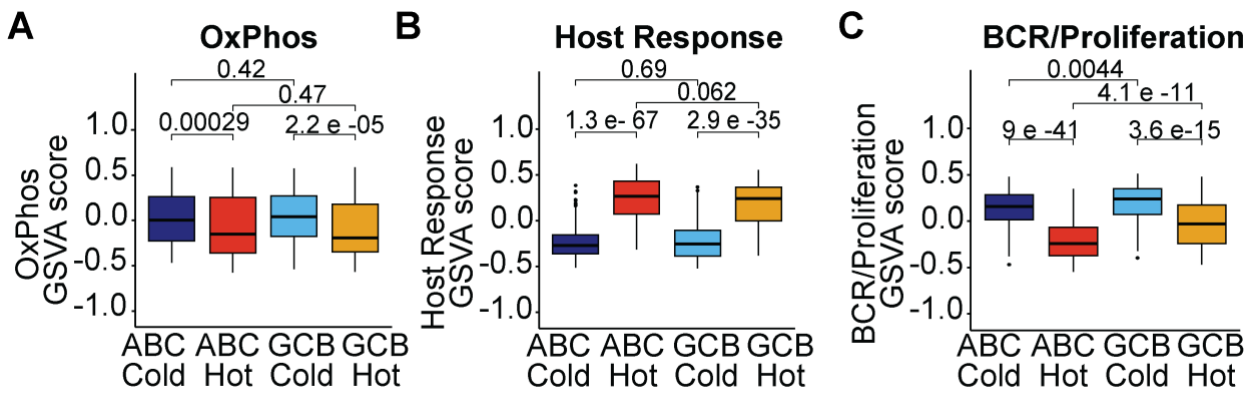

Figure 17. Association of immune-related clusters with previously defined DLBCL consensus clusters. A. Box plot showing GSVA expression scores for each immune-related cluster for genes that are highly expressed in OxPhos DLBCLs. **B.** Box plot showing GSVA expression scores for each immune-related cluster for genes that are highly expressed in host response DLBCLs. **C.** Box plot showing GSVA expression scores for each immune-related cluster for genes that are highly expressed in BCR/proliferation DLBCLs.

3.2.11. Association of immune-related clusters with previously defined lymphoma microenvironments (LME).

Kotlov et al. recently classified DLBCLs based on the expression of functional gene expression signatures (F^{GES}) reflecting the relative abundance and function of particular cellular constituents[246]. This analysis also identified four DLBCL clusters, termed "lymphoma microenvironments" (LMEs): 1) mesenchymal (LME-ME), characterized by high abundance of stromal and extracellular matrix components; 2) germinal center-like (LME-GC), characterized by presence of cells found in germinal centers; 3) inflammatory (LME-IN), harboring an inflammatory milieu; 4) depleted (LME-DE), characterized by a lack of immune cell infiltration. Therefore, we sought to determine the concordance between our GSVA-defined immune clusters and the defined LME categories. We found that the ABC hot cluster overlapped significantly with an inflamed microenvironment (LME-IN), which is characterized by a robust immune cell infiltrate **(Figure 18A)**. ABC hot DLBCLs had high F^{GES} scores for several gene sets that reflect

the presence and activation of T cell subsets including tumor infiltrating lymphocytes (TILs), Tregs, T-cell traffic, NK cells, and JAK-STAT signaling **(Figure 18B)**. LME-DE, which has low expression scores for all immune-related gene sets, was divided between GCB cold and ABC cold clusters. The remaining GSVA clusters, however, did not overlap significantly with other LMEs **(Figure 18A)**. LME-ME and LME-GC gene sets were both represented in the GCB hot cluster, and GCB hot DLBCLs had high F^{GES} scores for extracellular matrix components and endothelial cells, in addition to higher expression scores for gene sets related to TILs and other T cell subsets **(Figure 18B)**. GCB and ABC cold DLBCLs were characterized by low expression of T cell and myeloid cell-related gene sets and, conversely, higher expression of B cell signaling related gene sets compared to hot DLBCLs **(Figure 18B)**. These data suggest that these two analyses capture different aspects of the lymphoma microenvironment, and the contribution of different LMEs to immunotherapy response remains unknown.

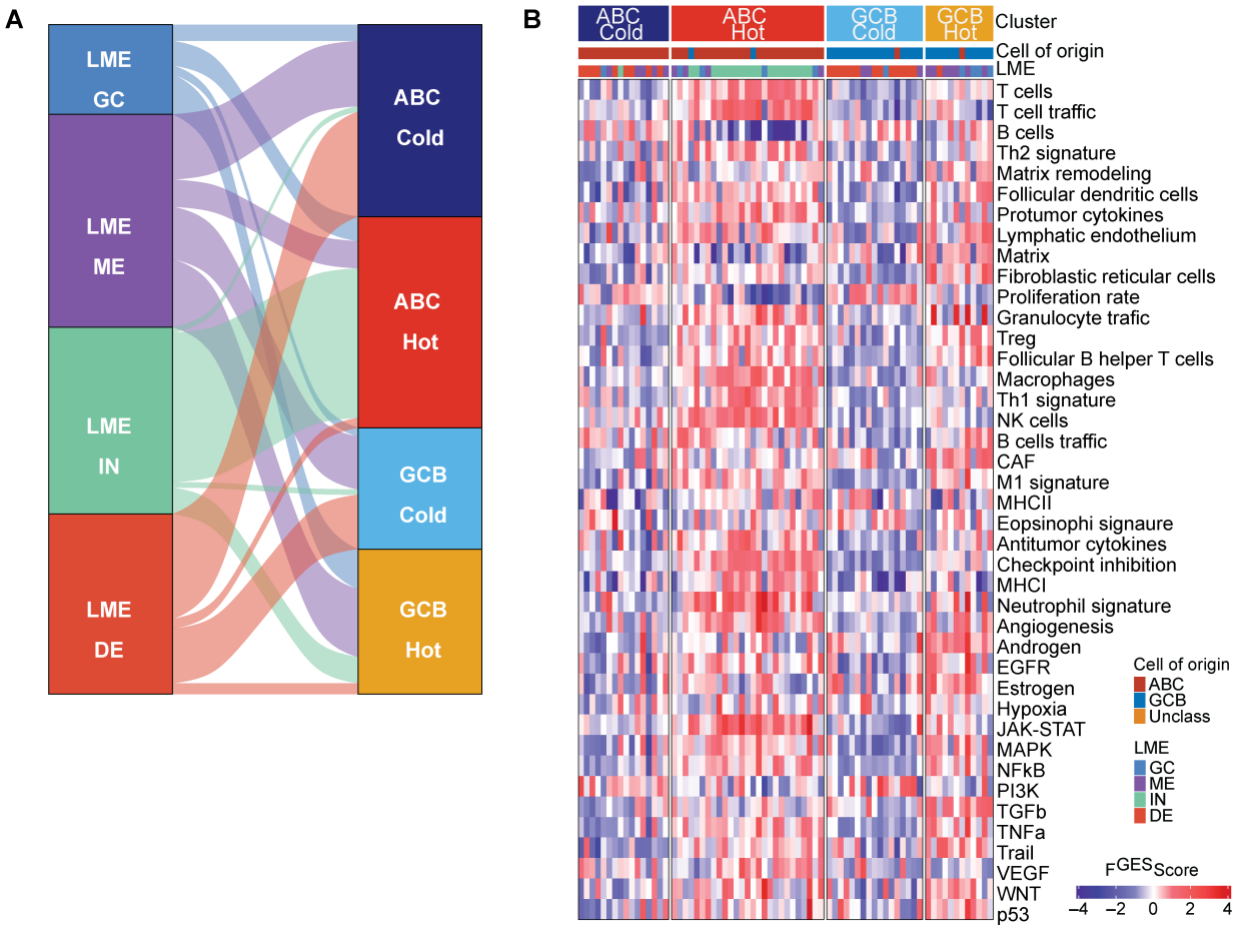

Figure 18. Overlap of GSVA-based immune clusters and lymphoma microenvironmental clusters (LME). A. Alluvial plot demonstrating overlap between LME clusters and GSVA-based immune-related clusters. **B.** Heatmap showing F^{GES} scores for DLBCLs in each immune-related cluster.

3.2.12 Similarity of DLBCL immune-related clusters with immune environments of other B cell lymphomas.

We then performed GSVA on a multi-lymphoma microarray dataset that contained gene expression profiling of DLBCL as well as classical Hodgkin lymphoma (cHL), PMBL, Burkitt lymphoma (BL), T cell histiocyte-rich large B cell lymphoma (THRLBCL), and gray zone lymphoma (GZL) **(Figure 19)**[273]. BL was associated with a decreased expression of all immune-

related gene sets, suggesting a lack of immune cells in the environment. This finding is consistent with other reports of a subset of "cold" DLBCLs that is transcriptionally similar to BL and shares significant overlap with DHITsig^{+} DLBCLs, known as molecular high grade (MHG) DLBCL[274]. On the other hand, PMBL, THRLBCL, and cHL, which are known to have robust immune cell infiltration, showed high expression of genes related to the immune environment and activated T cell subsets[275–278]. PMBL and cHL are exquisitely sensitive to CBT, suggesting that "inflamed" DLBCLs may also be similarly sensitive to T cell-based immunotherapy. However, little is known about the cellular mediators of response to CBT in PMBL and cHL. Moreover, the contribution of lymphoma cell-intrinsic alterations in regulating the immune environment in these lymphomas has not been elucidated. Recent genomic analyses have revealed that PMBL and cHL often possess alterations that lead to constitutive JAK/STAT activation, including loss-of-function mutations in *SOCS1*, gain-of-function mutations in *IL4R,* and *PD-L1* copy gains. However, the mechanism by which JAK/STAT activation may orchestrate an inflamed immune environment remains unknown. Taken together, these results support concordance between our transcriptionally defined, immune-related clusters and known immune environmental aspects of previously characterized DLBCL subsets as well as other B cell lymphomas.

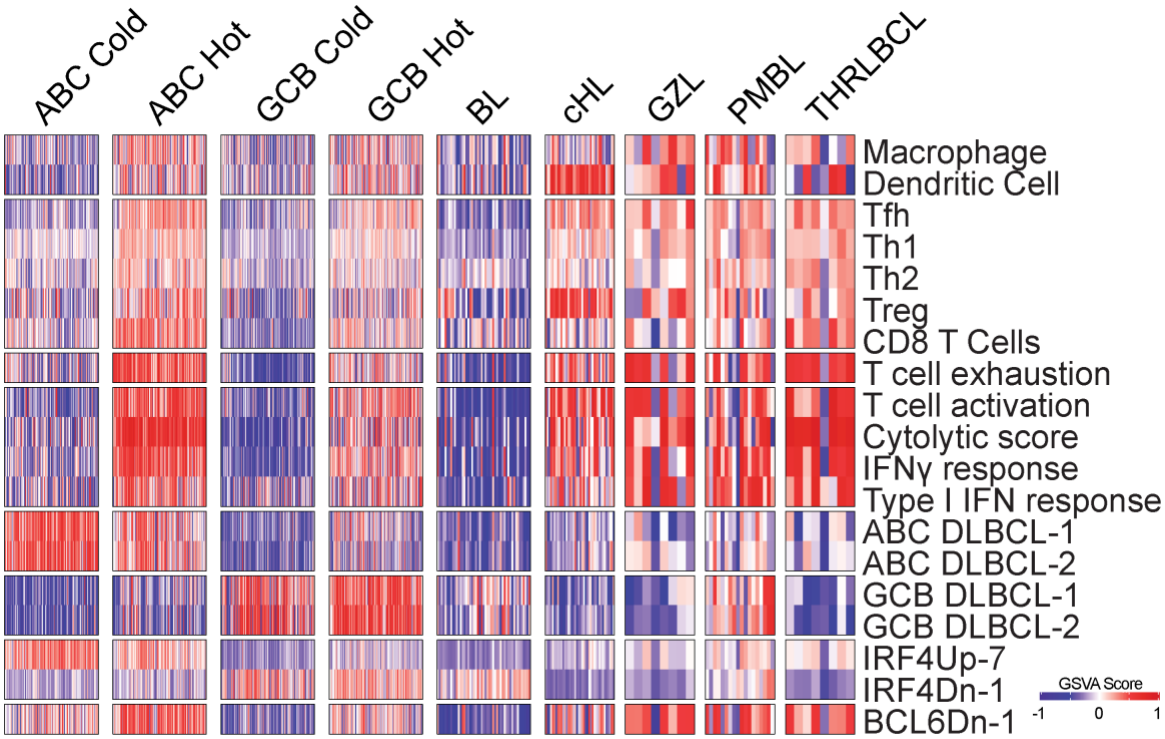

Figure 19. Overlap of GSVA-based immune clusters and lymphoma microenvironmental clusters (LME). Heatmap showing GSVA scores for immune-related gene sets and COO gene sets for DLBCL, Burkitt lymphoma (BL), Hodgkin lymphoma (cHL), gray zone lymphoma (GZL), Primary mediastinal B cell lymphoma (PMBL), and T cell rich/histiocyte rick large B cell lymphoma (THRLBCL).

3.2.13 Genomic features associated with different immune environments.

Emerging evidence indicates that specific oncogenic alterations and associated transcriptional programs can significantly impact the composition of the immune environment and vulnerability to particular immunotherapies[94,99,157,158,162,167]. Furthermore, genetic aberrations also represent novel therapeutic targets that may synergize with immunotherapies. Recently, several landmark studies have used an integrative approach to define new DLBCL clusters based on co-occurring genetic alterations[55,56,263]. One such analysis classified DLBCLs into seven subtypes based on distinct genetic features using an algorithm called LymphGen[55]; however, the impact of

the recurring genetic alterations associated with these DLBCL clusters on the local immune environment is not known. Therefore, we sought to determine whether these genetic clusters were recurrently associated with unique GSVA-predicted immune environments.

LymphGen cluster annotations were available for all DLBCLs in our discovery (NCI, UCMC) and validation datasets (BCCA). To power our analyses to identify meaningful differences given the striking genetic heterogeneity in DLBCL, we combined the validation and discovery cohorts. Broadly speaking, there was only modest overlap between GSVA-based immune environmental classification and LymphGen classification **(Figure 20A)**, with a few notable exceptions. For example, DLBCLs characterized by activating mutations in the NOTCH1 pathway (N1 subtype), which are predominantly ABC COO, were significantly enriched in the ABC hot cluster, while DLBCLs with *TP53* loss and aneuploidy (A53 subtype), also commonly of an ABC COO, were almost exclusively found in the ABC cold cluster. Lastly, DLBCLs with gain-of-function (GOF) mutations in *EZH2*, *BCL2* translocations, and *MYC* activation (EZB-MYC^{+}), were enriched in the GCB cold cluster. The other four LymphGen clusters showed little correlation with the GSVA-based immune-related clusters.

LymphGen uses a stringent probability threshold that only classifies ~60% of DLBCLs, and LymphGen unclassified DLBCLs were equally distributed among all four immune-related clusters **(Figure 20A)**. We hypothesized that individual mutations or CNAs might be recurrently associated with specific immune environments. Therefore, to the role of specific lymphoma cell-intrinsic alterations in orchestrating the DLBCL immune environment, we compared the genetic landscapes of DLBCLs in our four immune clusters. The analysis was restricted to essential driver genes that are mutated in >10% of DLBCLs to identify the genes most relevant to DLBCL biology.

Comparative analysis of the mutational profiles of hot DLBCLs to cold DLBCLs found that several alterations are associated with cold environments including, *BCL2*, *MYD88,* and *TP53*. *TP53* mutations are strongly enriched in A53 subtype DLBCLs, which are strongly associated with cold environments. Moreover, *TP53* mutations have been shown to be inversely correlated with response to bispecific antibodies and CAR T-cell therapy. Conversely, inflamed lymphomas are characterized by mutations in *SOCS1*, *TNFRSF14,* and *NFKBIA* **(Figure 20B)**.

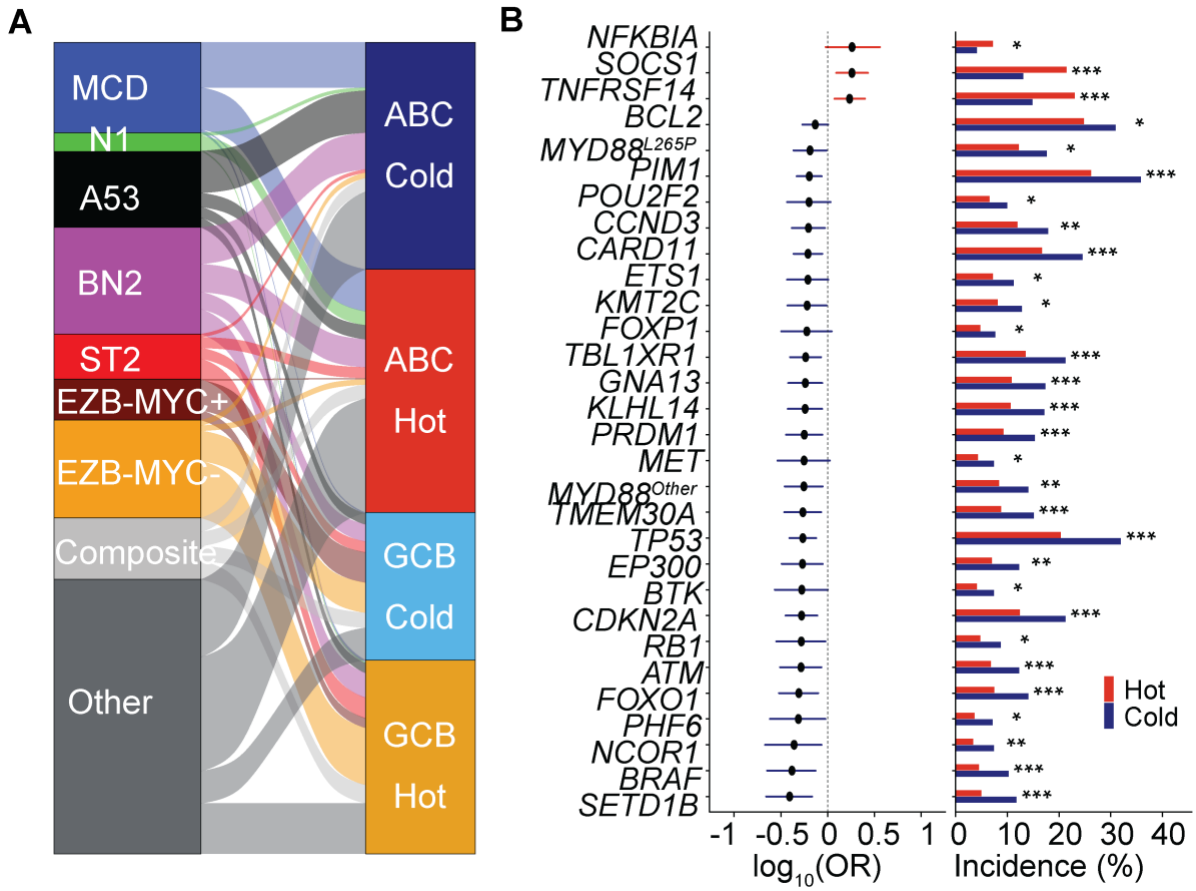

Figure 20. Genomic features associated with immune environments. A. Alluvial plot showing overlap between LymphGen clusters and immune clusters. **B.** Forest plot showing alterations recurrently enriched in hot (PC1 >0) or cold (PC1 <0) DLBCLs. Fisher's exact test, BH-adjusted p values reported ((* adj. $p < 0.1$, ** adj. $p < 0.05$, *** adj. $p < 0.01$). OR- odds ratio

ABC and GCB DLBCLs rely on distinct oncogenic pathways, leading to distinct genetic lesions that are recurrently associated with each COO. In order to control for this variance, we restricted the analysis to compare oncogenic alterations in ABC hot versus ABC cold DLBCLs (or GCB hot versus GCB cold DLBCLs) to identify genes that may be driving different immune environments. Genes such as *MYD88, TBL1XR1,* and *TMEM30A,* which have been shown to be potent drivers of chronic BCR signaling, are strongly associated with ABC cold DLBCLs. Alterations in *CD274* (PD-L1) are significantly enriched in ABC hot DLBCLs, concordant with our previous work **(Figure 21A)**. Mutations in *RB1*, *FOXO1*, and *GNA13* are enriched in the GCB cold cluster, while *TNFAIP3* and *SOCS1* are significantly associated with GCB hot DLBCLs **(Fig 21B)**.

Finally, in order to identify genetic alterations that may converge on shared oncogenic signaling pathways, we grouped mutations and CNAs into functional pathways. Genetic alterations in BCR-dependent NFκB signaling pathway[55] – a pathway that is critical for survival of ABC DLBCLs and leads to constitutive NFκB activity - were significantly enriched in ABC cold DLBCLs compared to ABC hot DLBCLs **(Figure 21C)**. Interestingly, MCD DLBCLs – which are characterized by mutations that lead to chronic NFκB signaling – have been demonstrated to have low expression scores for gene sets related to TFH and CD4T cells compared to all other DLBCLs. However, the contribution of individual mutations in BCR-dependent NFκB signaling, including *MYD88* and *CD79B* mutations, in orchestrating a cold environment has not been elucidated. ABC and GCB cold DLBCLs were also significantly enriched for lesions in genes involved in p53 signaling and cell cycle compared to ABC and GCB hot DLBCLs, respectively, suggesting loss of p53 or dysregulation of cell cycle pathway may lead to decreased immune cell infiltration **(Figure 21D).**

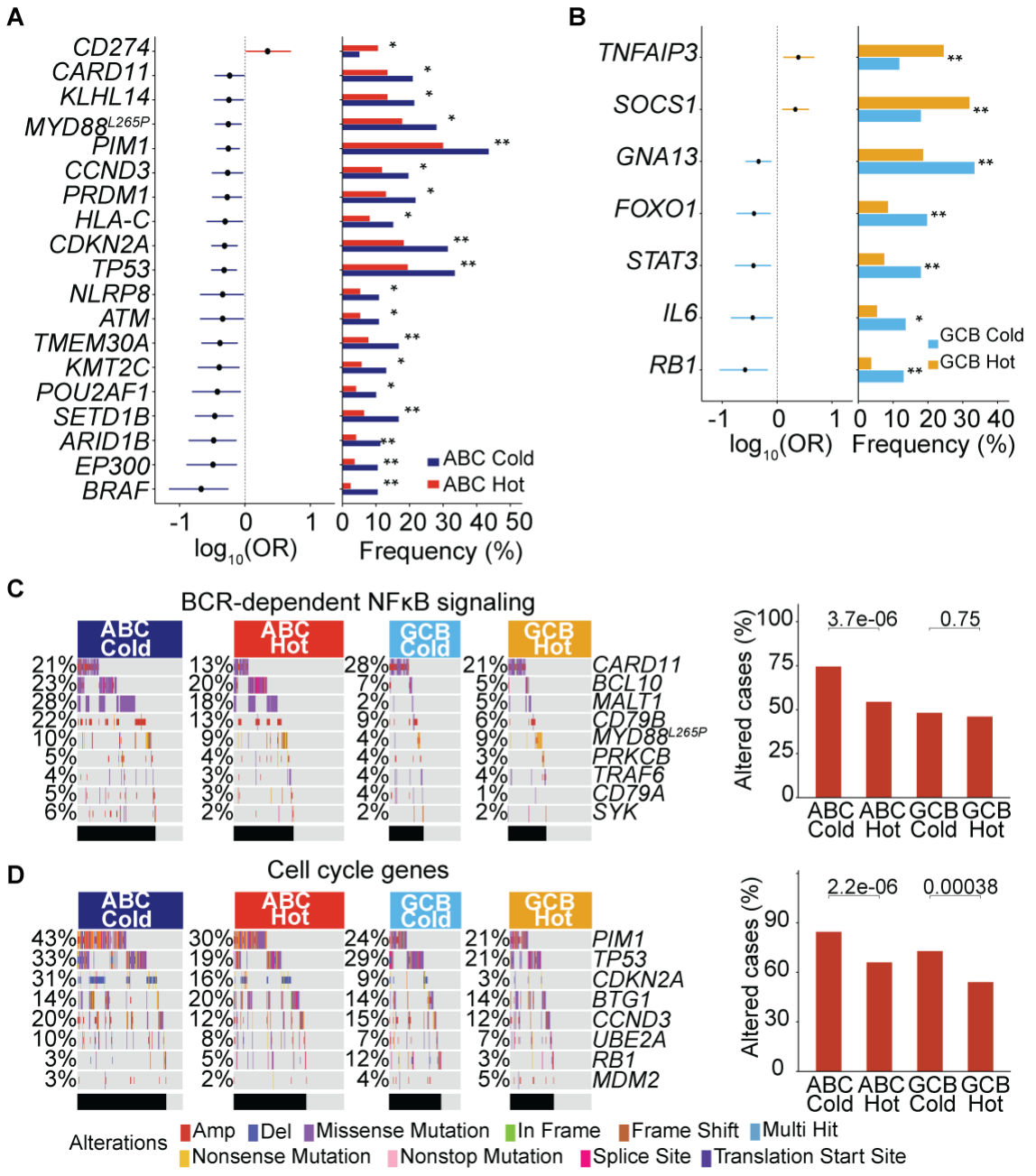

Figure 21. Genomic features associated with immune environments. A. Forest plot showing alterations recurrently associated with ABC hot or ABC cold DLBCLs. **B.** Forest plot showing alterations recurrently associated with GCB hot or GCB cold DLBCLs. Fisher's exact test, BH-adjusted p values reported ((* adj. $p < 0.1$, ** adj. $p < 0.05$, *** adj. $p < 0.01$). **C.** Oncoprint (left) and barplot (right) showing frequency of DLBCLs in each immune-related cluster with at least one alteration in BCR-dependent NFκB signaling pathway genes. **D.** Oncoprint (left) and barplot (right) showing frequency of DLBCLs in each immune-related cluster with at least one alteration in cell cycle related genes. Statistical testing by Fisher's exact test for ABC hot vs ABC cold and GCB hot vs GCB cold, unadjusted p-values reported. OR- odds ratio.

In support of this notion, gene set enrichment analysis (GSEA) demonstrated that ABC cold DLBCLs were significantly enriched for *MYC* target genes **(Figure 22A, 22B)**. Compared to GCB hot DLBCLs, GCB cold DLBCLs were also characterized by upregulation of MYC activation gene sets, likely due to EZB-MYC^{+} and DHITsig^{+} DLBCLs being enriched in the GCB cold cluster **(Figure 22B).** Consistent with the enrichment of mutations in p53 and cell cycle genes in ABC and GCB cold DLBCLs, GSEA also showed upregulation of G2M target gene sets in ABC and GCB cold DLBCL clusters, suggesting dysregulated cell cycling might be playing a role in orchestrating the immune environment in DLBCL **(Figure 22C)**.

Taken together, these data show shows that several genetic lesions and oncogenic pathways are recurrently associated with our immune-related clusters, suggesting that lymphoma cell-intrinsic alterations may impact the immune environment in DLBCL.

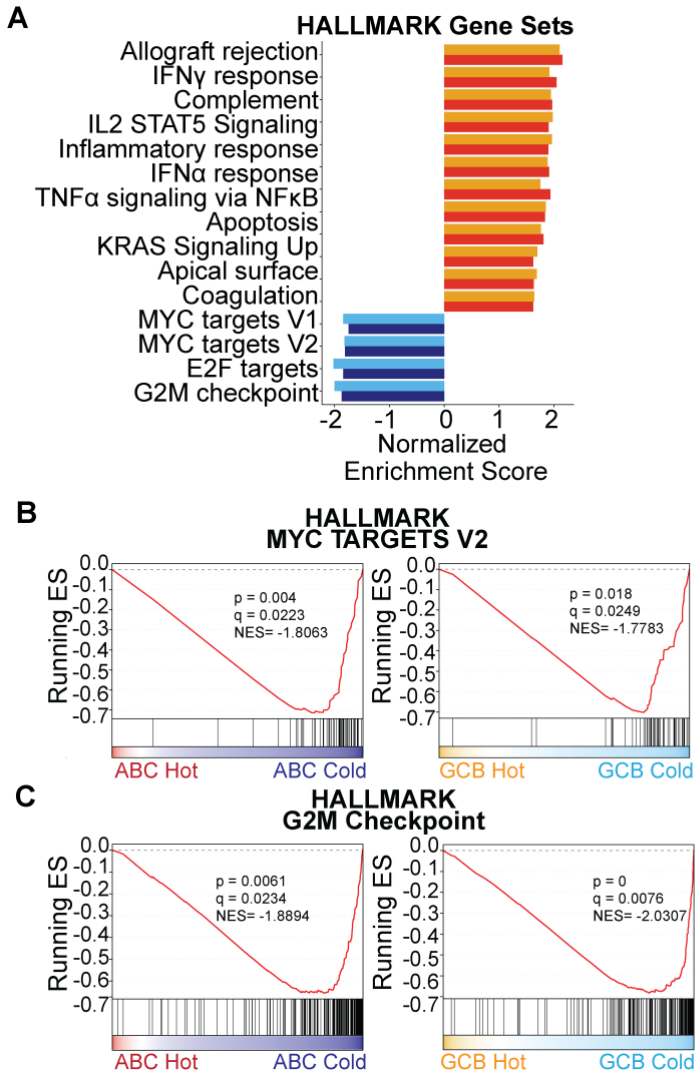

Figure 22. Genomic features associated with immune environments. A. Bar plot of gene set enrichment analysis (GSEA) showing gene sets significantly enriched in each immune-related cluster. **B.** GSEA plots showing upregulation of *MYC* target gene sets in ABC cold and GCB cold DLBCLs. **C.** GSEA plots showing upregulation of G2M checkpoint related genes in ABC cold DLBCLs. ES- enrichment score; NES – normalized enrichment score.

3.2.14 MYC activation is associated with cold immune environments.

MYC expression has been associated with resistance to bsAb therapy in DLBCL, suggesting that MYC may play a role in regulating the immune environment within tumors[245]. However, the mechanism through which MYC may do so remains unclear. We devised a MYC signature score using genes from a previously published target gene signature (MycUp-4) to assign DLBCLs to a "*MYC*-high," "*MYC*-low", or "*MYC*-intermediate" group. IHC for MYC expression was performed on DLBCLs (n = 107) with paired transcriptomic data. DLBCLs with high MYC protein expression were also consistently classified as *MYC*-high transcriptionally. Conversely, DLBCLs that were identified as *MYC*-low were characterized by low MYC protein expression, showing a transcriptional *MYC* signature is identifying MYC-driven DLBCLs **(Figure 23A)**.

ABC cold and GCB cold DLBCLs showed significantly higher expression of the *MYC* activation signature compared to ABC hot or GCB hot DLBCLs (**Figure 23B)** and *MYC*-high DLBCs equally distributed between ABC cold (40%) and GCB cold (40%) clusters **(Figure 23C)**. Moreover, *MYC*-high DLBCLs in both the ABC and GCB clusters contained significantly lower inferred proportions of several immune cell subsets **(Figure 23D),** including CD8+ T cells **(Figure 23E)** and CD4+ T cells **(Figure 23F),** suggesting a negative correlation between *MYC* activation and the presence of an inflamed environment. DLBCLs in the *MYC*-high group were characterized by lower $CD8^+$ T cell : DLBCL compared to *MYC*-low DLBCLs **(Figure 23G).** CD8+ T cell : DLBCL ratios were also negatively correlated with a sample wise *MYC* GSVA score **(Figure 23H).** CD4+ T cell: DLBCL ratios were similarly negatively associated with the *MYC*-high cluster **(Figure 23I)** and a sample wise *MYC* GSVA score **(Figure 23J)**.

The molecular mechanisms underlying the activation of MYC signaling differ in ABC and GCB DLBCLs. For example, *MYC* translocations to the immunoglobulin heavy chain (*IGH*) locus

are commonly found in GBC DLBCLs, while ABC DLBCLs may activate *MYC* downstream of other oncogenic events[55,271,279–283]. Interestingly, ABC cold DLBCLs had a significantly higher MYCUp-4 score compared to GCB cold DLBCLs (**Figure 23B)**, suggesting that ABC DLBCLs may have a distinct mechanism of driving *MYC* activation. Comparative analysis of the genomes of GCB *MYC*-high and *MYC*-low groups showed *MYC*-high GCB DLBCLs were enriched for alterations in *MYC* and *DDDX3X* consistent with published reports of the oncogenic profiles of DHIT-sig+ and EZB-MYC+ DLBCLs which share considerable overlap with our GSVA defined GCB *MYC*-high DLBCLs **(Figure 23K)**[55,271]. ABC *MYC*-high DLBCLs showed recurrent alterations in *MYD88L265P, CD79B, and PRDM1* compared to ABC *MYC*-low DLBCLs **(Figure 23L).** Several genes that were enriched in ABC *MYC*-high DLBCLs fell into the "BCR-dependent NFκB" pathway, suggesting that activation of chronic NFκB signaling may drive *MYC* activity in ABC DLBCLs and lead to cold environments.

Further research is needed to understand whether distinct mechanisms of MYC-mediated immune suppression are present in activated B-cell-like (ABC) or germinal center B-cell-like (GCB) DLBCL. It is possible that MYC may have different effects on the immune environment depending on the molecular subtype of DLBCL, as these subtypes have distinct genetic and epigenetic profiles that may influence immune regulation. This knowledge may ultimately lead to the development of novel therapies that can target MYC-mediated immune suppression and improve the efficacy of immunotherapies in patients with cancer.

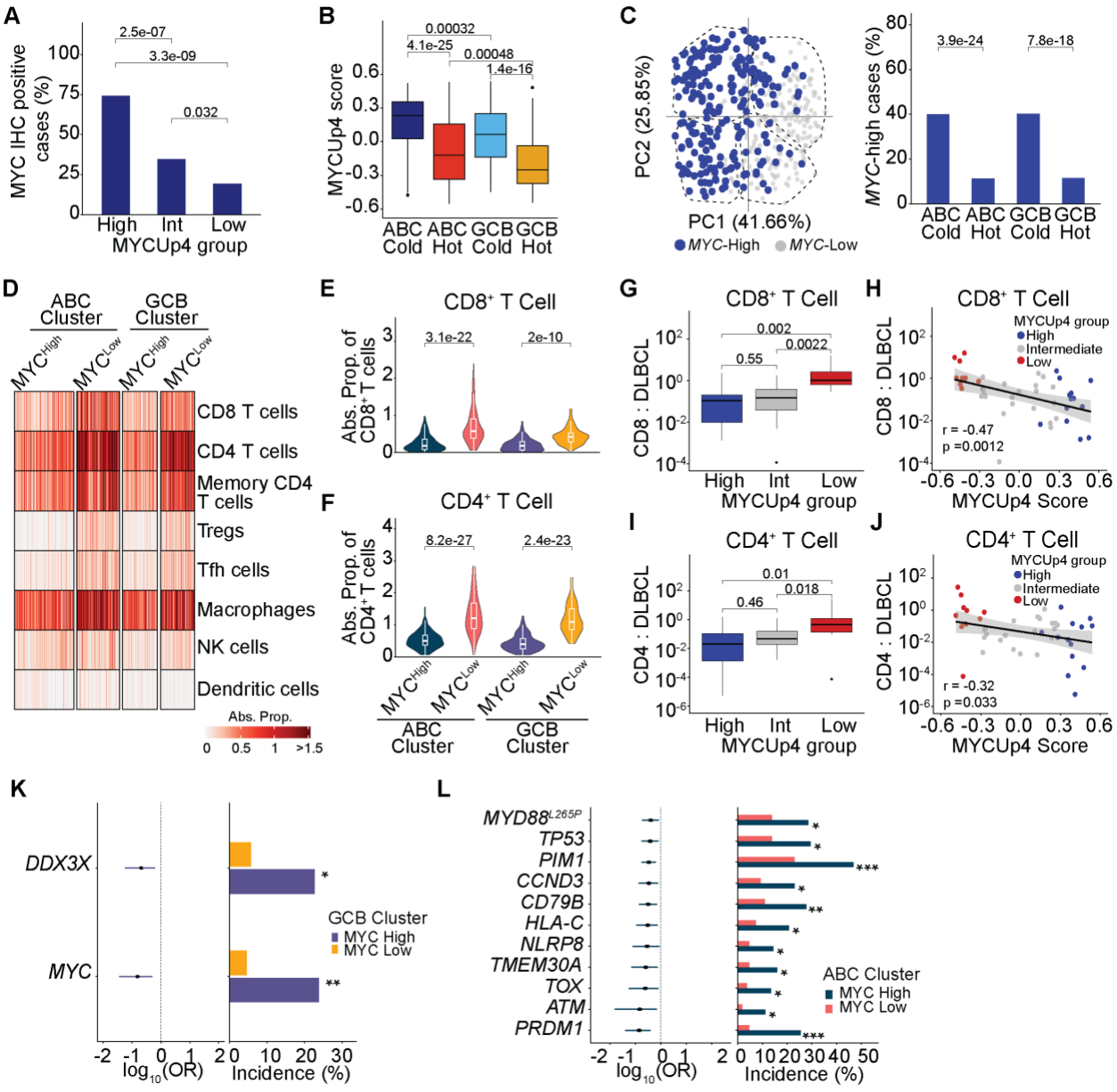

Figure 23. *MYC* activity is associated with "cold" DLBCL environments. A. Barplot showing frequency of MYC+ DLBCLs in transcriptionally defined *MYC*-high, MYC-intermediate, *MYC*-low groups. **B.** Box plot showing MYCUp4 score in immune clusters. **C.** PCA plot (left) and barplot (right) showing frequency of *MYC*-high DLBCLs in immune clusters. **D.** Heatmap showing absolute inferred proportions of immune cell subsets in *MYC*-high and *MYC*-low DLBCLs from ABC and GCB clusters. **E, F.** Violin plots showing absolute inferred proportions of CD8 **(E)** and CD4 **(F)** T cells in *MYC*-high and *MYC*-low DLBCLs in ABC and GCB clusters. **G.** Boxplot showing CD8+T cell : DLBCL ratio in *MYC*-high, *MYC*-int, and *MYC*-low groups. **H.** Scatterplot showing correlation of MYCUp4 score and CD8+ T cell : DLBCL ratio. Colored by MYCUp4 group classification (*MYC*-high – blue, *MYC*-int – gray *MYC*-low – red). **I.** Boxplot

Figure 23 continued. showing CD4+T cell : DLBCL ratio in *MYC*-high, *MYC*-int, and *MYC*-low groups. **J.** Scatterplot showing correlation of MYCUp4 score and CD4+ T cell : DLBCL ratio. Colored by MYCUp4 group classification (*MYC*-high – blue, *MYC*-int – gray *MYC*-low – red). **K.** Forest plot showing alterations enriched in ABC *MYC*-high and *MYC*- low DLBCLs. **L.** Forest plot showing recurrent alterations in GCB *MYC*- high and GCB *MYC*-low DLBCLs. Fisher's exact test with BH-adjusted p-values for categorical variables. Kruskal-Wallis test followed by post-hoc Dunn's test with adjusted p-values for continuous variables.

3.2.15 *SOCS1* mutations are associated with immune inflamed environments in DLBCL.

SOCS1 is a potent negative regulator of JAK/STAT signaling downstream of a critical T-cell effector cytokine, IFNγ[108,126,156,267,284–286]. Enrichment of *SOCS1* mutations in GCB hot DLBCLs was particularly interesting, as LOF *SOCS1* mutations are highly prevalent in CBT-responsive lymphomas such as primary mediastinal B cell lymphoma (PMBL) and classical Hodgkin lymphoma (cHL)[248,272,287–289]. One reason for the sensitivity of cHL to anti-PD1 therapy is due to a robust T cell infiltrate[276,290,291]. Moreover, GSVA showed that both cHL and PMBL scored highly for immune-related gene sets (**Figure 19**). Therefore, we hypothesized that *SOCS1* mutant DLBCLs might represent a subset of inflamed lymphomas that are sensitive to T cell-mediated immunotherapies (CAR T-cell therapy, bsAb therapy, or CBT).

SOCS1 mutations occurred in 15.8% of DLBCLs in our cohort, and were significantly associated with GCB DLBCLs. Intriguingly, the incidence of *SOCS1* mutations was significantly higher in the GCB hot cluster compared to other clusters, representing 30% of all lymphomas classified as GCB hot **(Figure 24A)**. *SOCS1* mutations were often missense or nonsense, and occurred with similar frequencies across the length of the *SOCS1* protein**,** consistent with the role of SOCS1 as a tumor suppressor gene. Immune cell deconvolution revealed an increased inferred fraction of several immune cell subsets, including CD8 T cells and CD4 T cells, in *SOCS1* mutant

compared to *SOCS1* wt GCB DLBCLS **(Figure 24B)**. Finally, GSEA demonstrated increased expression of IFNγ - and IFNα- associated genes in *SOCS1* mutant DLBCLs relative to *SOCS1* wt DLBCLs **(Figure 24 C, 24D)**. Together, these data indicate that *SOCS1* loss of function mutations are associated with inflamed immune environments. Therefore, *SOCS1* mutant DLBCLs may represent a novel subset that is sensitive to CAR T-cell, bsAb, or CBT therapies.

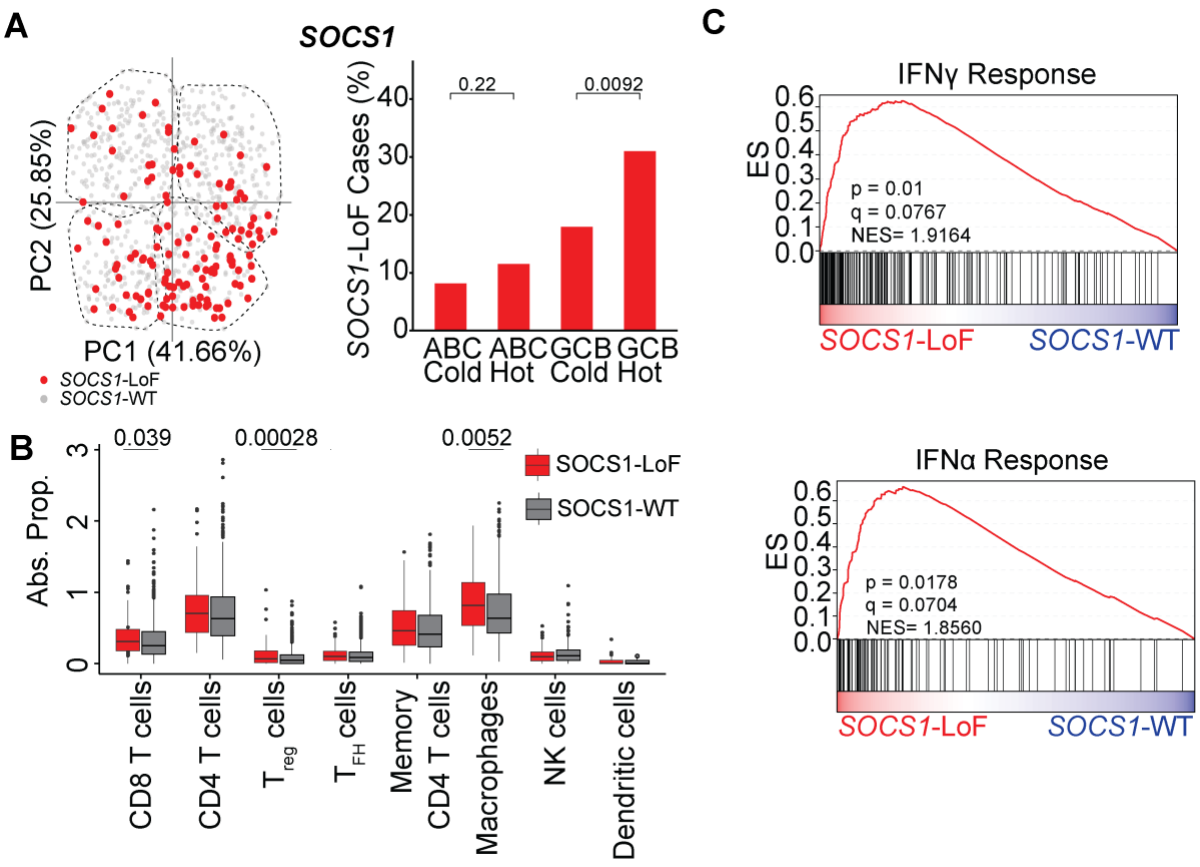

Figure 24. A. *SOCS1* mutations are associated with immune inflamed environments in DLBCL. PCA plot (left) and bar plot (right) showing the frequency of *SOCS1* loss of function (LoF) alterations in immune clusters. **B.** Immune cell deconvolution (CibersortX) showing absolute inferred proportions of immune cell subsets in *SOCS1*-LoF DLBCLs compared to *SOCS1*-WT DLBCLs. **C.** GSEA plots showing upregulation of Interferon gamma **(top)** related genes and Interferon alpha response genes **(bottom)** in *SOCS1*-LoF DLBCLs compared to *SOCS1*-WT. Fisher's exact test with BH-adjusted p-values for categorical variables. Kruskal-Wallis test followed by post-hoc Dunn's test with adjusted p-values for continuous variables.

3.2.16 *Socs1* deficiency enhances sensitivity to IFNγ.

As *SOCS1* mutant DLBCLs are associated with inflamed environments, we hypothesized that *SOCS1* mutations might enhance the anti-tumor effects of IFNγ, thus rendering lymphoma cells more sensitive to T cell-mediated immunotherapies. In order to test this hypothesis, we subjected $CD19^+$ B cells isolated from the spleens of *Socs1*- deficient ($Cd19^{Cre/+}$ $Socs1^{fl/fl}$) or *Socs1*-sufficient mice ($Cd19^{Cre/wt}$) to IFNγ stimulation. IFNγ response genes such as MHC II, and PD-L1 were significantly more inducible in a dose-dependent manner in $CD19^+$ B cells from mice lacking *Socs1* compared to wildtype controls **(Figure 25A)**. These data suggest that genetic ablation of *Socs1* leads to increased IFNγ sensitivity in non-malignant B cells.

In order to determine the extent to which *Socs1* deficiency renders cancer cells more sensitive to IFNγ, we generated a *Socs1*-deficient murine B cell lymphoma cell line (A20) and a melanoma cell line (B16). Relative to $A20^{WT}$, $A20^{Socs1-/-}$ cells were characterized by increased pStat1 levels upon IFNγ stimulation, suggesting activation of JAK/STAT signaling (**Fig 25B).** However, MHC-I, MHC-II, and PD-L1 were not more inducible upon IFNγ stimulation in $A20^{Socs1-/-}$ cells compared to $A20^{WT}$ (**Figure 25C)**. Moreover, relative to wildtype cells, $A20^{Socs1-/-}$ lymphoma cells did not exhibit reduction in proliferation upon exposure to IFNγ **(Figure 25D)**.

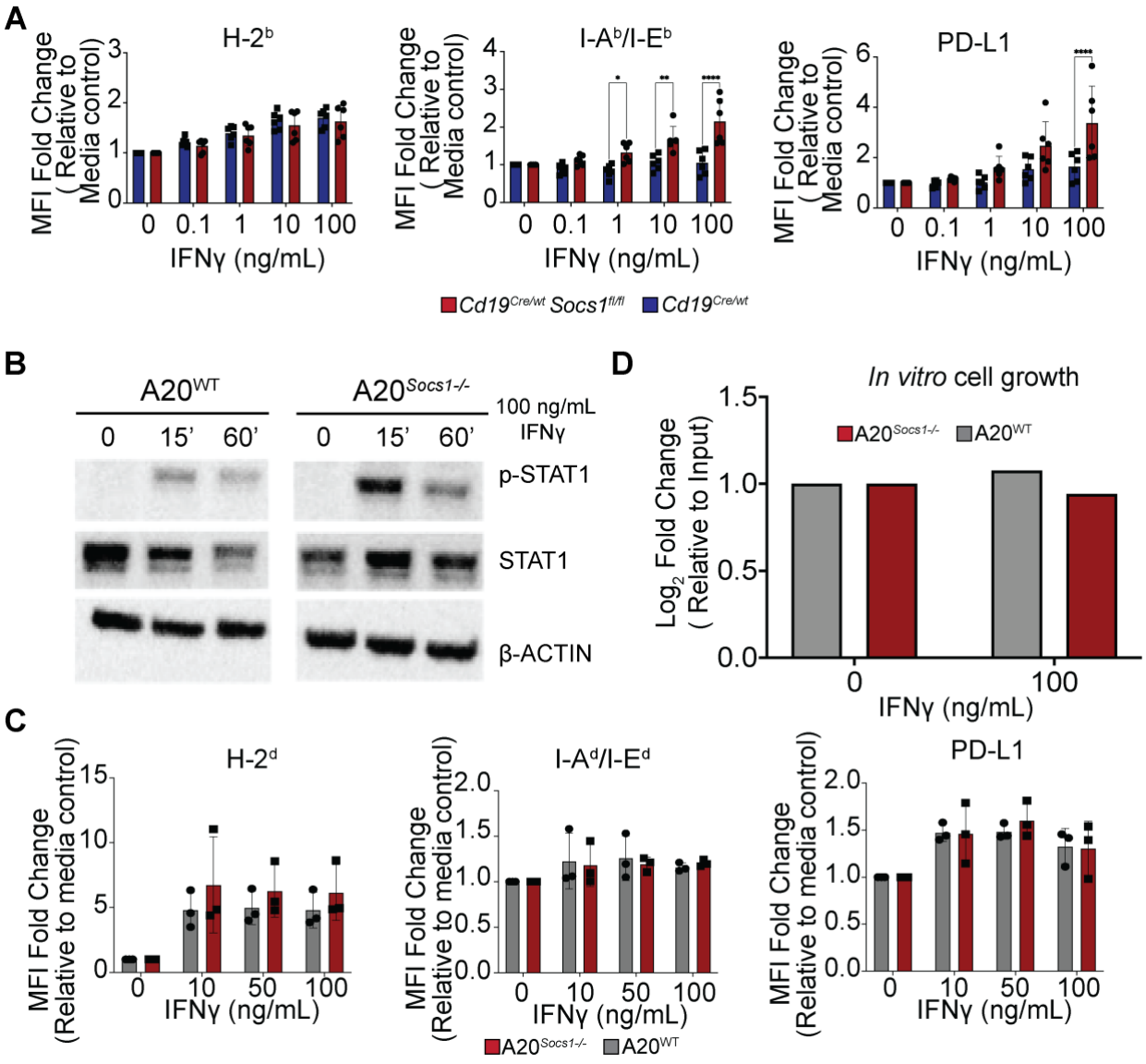

Figure 25. *Socs1* deficiency enhances sensitivity to IFNγ. A. Mean fluorescence intensity (MFI) of MHC-I, MHC-II, and PD-L1 expression in B cells isolated from the spleens of *Socs1*-sufficient (blue) and *Socs1*-deficient (red) mice and stimulated with IFNγ *in vitro* for 48 hours. **B.** Western blot showing pSTAT1, STAT1, and B-ACTIN expression in $A20^{WT}$ and $A20^{Socs1-/-}$lymphoma cells upon IFNγ stimulation (100ng/mL). 1 x 10^6 cells were stimulated for 15 mins or 60mins and whole cell lysates were blotted for pSTAT1, STAT1, and B-ACTIN. **C.** MFI of MHC-I, MHC-II, and PD-L1 expression in $A20^{WT}$ and $A20^{Socs1-/-}$ cells stimulated with IFNγ *in vitro* for 48 hours. **D.** *In vitro* cell growth of $A20^{WT}$ and $A20^{Socs1-/-}$ cells with media only or 100ng/mL IFNγ exposure for 72 hours. Cell count is normalized to number of input cells (5 x 10^4 cells).

While Socs1-deficient A20 lymphoma cells were not more sensitive to the effects of IFNγ *in vitro*, A20$^{Socs1-/-}$ tumors may be more sensitive to T cell-mediated cytolysis *in vivo*. A20^{WT} and A20$^{Socs1-/-}$ tumors grew similarly in NSG mice, which lack an adaptive immune system **(Figure 26A)**. In syngeneic Balb/c mice, however, A20$^{Socs1-/-}$ tumors demonstrated highly variable growth. Some A20$^{Socs1-/-}$ tumors grew rapidly while others regressed spontaneously **(Figure 26B)**. Overall, A20$^{Socs1-/-}$ tumors exhibited a trend toward higher rates of spontaneous regression compared to A20^{WT} tumors **(Figure 26C)**. These data suggest that A20 lymphoma cells may have other mechanisms that compensate for *Socs1* deficiency.

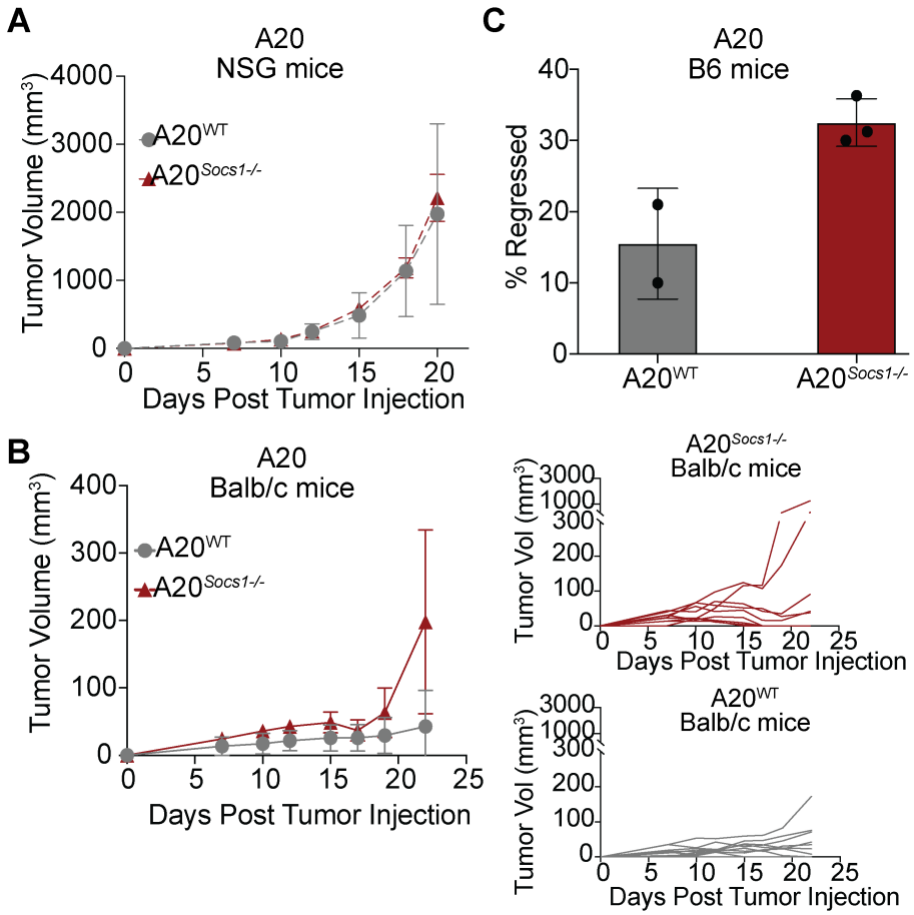

Figure 26. *Socs1* deficiency does not enhance T cell-mediated control of A20 lymphoma. A. Average tumor volume (mm^3) of A20^{WT} (gray) or A20$^{Socs1-/-}$ tumors in immunodeficient NSG mice (n=5 mice per group). Mice were inoculated subcutaneously in the left flank. **B.** Average tumor

Figure 26 continued. volume (mm^3) of $A20^{WT}$ (gray) or $A20^{Socs1-/-}$ tumors in Balb/c mice (n =11 mice per group) for two independent biological replicates. Individual tumor growth plots for $A20^{Socs1-/-}$ (top panel), and $A20^{WT}$ (bottom). **C.** Rate of spontaneous regression of $A20^{WT}$ or $A20^{Socs1-/-}$ tumors across 3 independent experiments. Regression was defined as tumors that were palpable (50-100mm^3) and then decreased in volume until no longer palpable.

We sought to test our hypothesis that *Socs1* deficiency leads to increased JAK/STAT activation and sensitivity to IFNγ using a different syngenic mouse model, B16 melanoma. In contrast to A20 lymphoma cells, $B16^{Socs1-/-}$ melanoma cells showed increased expression of pSTAT1 after treatment with IFNγ compared to $B16^{WT}$ cells **(Figure 27A)**. Loss of function of *Socs1* led to a significant, dose-dependent increase in expression of IFNγ response genes such as MHC-I, MHC-II, and PD-L1, confirming that JAK/STAT signaling was increased in IFNγ stimulated $B16^{Socs1-/-}$ melanoma cells **(Figure 27B)**. Moreover, $B16^{Socs1-/-}$ cells stimulated with IFNγ were characterized by increased expression of *Cxcl9, Cxcl10,* and *Cd274* compared to $B16^{WT}$ cells **(Figure 27C)**. *In vitro,* it was found that exposure to IFNγ had a significant inhibitory effect on the growth of B16iSocs1-/- melanoma cells compared to $B16^{WT}$ cells **(Figure 20D)**. When subcutaneously inoculated in NSG mice, B16.SIY Socs1-/- tumors, which express an MHC-I restricted model antigen (SIY), exhibited similar growth rates as $B16.SIY^{WT}$ tumors **(Figure 28A)**. However, the B16.SIY Socs1-/- tumors experienced a significant growth disadvantage in immunocompetent B6 mice **(Figure 28B)**. This suggests that the presence of T cell immunity is an important factor in inhibiting the growth of these tumors. Taken together, these data suggest that melanoma-cell intrinsic JAK/STAT activation via *Socs1* ablation increases B cell and melanoma cell sensitivity to IFNγ.

SOCS1 is a potent negative regulator of JAK/STAT signaling. Genetic ablation of *Socs1* in splenocytes and in B16 melanoma cells resulted in increased sensitivity to IFNγ. However, the

increased JAK/STAT activation in *Socs1*-deficient A20 lymphoma upon IFNγ exposure did not result in a concordant upregulation of IFNγ-dependent genes. These conflicting results suggest that A20 may have other mechanisms of inhibiting JAK/STAT signaling. Therefore, a more representative autochthonous DLBCL model may better address the questions raised by these results.

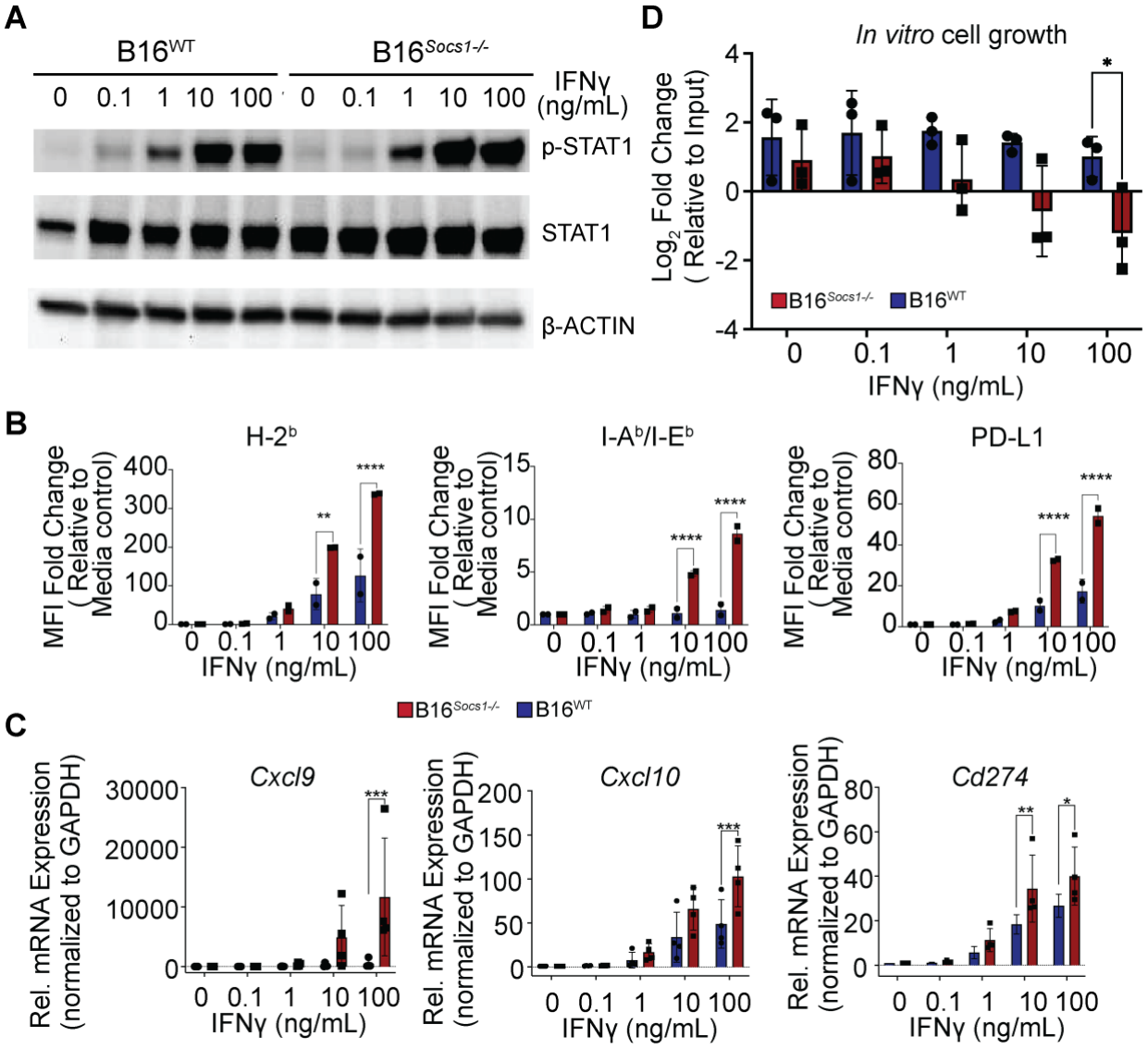

Figure 27. *Socs1* deficiency enhances sensitivity of B16 melanoma to IFNγ. A. Western blot showing pSTAT1, STAT1, and B-ACTIN expression in B16^{WT} and B16$^{Socs1-/-}$ lymphoma cells upon IFNγ stimulation (0,0.1,1,10, 100ng/mL). 1 x 10^6 cells were stimulated for 15 mins and whole cell lysates were blotted for pSTAT1, STAT1, and B-ACTIN.**B.** MFI of MHC-I, MHC-II, and PD-L1 expression in B16^{WT} and B16$^{Socs1-/-}$cells stimulated with IFNγ *in vitro* for 48 hours. **C.** Relative mRNA expression of *Cxcl9, Cxcl10,* and *Cd274* in B16^{WT} and B16$^{Socs1-/-}$cells stimulated with IFNγ *in vitro* for 18-24 hours. **D.** *In vitro* cell growth of B16^{WT} and B16$^{Socs1-/-}$ cells with media only or 100ng/mL IFNγ exposure for 72 hours. Cell count is normalized to number of input cells (5 x 10^4 cells). Average of 3 or more independent biological replicates, two-way ANOVA with Bonferroni post-hoc correction for multiple comparisons, adjusted p values are reported. (* adj. $p < 0.1$, ** adj. $p < 0.05$, *** adj. $p < 0.01$).

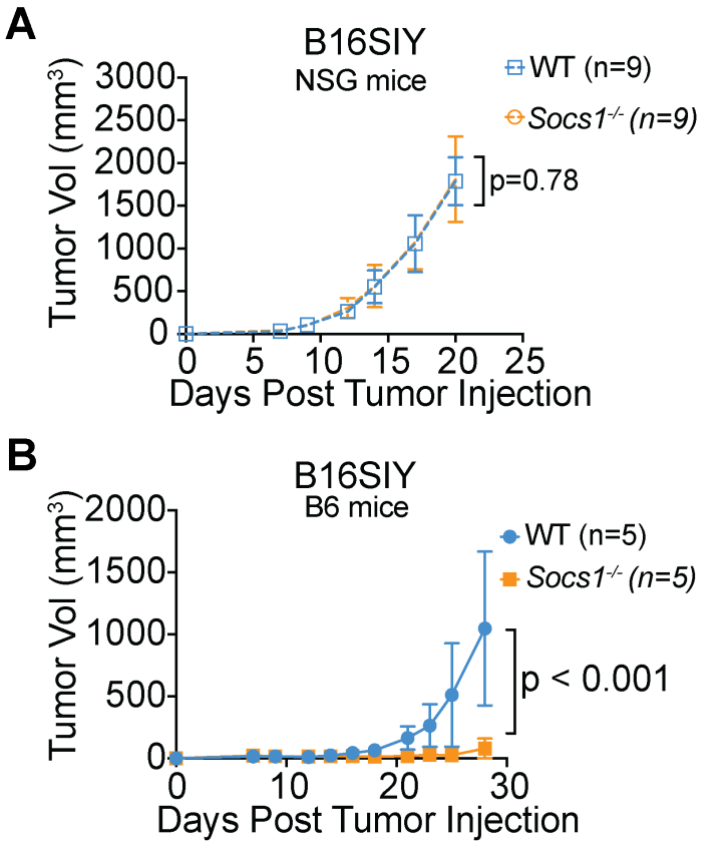

Figure 28. *Socs1* deficiency enhances T cell-mediated control of B16 melanoma. Average tumor volume (mm^3) of $B16^{WT}$ (blue) or $B16^{Socs1-/-}$ (orange) tumors in immunodeficient NSG mice (n=9 mice per group). Mice were inoculated subcutaneously in the left flank. **B.** Average tumor volume (mm^3) of $B16^{WT}$ (blue) or $B16^{Socs1-/-}$ (orange) tumors in B6 mice (n = 5mice per group).

4. Discussion

DLBCL is an aggressive malignancy that is often cured with R-CHOP chemoimmunotherapy; however, the remaining 40% of patients with r/r DLBCL often succumb to their disease[4,30]. Immunotherapies, such as CAR T-cell therapy, bispecific antibodies, or anti-PD1 therapy, have shown clinical benefit in a subset of patients with r/r DLBCL[5–12]. However, the majority of patients either fail to respond or eventually relapse, suggesting more work needs to be done to improve immunotherapy efficacy in r/r DLBCL.

The response to immunotherapy in solid tumors is strongly associated with the immune environment and activation status of CD8+ T cells[108,267–269,292,293]. Furthermore, certain oncogenic alterations in certain types of cancer have been linked to either promoting or suppressing anti-tumor immune responses[94,99,157,158,294–296]. Recent genomic analyses have described the genetic landscape of DLBCL[55,56,263]; however, the immune environment of DLBCL, and the role of specific mutations in orchestrating the immune environment, is less well characterized. Classifying DLBCLs according to the immune environment may identify subsets that are more vulnerable to immunotherapies such as CAR T-cell therapy, bsAbs, or CBT. Moreover, identifying recurrent genetic alterations associated with particular DLBCL immune environments may uncover mechanisms by which oncogenic pathways shape the immune landscape. This knowledge could identify new therapeutic targets that may synergize with immunotherapy to expand the proportion of patients that benefit from these treatments.

In this thesis, I aimed to 1) define the spectrum of immune environments that exist in DLBCL, as well as the extent to which particular immune environments are associated with immunotherapy response, and 2) identify recurrent oncogenic alterations that impact the DLBCL immune environment.

By analyzing bulk transcriptomes of >800 diagnostic DLBCL specimens, I identified four immune-related clusters in DLBCL – ABC hot, ABC cold, GCB hot, and GCB cold – segregated by expression of immune-related and cell-of origin related gene sets. ABC hot and GCB hot DLBCLs were characterized by increased CD8+ and CD4+ T cell infiltration compared to ABC cold and GCB cold DLBCLs, respectively. Per sample GSVA expression scores for immune-related gene sets were significantly correlated with CD8+ T cell and CD4+ T cell infiltration as assessed by mIF analysis, demonstrating transcriptional clustering accurately identifies DLBCLs with an inflamed microenvironment. To confirm the association of immune-related DLBCL clusters with response to immunotherapy, I intend to analyze transcriptomic data from a cohort of patients who have received CD20/CD3 bsAb treatment (mosunetuzumab) or CAR T-cell therapy. Patients that fall in ABC or GCB hot clusters may be more sensitive to bsAb therapy.

Each immune-related cluster was associated with specific recurrent oncogenic alterations and pathways, suggesting that the genetic landscape of DLBCL may play a crucial role in shaping its immune environment. For instance, the expression of MYC gene signatures was notably higher in "cold" DLBCLs, indicating that MYC may contribute to the development of "cold" immune environments. Therefore, these DLBCLs may be less sensitive to CAR T-cell therapy, bsAbs, or CBT. However, the mechanism by which MYC activation may lead to cold environments is still unknown.

This analysis also identified that *SOCS1* LoF mutations were enriched in GCB hot DLBCLs. This observation was intriguing as *SOCS1* plays a critical role in suppressing the JAK/STAT signaling pathway that is activated by various cytokines, such as IFNγ, which has significant anti-tumor properties. Therefore, *SOCS1* mutant DLBCLs may be more sensitive to T cell-mediated immunotherapies that rely on IFNγ. In support of this notion, mechanistic studies

using *Socs1*-deficient B cells demonstrated that *Socs1*-deficient B cells may be more sensitive to IFNγ. However, *Socs1*-deficient A20 lymphoma cells – which represent a syngeneic B cell lymphoma model – were not more sensitive to IFNγ. To better understand the role of loss of function mutations in Socs1 in shaping an inflamed immune environment and influencing the response to immunotherapy, it may be necessary to conduct mechanistic studies using cell lines derived from autochthonous mouse models of DLBCL.

Study limitations. There were also some limitations to this study. First, treatments such as CAR T-cell therapy, bispecific antibodies (bsAbs), or checkpoint blockade therapy (CBT) are typically used in patients who have failed multiple lines of therapy. The DLBCL specimens we analyzed were diagnostic biopsies taken before treatment. The immune landscapes of treatment-naïve versus relapsed/refractory DLBCL likely differ, at least to some extent. However, our characterization of the immune environments associated with untreated DLBCL may facilitate identification of patients more likely to benefit from immunotherapies, thereby limiting use of additional chemotherapies or targeted therapies that are unlikely to provide meaningful clinical benefit. I plan to address this gap in knowledge by using transcriptomic data from a cohort of DLBCLs treated with mosunetuzumab. By comparing the immune landscape of r/r DLBCLs with the diagnostic biopsies, I hope to capture the heterogeneity in the immune environment of diagnostic and r/r DLBCLs.

Second, effector T cells are important for mediating anti-tumor immunity, but the tumor microenvironment also includes other immune cell subsets such as DCs, macrophages, and NK cells that contribute to the host immune response. In our analysis gene sets representing DCs and macrophages were correlated with T cell-based gene sets. However, mIF analysis did not reveal

significantly enriched infiltration of DCs or macrophages in hot DLBCLs compared to cold DLBCLs. As DCs are rare in tumors, their identification through a transcriptomic signature may be more sensitive than mIF. Additionally, DLBCL often arises in lymph nodes where multiple populations of DCs and macrophages naturally exist, and the accumulation of DCs may not be correlated with the generation of a productive anti-tumor immune response. Therefore, clustering DLBCLs based on their transcriptional profile may allow for identification of inflamed lymphomas that have both innate and adaptive components critical for anti-tumor immunity.

Third, previous studies have employed transcriptional-based clustering of DLBCLs, which in some cases, has yielded insights into the DLBCL immune environment. For example, host response (HR)[52] and LME-IN (inflamed lymphoma micro environment)[246] DLBCLs are characterized by upregulation of immune-related transcripts, suggesting that anti-lymphoma immune responses are activated in a subset of DLBCLs. Interestingly, in these studies, the HR and LME-IN DLBCLs were not enriched for a particular COO. Similarly, our GSVA-based clustering found that both ABC and GCB DLBCLs were associated with a spectrum of immune environments, with ABC hot DLBCLs scoring overall higher in immune-related gene sets and exhibiting higher T cell infiltration compared to GCB hot DLBCLs when assessed by mIF. These observations suggest there may be COO-related differences in the immune environment of DLBCL. However, our analysis utilized bulk transcriptomic data, which lacks the granularity to effectively capture the immune cell heterogeneity that may exist in particular DLBCL microenvironments. This was indeed shown to be the case in a recent single-cell transcriptomic analysis of a small cohort of DLBCLs that revealed COO-specific immune cell heterogeneity[297]. Here, M2-macrophages and T_{FH} cells were more prevalent in ABC DLBCLs and metabolically active T_{regs} were enriched in GCB DLBCLs. Other features, such as activated CD8+ T cells and

"stem-cell like" CD8+ T cells, were present in both ABC and GCB DLBCLs, highlighting the need for more comprehensive single cell analyses to fully define how and why COO impacts the DLBCL immune environment.

The immune environment and response or resistance to immunotherapy.

Recently, the presence of a "T cell inflamed" immune environment has been shown to be correlated with improved response to CD19 CAR T-cell therapy (ZUMA-1)[237]. However, the mechanism(s) by which the DLBCL immune environment affects the persistence, durability, or function of CAR T-cells has not been dissected. CAR T-cell tumoricidal activity may act through 1) direct killing of tumor cells or 2) activation of a local immune response. T cells and other immune cells in the tumor may indirectly support the persistence and/or function of lymphoma infiltrating CAR T-cells or may actively be recruited to participate in the anti-tumor immune response following CAR T-cell infusion.

First, endogenous immune cells resident in the lymphoma environment may facilitate the recruitment, proliferation of CAR T-cells through chemokine and cytokine secretion[298]. In addition to chemokine-mediated recruitment, the activation and expansion of CAR T-cells may also be influenced by other factors in the immune microenvironment. Additionally, the cytokine milieu within the tumor microenvironment can affect CAR T-cell function, as certain cytokines such as IL-12[299] and IL-18[300–302] can enhance CAR T-cell activity while others such as TGFβ can inhibit it. Therefore, the immune environment of DLBCLs may influence response to CAR T-cell therapy not only through recruitment of CAR T-cells, but also through regulation of CAR T-cell activation and function.

Alternatively, CAR T-cell activity may lead to the activation of T cells in the TME. Following recognition of the cognate antigen, CAR T-cells secrete cytolytic molecules (GZMdB, PRF1) and effector cytokines (TNFα and IFNγ)[236]. The increase in effector cytokines in the tumor environment may initiate a positive feedback loop that improves the function of existing tumor antigen-specific T cells in the environment or lead to epitope spreading that activates new tumor specific T cells. This inflammatory environment may also activate "bystander" non-lymphoma antigen-specific $CD8^+$ and $CD4^+$ T cells in the environment, though the contribution of these T cells to the anti-tumor immune response has not been thoroughly described.

One study exploring the immune environment of patients treated with CD19 CAR T-cell therapy (ZUMA-1) found that the majority of non-CAR T-cells in the TME expressed markers of activation (Ki67, GzmB, IFNγ) after therapy[303]. It is important to note that patients receive lymphodepleting therapy prior to CAR T-cell infusion, which may deplete T cells in the immune environment. Therefore, the source of the activated non-CAR T-cells in the environment could be untransduced T cells that were present in the CAR T-cell product, suggesting more work needs to be done to longitudinally track CAR T-cells and non-CAR T-cells in the lymphoma environment.

Similarly, correlative analyses performed on pretreatment biopsies of patients treated with a CD20/CD3 bsAb (Glofitamab) demonstrated a trend toward higher CD8+ T effector cell transcripts in the lymphomas of patients who achieved a complete response to this therapy[245]. However, the mechanism by which an inflamed environment leads to response to bsAbs has not been defined. BsAbs may mediate anti-tumor immunity thorough redirecting peripheral T cells to the TME. Additionally, bsAbs may also induce local T cell activation in the tumor, leading to antigen spreading and activation of additional tumor-specific T cells. The immune environment of

DLBCL can influence the recruitment and function of these T cells, as well as the overall efficacy of bsAb therapy.

The contribution of the immune environment to CAR T-cell therapy response and bsAb response may also differ. Naïve T cells require TCR stimulation (signal 1), co-stimulation (signal 2), and soluble factors (signal 3) for full activation. In the case of bispecific antibody therapy, the requirement for co-stimulation may make the presence of DCs in the TME or CD80/CD86 expression on lymphoma cells important for efficacy. In support of this notion, addition of a CD28/CD22 targeting bsAb to a CD20/CD3 bsAb regimen enhanced T cell activation and function over either bsAb alone[304]. In contrast, CAR T-cells contain intracellular co-stimulatory domains, which may decrease the requirement for such signals from immune cells in the environment.

Recent advances in the field of cancer immunotherapy have led to several clinical trials of CAR T-cell therapy or bsAb therapy in DLBCL. Currently, it is unknown if CAR T-cell therapy and bsAb therapy lead to clinical benefit in the same population of patients. Therefore, leveraging transcriptomic and genetic data combined with paired clinical response information, from these studies may allow researchers to compare the population of patients that benefit from CAR T-cell therapy or bsAb therapy. Such analyses may enable identification of other factors that may lead to sensitivity to either CAR T-cell or bsAb therapy.

Currently, investigation of methods to improve CAR T or bsAb therapy relies on the use of human cell lines xenografted in immunodeficient mice followed by transfer of allogeneic CAR T-cells, which does not recapitulate the immune environment of DLBCL. Therefore, the development of novel syngeneic or autochthonous murine models of DLBCL may facilitate in-depth investigation into the underlying mechanisms of action of these immunotherapies. For example, cell lines generated from mice in which conditional expression of a gain of function

EZH2 mutation and conditional BCL2 overexpression leads to lymphomagenesis (*Cd19*$^{Cre+/-}$,*Ezh2*$^{Y641S/F}$, *Rosa26*$^{LSL\text{-}BCL2\text{-}IRES\text{-}GFP}$, gift from Dr. Ari Melnick) may be engineered to express a model antigen (Ovalbumin). This system would allow for adoptive transfer of congenically marked OVA-specific CD8+ T cells (OT-1) or CD4+ T cells (OT-II) to track OVA-specific T cells' response with or without bsAb therapy. Additionally, endogenous OVA-specific T cells could also be monitored using this system. A tractable system using a model antigen may also be useful to understand the contribution of the immune environment to response to CAR T-cell therapy. Adoptive transfer of OVA-specific T cells prior to CAR T-cell transfer may simulate an inflamed environment. Ultimately, the development of autochthonous models of DLBCL that recapitulate lymphoma-cell intrinsic features as well as the immune environment will be required to fully understand the complex interplay between malignant lymphoma cells and the immune environment.

The generation of an effective anti-tumor immune response is a complex process that involves multiple mechanisms in the tumor microenvironment. Therefore, more work is needed to fully understand the contribution of the local immune environment in facilitating response to CAR T-cell therapy, bsAbs, and other immunotherapies.

Role of lymphoma cell-intrinsic alterations in orchestrating the DLBCL immune environment.

While genetic alterations have been shown to play a crucial role in modulating the immune environment in various types of cancer, their impact on immune environments in DLBCL is not yet fully understood. Our study aimed to address this gap in knowledge by investigating the relationship between our transcriptionally-based immune-related DLBCL clusters and oncogenic alterations in DLBCL. We discovered that each of the four immune-related clusters was associated

with several oncogenic alterations, which implicated a role for lymphoma cell-intrinsic alterations in shaping the immune environment. It is noteworthy that multiple alterations were consistently linked to cold environments, while only a few were linked to hot environments. One possible explanation for this trend is that cancer cells would be at a disadvantage if they acquired mutations that create a T cell inflamed environment, as they would be more vulnerable to T cell-mediated cytolysis. Hence, lymphomas may develop mutations that generate an immune-devoid environment. Intriguingly, almost half of all DLBCLs have mutations in β2M or HLA-A,B,C, indicating a potential anti-tumor immune response, suggesting DLBCLs could be subject to intense immune surveillance due to their development in the lymph node. Consequently, DLBCLs may be even less prone to acquiring or propagating genetic mutations that foster an "inflamed" environment relative to other cancer types.

A particularly interesting and recurring LoF genetic alteration in GCB hot DLBCLs occurred in *SOCS1,* which garnered our interest given the high frequencies of LoF *SOCS1* alterations in other CBT responsive lymphomas such as cHL and PMBL. However, *SOCS1* mutant DLBCLs were also observed in the GCB cold cluster, suggesting *SOCS1* LoF mutations may not be sufficient in isolation to effectively identify inflamed DLBCLs. For example, other genetic factors – such as *JAK2* amplifications or GoF *STAT3/6* mutations- may cooperate with *SOCS1* mutations to orchestrate an inflamed immune environment.

LoF mutations in SOCS1 can enhance oncogenic JAK/STAT signaling, but they may also offer a therapeutic opportunity. Genome wide CRISPR screens have demonstrated the requirement for tumor cell-intrinsic IFNγ signaling in mediating response to CBT. For example, mutations in *IFNγR*, *JAK2*, *or STAT1* renders B16 melanoma cells less sensitive to the effects of CBT[157–159]. Conversely, loss of negative regulators of JAK/STAT signaling – such as *PTPN2*- can sensitize

B16 melanoma cells to immunotherapy. Similarly, patients who develop acquired resistance to CBT have been shown to acquire mutations in *JAK2*, leading to decreased IFNγ sensing. Therefore, I hypothesized that mutations in *Socs1* may render lymphoma cells more sensitive to IFNγ. Interestingly, I show that murine non-malignant B cells, murine B lymphoma cells (A20) and murine melanoma cells (B16) displayed different behavior after exposure to IFNγ, which indicates potential broad differences in cell type-specific sensitivity to IFNγ. Compared to wildtype cells, B16 melanoma cells deficient in Socs1 showed increased expression of pSTAT1 and IFNγ-dependent genes, including MHC-I, MHC-II, and PD-L1, upon exposure to IFNγ. Additionally, these B16$^{Socs1-/-}$ cells displayed growth inhibition in vitro and significant growth disadvantage in vivo in the presence of adaptive immunity. In contrast, A20 lymphoma cells displayed intact IFNγ sensing, as evidenced by increased pSTAT1 expression upon IFNγ stimulation, but A20$^{Socs1-/-}$ cells did not show increased sensitivity to the anti-proliferative effects of IFNγ relative to A20WT cells. B cells from Socs1-deficient mice showed marked upregulation of MHC-II and PD-L1 at high IFNγ concentrations, but MHC-I was inducible similarly in Socs1-deficient and Socs1-sufficient B cells, indicating that the regulation of IFNγ signaling may differ across cell types.

While IFNγ is known to induce anti-proliferative effects in many cell types, the extent to which these effects are observed may vary depending on the specific cell type and the signaling pathways that are activated. In the case of mouse B cells, it is known that IFNγ signaling can lead to the production of IgG2a antibodies through the induction of class switch recombination (CSR)[14,15,305,306]. However, B cells may have developed mechanisms to avoid the anti-proliferative effects of IFNγ in order to facilitate this process. One potential mechanism may involve the expression of negative regulators of JAK/STAT signaling, such as SOCS3, which can help to limit

the extent of IFNγ signaling and prevent excessive cell death. In addition, it is possible that B cells may signal through other pathways, such as the PI3K or NFκB pathways, upon B cell receptor (BCR) stimulation that counteract the anti-proliferative effects of IFNγ. These pathways may be hijacked by malignant lymphoma cells and can promote cell survival and proliferation and may therefore help to offset the anti-proliferative effects of IFNγ in B cells. Therefore, investigating transcriptional changes in A20 lymphoma cells and B16 melanoma cells, as well as normal B cell and epithelial cell counterparts, upon stimulation with IFNγ may shed light on the differential sensitivity of various cell types to IFNγ. Furthermore, it is currently unknown whether the depth and duration of clinical responses to immunotherapy is related to the sensitivity of different cell types to IFNγ. Therefore, identifying such features may enable development of targeted therapies that can synergize with immunotherapies in cancer.

Overall, the sensitivity of different cell types to IFNγ likely reflects a complex interplay between various signaling pathways and feedback mechanisms. Further research is needed to fully understand the mechanisms underlying these differences and their implications for immune function and cancer immunotherapy.

ABC cold DLBCLs were characterized mutations in BCR signaling components that may lead to constitutive NFκB signaling– *MYD88*^{L265P}, *CARD11, KLHL14, CD79B*– suggesting activation of this pathway may lead to immune suppression. A recent genomic analysis of DLBCL identified several oncogenic alterations that were correlated with decreased expression of immune cell-related genes. Among the genes identified, *MYD88* was significantly negatively associated with expression of T cell and NK cell-related genes[263]. BCR activating mutations are also enriched in MCD DLBCLs, which were demonstrated to be negatively associated with genes related to T_{FH}

and CD4+ T cells compared to other LymphGen genetic clusters[55]. These data are particularly interesting as NFκB signaling results in secretion of pro-inflammatory cytokines in immune cells – which should lead to increased recruitment of anti-tumor immune cells to the microenvironment. However, the mechanism by which BCR activation and concomitant NFκB signaling leads to cold environments has not yet been elucidated.

One possibility is through the activation of *MYC* signaling. We found that ABC cold DLBCLs strongly upregulated transcriptional programs associated with *MYC* activity compared to ABC hot DLBCLs. In the germinal center, B cells bind antigen through the BCR, leading to BCR activation, followed by presentation of antigen derived peptides on MHC-II to cognate T_{FH} cells[14,15]. *MYC* expression is transiently induced in a proportion of B cells that have been positively selected for cyclic re-entry into the dark zone, and is critical for affinity maturation[15,307–310]. *MYC* expression in GC B cells is tightly regulated and relies on cooperation between PI3K activation downstream of BCR activation and CD40-dependent NFκB activation[307,309]. Extending this concept to lymphoma, ABC DLBCLs are driven by alterations that lead to constitutive NFκB activation and activation of BCR signaling, and may have a similar *MYC* driven transcriptional program to positively selected GC B cells. However, the strength of *MYC* upregulation or activity may depend on the genetic alteration, leading to heterogeneity in *MYC* activity amongst ABC DLBCLs.

Mechanistically, *MYC* upregulation has been implicated in immune evasion in lymphoma through mediating downregulation of HLA-I/II molecules[271,311] and adhesion molecules[312]. *MYC* has been shown to induce metabolic reprogramming in lymphoma cells[313–316], leading to a shortage of key metabolites in the tumor microenvironment and decreased T cell fitness and survival[313].

MYC activity also leads to increased proliferation of the lymphoma cells, further altering the balance between lymphoma cells and T cells.

The aforementioned studies have been conducted *in vitro* and *in vivo* using models of Burkitt lymphoma, in which chromosomal rearrangement of *MYC* to the immunoglobulin heavy chain (*IGH*) locus leads to aberrant MYC activity. Whether similar mechanisms of immune escape are active in ABC DLBCLs, where *MYC* upregulation is driven by mutations in the "BCR dependent NFκB" pathway, is unknown. Interestingly, we found that ABC cold DLBCLs were characterized by higher expression of *MYC* related gene sets compared to GCB cold DLBCLs, suggesting the strength of *MYC* upregulation and activation may differ by COO.

In order to first test whether ABC and GCB DLBCLs differ in strength of *MYC* activation, a panel of human DLBCL cell lines could be stimulated with anti-IgM and CD40L to measure *MYC* expression and transcription of *MYC* target genes. In addition, a mouse B cell lymphoma cell line that expresses doxycycline-inducible *MYC* could be used as a syngeneic model to investigate the impact of *MYC* activation on creating a cold tumor environment. This model would offer the ability to control the strength and timing of *MYC* activation. Overall, the specific role of MYC in orchestrating a cold tumor microenvironment in DLBCL and the impact of its mechanism of activation on this process require further investigation.

The genetic landscape of diffuse large B-cell lymphoma (DLBCL) is highly heterogeneous, with a wide variety of mutations and genetic alterations that can drive tumor growth and progression. This heterogeneity can make it challenging to study the role of individual mutations in the orchestration of the immune environment in DLBCL. Genetically engineered mouse models (GEMMs) can be a valuable tool for studying the effects of specific mutations on tumor development and the immune response. However, the complexity of the genetic landscape of

DLBCL, as well as the fact that DLBCLs arise within the lymph node microenvironment, may require the use of more sophisticated GEMMs to fully capture the heterogeneity and complexity of the disease. For example, GEMMs that incorporate multiple mutations that are commonly observed in DLBCLs, as well as models that allow for the study of tumor development within the lymph node microenvironment, could be useful for investigating the role of these mutations in shaping the immune environment in DLBCL.

Conclusion

The identification of four unique DLBCL immune environments and their association with specific oncogenic alterations is an important step towards understanding the complex interplay between tumor cells and the immune system in DLBCL. Validation of these immune environments in response to immunotherapies such as bsAb therapy or CAR T-cell therapy could provide valuable insights into the mechanisms underlying response and resistance to these treatments. The development of a clinically translatable "immune score" for DLBCL could also have significant clinical implications by helping to identify patients who are most likely to respond to immunotherapy. This type of score could potentially be used to guide treatment decisions and improve patient outcomes.

Mechanistic studies that investigate the causal role of lymphoma cell-intrinsic alterations in regulating the immune environment will also be important for identifying new therapeutic targets. By understanding the molecular mechanisms underlying the immune environment in DLBCL, researchers may be able to identify novel targets for therapeutic intervention that can help to turn "cold" DLBCLs into "hot" DLBCLs and improve the efficacy of immunotherapy.

Overall, these studies have the potential to significantly improve our understanding of the immune environment in DLBCL and facilitate the development of more effective immunotherapeutic approaches for patients with this disease.

Bibliography

1. Siegel RL, Miller KD, Fuchs HE, Jemal A. Cancer statistics, 2022. *CA: A Cancer Journal for Clinicians*. 2022;72(1):7-33. doi:10.3322/caac.21708

2. Swerdlow SH, Campo E, Pileri SA, et al. The 2016 revision of the World Health Organization classification of lymphoid neoplasms. *Blood*. 2016;127(20):2375-2390. doi:10.1182/blood-2016-01-643569

3. Vitolo U, Seymour JF, Martelli M, et al. Extranodal diffuse large B-cell lymphoma (DLBCL) and primary mediastinal B-cell lymphoma: ESMO Clinical Practice Guidelines for diagnosis, treatment and follow-up †. *Annals of Oncology*. 2016;27:v91-v102. doi:10.1093/annonc/mdw175

4. Crump M, Neelapu SS, Farooq U, et al. Outcomes in refractory diffuse large B-cell lymphoma: results from the international SCHOLAR-1 study Key Points. Published online 2017. doi:10.1182/blood-2017-03

5. Neelapu SS, Locke FL, Bartlett NL, et al. Axicabtagene Ciloleucel CAR T-Cell Therapy in Refractory Large B-Cell Lymphoma. *N Engl J Med*. 2017;377(26):2531-2544. doi:10.1056/NEJMoa1707447

6. Schuster SJ, Bishop MR, Tam CS, et al. Tisagenlecleucel in Adult Relapsed or Refractory Diffuse Large B-Cell Lymphoma. *https://doi.org/101056/NEJMoa1804980*. 2018;380(1):45-56. doi:10.1056/NEJMOA1804980

7. Budde LE, Assouline S, Sehn LH, et al. Single-Agent Mosunetuzumab Shows Durable Complete Responses in Patients With Relapsed or Refractory B-Cell Lymphomas: Phase I Dose-Escalation Study. *JCO*. 2022;40(5):481-491. doi:10.1200/JCO.21.00931

8. Dickinson MJ, Carlo-Stella C, Morschhauser F, et al. Glofitamab for Relapsed or Refractory Diffuse Large B-Cell Lymphoma. *New England Journal of Medicine*. 2022;387(24):2220-2231. doi:10.1056/NEJMoa2206913

9. Ansell SM. Checkpoint Blockade in Lymphoma. *Journal of Clinical Oncology*. Published online January 12, 2021. doi:10.1200/JCO.20.01522

10. Ansell SM, Minnema MC, Johnson P, et al. Nivolumab for Relapsed/Refractory Diffuse Large B-Cell Lymphoma in Patients Ineligible for or Having Failed Autologous Transplantation: A Single-Arm, Phase II Study. *JCO*. 2019;37(6):481-489. doi:10.1200/JCO.18.00766

11. Kline J, Godfrey J, Ansell SM. The immune landscape and response to immune checkpoint blockade therapy in lymphoma. *Blood*. 2020;135(8):523-533. doi:10.1182/blood.2019000847

12. Villasboas JC, Reeder CB, Tun HW, et al. The DIAL Study (Dual Immunomodulation in Aggressive Lymphoma): A Randomized Phase 2 Study of CDX-1127 (Varlilumab) in Combination with Nivolumab in Patients with Relapsed or Refractory Aggressive B-Cell Lymphomas (NCI 10089 / NCT03038672). *Blood*. 2019;134(Supplement_1):1591-1591. doi:10.1182/BLOOD-2019-130449

13. Basso K, Dalla-Favera R. Germinal centres and B cell lymphomagenesis. *Nat Rev Immunol*. 2015;15(3):172-184. doi:10.1038/nri3814

14. Mesin L, Ersching J, Victora GD. Germinal Center B Cell Dynamics. *Immunity*. 2016;45(3):471-482. doi:10.1016/j.immuni.2016.09.001

15. Victora GD, Nussenzweig MC. Germinal Centers. *Annual Review of Immunology*. 2022;40(1):413-442. doi:10.1146/annurev-immunol-120419-022408

16. Victora GD, Schwickert TA, Fooksman DR, et al. Germinal Center Dynamics Revealed by Multiphoton Microscopy Using a Photoactivatable Fluorescent Reporter. *Cell*. 2010;143(4):592-605. doi:10.1016/j.cell.2010.10.032

17. Bahler D, Campbell M, Hart S, Miller R, Levy S, Levy R. Ig VH gene expression among human follicular lymphomas. *Blood*. 1991;78(6):1561-1568. doi:10.1182/blood.V78.6.1561.1561

18. Chapman C, Mockridge C, Rowe M, Rickinson A, Stevenson F. Analysis of VH genes used by neoplastic B cells in endemic Burkitt's lymphoma shows somatic hypermutation and intraclonal heterogeneity. *Blood*. 1995;85(8):2176-2181. doi:10.1182/blood.V85.8.2176.bloodjournal8582176

19. Klein U, Klein G, Ehlin-Henriksson B, Rajewsky K, Küppers R. Burkitt's Lymphoma Is a Malignancy of Mature B Cells Expressing Somatically Mutated V Region Genes. *Mol Med*. 1995;1(5):495-505. doi:10.1007/BF03401587

20. Bakkus M, Heirman C, Van Riet I, Van Camp B, Thielemans K. Evidence that multiple myeloma Ig heavy chain VDJ genes contain somatic mutations but show no intraclonal variation. *Blood*. 1992;80(9):2326-2335. doi:10.1182/blood.V80.9.2326.2326

21. Baker BW, Deane M, Gilleece MH, Johnston D, Scarffe JH, Norton JD. Distinctive Features of Immunoglobulin Heavy Chain Variable Region Gene Rearrangement in Multiple Myeloma. *Leukemia & Lymphoma*. 1994;14(3-4):291-301. doi:10.3109/10428199409049681

22. Küppers R, Rajewsky K, Zhao M, et al. Hodgkin disease: Hodgkin and Reed-Sternberg cells picked from histological sections show clonal immunoglobulin gene rearrangements and appear to be derived from B cells at various stages of development. *Proceedings of the National Academy of Sciences*. 1994;91(23):10962-10966. doi:10.1073/pnas.91.23.10962

23. Kanzler H, Küppers R, Hansmann ML, Rajewsky K. Hodgkin and Reed-Sternberg cells in Hodgkin's disease represent the outgrowth of a dominant tumor clone derived from (crippled) germinal center B cells. *Journal of Experimental Medicine*. 1996;184(4):1495-1505. doi:10.1084/jem.184.4.1495

24. Küppers R, Rajewsky K, Hansmann ML. Diffuse large cell lymphomas are derived from mature B cells carrying V region genes with a high load of somatic mutation and evidence of selection for antibody expression. *European Journal of Immunology*. 1997;27(6):1398-1405. doi:10.1002/eji.1830270616

25. Küppers R, Klein U, Hansmann ML, Rajewsky K. Cellular Origin of Human B-Cell Lymphomas. *New England Journal of Medicine*. 1999;341(20):1520-1529. doi:10.1056/NEJM199911113412007

26. Hsu F, Levy R. Preferential use of the VH4 Ig gene family by diffuse large-cell lymphoma. *Blood*. 1995;86(8):3072-3082. doi:10.1182/blood.V86.8.3072.3072

27. Küppers R, Klein U, Hansmann ML, Rajewsky K. Cellular Origin of Human B-Cell Lymphomas. *New England Journal of Medicine*. 1999;341(20):1520-1529. doi:10.1056/NEJM199911113412007

28. Mlynarczyk C, Fontán L, Melnick A. Germinal center-derived lymphomas: The darkest side of humoral immunity. *Immunological Reviews*. 2019;288(1):214-239. doi:10.1111/imr.12755

29. Pasqualucci L. Molecular pathogenesis of germinal center-derived B cell lymphomas. *Immunological Reviews*. 2019;288(1):240-261. doi:10.1111/imr.12745

30. JW F. Relapsed/refractory diffuse large B-cell lymphoma. *Hematology American Society of Hematology Education Program*. 2011;2011:498-505. doi:10.1182/ASHEDUCATION-2011.1.498

31. Menon MP, Pittaluga S, Jaffe ES. The Histological and Biological Spectrum of Diffuse Large B-cell Lymphoma in the WHO Classification. *Cancer J*. 2012;18(5):411-420. doi:10.1097/PPO.0b013e31826aee97

32. Xie Y, Pittaluga S, Jaffe ES. The Histological Classification of Diffuse Large B-cell Lymphomas. *Semin Hematol*. 2015;52(2):57-66. doi:10.1053/j.seminhematol.2015.01.006

33. Engelhard M, Brittinger G, Huhn D, et al. Subclassification of Diffuse Large B-Cell Lymphomas According to the Kiel Classification: Distinction of Centroblastic and Immunoblastic Lymphomas Is a Significant Prognostic Risk Factor. *Blood*. 1997;89(7):2291-2297. doi:10.1182/blood.V89.7.2291

34. Alizadeh AA, Eisen MB, Davis RE, et al. Distinct types of diffuse large B-cell lymphoma identified by gene expression profiling. *Nature*. 2000;403(6769):503-511. doi:10.1038/35000501

35. Hans CP, Weisenburger DD, Greiner TC, et al. Confirmation of the molecular classification of diffuse large B-cell lymphoma by immunohistochemistry using a tissue microarray. *Blood*. 2004;103(1):275-282. doi:10.1182/blood-2003-05-1545

36. Young RM, Phelan JD, Shaffer AL, et al. Taming the Heterogeneity of Aggressive Lymphomas for Precision Therapy. *Annual Review of Cancer Biology*. 2019;3(1):429-455. doi:10.1146/annurev-cancerbio-030518-055734

37. Davis RE, Ngo VN, Lenz G, et al. Chronic active B-cell-receptor signalling in diffuse large B-cell lymphoma. *Nature*. 2010;463(7277):88-92. doi:10.1038/nature08638

38. Staudt LM. Oncogenic Activation of NF-κB. *Cold Spring Harb Perspect Biol*. 2010;2(6):a000109. doi:10.1101/cshperspect.a000109

39. Yang Y, Shaffer AL, Emre NCT, et al. Exploiting Synthetic Lethality for the Therapy of ABC Diffuse Large B Cell Lymphoma. *Cancer Cell*. 2012;21(6):723-737. doi:10.1016/j.ccr.2012.05.024

40. Camicia R, Winkler H, Hassa P. Novel drug targets for personalized precision medicine in relapsed/refractory diffuse large B-cell lymphoma: A comprehensive review. *Molecular Cancer*. 2015;14. doi:10.1186/s12943-015-0474-2

41. Wilson WH, Wright GW, Huang DW, et al. Effect of ibrutinib with R-CHOP chemotherapy in genetic subtypes of DLBCL. *Cancer Cell*. 2021;39(12):1643-1653.e3. doi:10.1016/j.ccell.2021.10.006

42. Yang Y, Shaffer AL, Emre NCT, et al. Exploiting Synthetic Lethality for the Therapy of ABC Diffuse Large B Cell Lymphoma. *Cancer Cell*. 2012;21(6):723-737. doi:10.1016/j.ccr.2012.05.024

43. Wilson WH, Young RM, Schmitz R, et al. Targeting B cell receptor signaling with ibrutinib in diffuse large B cell lymphoma. *Nat Med*. 2015;21(8):922-926. doi:10.1038/nm.3884

44. Witzig TE, Vose JM, Zinzani PL, et al. An international phase II trial of single-agent lenalidomide for relapsed or refractory aggressive B-cell non-Hodgkin's lymphoma. *Ann Oncol*. 2011;22(7):1622-1627. doi:10.1093/annonc/mdq626

45. Ghesquieres H, Houillier C, Chinot S, Choquet C. Rituximab-Lenalidomide (REVRI) in Relapse or Refractory Primary Central Nervous System (PCNSL) or Vitreo Retinal Lymphoma (PVRL): Results of a "Proof of Concept" Phase II Study of the French LOC Network. 2016;128:785 ab.

46. Dunleavy K, Pittaluga S, Czuczman MS, et al. Differential efficacy of bortezomib plus chemotherapy within molecular subtypes of diffuse large B-cell lymphoma. *Blood*. 2009;113(24):6069-6076. doi:10.1182/blood-2009-01-199679

47. Davies A, Cummin TE, Barrans S, et al. Gene-expression profiling of bortezomib added to standard chemoimmunotherapy for diffuse large B-cell lymphoma (REMoDL-B): an open-label, randomised, phase 3 trial. *The Lancet Oncology*. 2019;20(5):649-662. doi:10.1016/S1470-2045(18)30935-5

48. Pasqualucci L, Trifonov V, Fabbri G, et al. Analysis of the coding genome of diffuse large B-cell lymphoma. *Nature Genetics*. 2011;43(9):830-837. doi:10.1038/ng.892

49. Shaffer AL, Young RM, Staudt LM. Pathogenesis of Human B Cell Lymphomas. *Annual Review of Immunology*. 2012;30(1):565-610. doi:10.1146/annurev-immunol-020711-075027

50. Morin RD, Mendez-Lago M, Mungall AJ, et al. Frequent mutation of histone-modifying genes in non-Hodgkin lymphoma. *Nature*. 2011;476(7360):298-303. doi:10.1038/nature10351

51. Victora GD, Dominguez-Sola D, Holmes AB, Deroubaix S, Dalla-Favera R, Nussenzweig MC. Identification of human germinal center light and dark zone cells and their relationship to human B-cell lymphomas. *Blood*. 2012;120(11):2240-2248. doi:10.1182/blood-2012-03-415380

52. Monti S, Savage KJ, Kutok JL, et al. Molecular profiling of diffuse large B-cell lymphoma identifies robust subtypes including one characterized by host inflammatory response. *Blood*. 2005;105(5):1851-1861. doi:10.1182/blood-2004-07-2947

53. Caro P, Kishan AU, Norberg E, et al. Metabolic Signatures Uncover Distinct Targets in Molecular Subsets of Diffuse Large B Cell Lymphoma. *Cancer Cell*. 2012;22(4):547-560. doi:10.1016/j.ccr.2012.08.014

54. Chen L, Monti S, Juszczynski P, et al. SYK-dependent tonic B-cell receptor signaling is a rational treatment target in diffuse large B-cell lymphoma. *Blood*. 2008;111(4):2230-2237. doi:10.1182/blood-2007-07-100115

55. Wright GW, Huang DW, Phelan JD, et al. A Probabilistic Classification Tool for Genetic Subtypes of Diffuse Large B Cell Lymphoma with Therapeutic Implications. *Cancer Cell*. 2020;37(4):551-568.e14. doi:10.1016/j.ccell.2020.03.015

56. Chapuy B, Stewart C, Dunford AJ, et al. Molecular subtypes of diffuse large B cell lymphoma are associated with distinct pathogenic mechanisms and outcomes. *Nat Med*. 2018;24(5):679-690. doi:10.1038/s41591-018-0016-8

57. Fehleisen F. Ueber die Züchtung der Erysipelkokken auf künstlichem Nährboden und ihre Übertragbarkeit auf den Menschen. *Dtsch Med Wochenschr*. 1882;8(31):553-554.

58. Busch W. Aus der Sitzung der medicinischen Section vom 13 November 1867. *Berl Klin Wochenschr*. 1868;5(5):137.

59. Coley WB. The Treatment of Malignant Tumors by Repeated Inoculations of Erysipelas: With a Report of Ten Original Cases.1: Bibliography. *The American Journal of the Medical Sciences (1827-1924)*. 1893;105(6):487.

60. COLEY WB. THE TREATMENT OF INOPERABLE SARCOMA WITH THE 'MIXED TOXINS OF ERYSIPELAS AND BACILLUS PRODIGIOSUS.: IMMEDIATE AND FINAL RESULTS IN ONE HUNDRED AND FORTY CASES. *Journal of the American Medical Association*. 1898;XXXI(9):456-465. doi:10.1001/jama.1898.92450090022001g

61. Starnes CO. Coley's toxins in perspective. *Nature*. 1992;357(6373):11-12. doi:10.1038/357011a0

62. Ribatti D. The concept of immune surveillance against tumors: The first theories. *Oncotarget*. 2016;8(4):7175-7180. doi:10.18632/oncotarget.12739

63. Gross L. Intradermal immunization of C3H mice against a sarcoma that originated in an animal of the same line. *Cancer research*. 1943;3(5):326-333.

64. Foley EJ. Antigenic properties of methylcholanthrene-induced tumors in mice of the strain of origin. *Cancer Res*. 1953;13(12):835-837.

65. Prehn RT, Main JM. Immunity to Methylcholanthrene-Induced Sarcomas. *JNCI: Journal of the National Cancer Institute*. 1957;18(6):769-778. doi:10.1093/jnci/18.6.769

66. Krikorian JG, Anderson JL, Bieber CP, Penn I, Stinson EB. Malignant Neoplasms Following Cardiac Transplantation. *JAMA*. 1978;240(7):639-643. doi:10.1001/jama.1978.03290070041012

67. Penn I. Development of cancer as a complication of clinical transplantation. *Transplant Proc*. 1977;9(1):1121-1127.

68. Sheil AG, Mahony JF, Horvath JS, et al. Cancer following successful cadaveric donor renal transplantation. *Transplant Proc*. 1981;13(1 Pt 2):733-735.

69. Thomas L. On Immunosurveillance in Human Cancer.

70. Burnet M. Cancer—A Biological Approach. *Br Med J*. 1957;1(5022):779-786.

71. Stutman O. Tumor Development after 3-Methylcholanthrene in Immunologically Deficient Athymic-Nude Mice. *Science*. 1974;183(4124):534-536. doi:10.1126/science.183.4124.534

72. Stutman O. Immunodepression and Malignancy. In: Klein G, Weinhouse S, Haddow A, eds. *Advances in Cancer Research*. Vol 22. Academic Press; 1976:261-422. doi:10.1016/S0065-230X(08)60179-7

73. Dighe AS, Richards E, Old LJ, Schreiber RD. Enhanced in vivo growth and resistance to rejection of tumor cells expressing dominant negative IFNγ receptors. *Immunity*. 1994;1(6):447-456. doi:10.1016/1074-7613(94)90087-6

74. Kaplan DH, Shankaran V, Dighe AS, et al. Demonstration of an interferon gamma-dependent tumor surveillance system in immunocompetent mice. *Proc Natl Acad Sci U S A*. 1998;95(13):7556-7561. doi:10.1073/pnas.95.13.7556

75. Demonstration of an interferon γ-dependent tumor surveillance system in immunocompetent mice. doi:10.1073/pnas.95.13.7556

76. Chen DS, Mellman I. Oncology Meets Immunology: The Cancer-Immunity Cycle. *Immunity*. 2013;39(1):1-10. doi:10.1016/j.immuni.2013.07.012

77. Girardi M, Oppenheim DE, Steele CR, et al. Regulation of Cutaneous Malignancy by γδ T Cells. *Science*. 2001;294(5542):605-609. doi:10.1126/science.1063916

78. Shinkai Y, Rathbun 0Gary, Lam KP, et al. RAG-2-deficient mice lack mature lymphocytes owing to inability to initiate V(D)J rearrangement. *Cell*. 1992;68(5):855-867. doi:10.1016/0092-8674(92)90029-C

79. Mitra-Kaushik S, Harding J, Hess J, Schreiber R, Ratner L. Enhanced tumorigenesis in HTLV-1 Tax-transgenic mice deficient in interferon-gamma. *Blood*. 2004;104(10):3305-3311. doi:10.1182/blood-2004-01-0266

80. Shankaran V, Ikeda H, Bruce AT, et al. IFNγ and lymphocytes prevent primary tumour development and shape tumour immunogenicity. *Nature*. 2001;410(6832):1107-1111. doi:10.1038/35074122

81. Bolitho P, Street SEA, Westwood JA, et al. Perforin-mediated suppression of B-cell lymphoma. *Proceedings of the National Academy of Sciences*. 2009;106(8):2723-2728. doi:10.1073/pnas.0809008106

82. Smyth MJ, Thia KYT, Street SEA, MacGregor D, Godfrey DI, Trapani JA. Perforin-Mediated Cytotoxicity Is Critical for Surveillance of Spontaneous Lymphoma. *Journal of Experimental Medicine*. 2000;192(5):755-760. doi:10.1084/jem.192.5.755

83. JCI - TRAIL-R deficiency in mice promotes susceptibility to chronic inflammation and tumorigenesis. Accessed February 4, 2023. https://www.jci.org/articles/view/29900

84. Davidson WF, Giese T, Fredrickson TN. Spontaneous Development of Plasmacytoid Tumors in Mice with Defective Fas–Fas Ligand Interactions. *Journal of Experimental Medicine*. 1998;187(11):1825-1838. doi:10.1084/jem.187.11.1825

85. Schreiber RD, Old LJ, Smyth MJ. Cancer Immunoediting: Integrating Immunity's Roles in Cancer Suppression and Promotion. *Science*. 2011;331(6024):1565-1570. doi:10.1126/science.1203486

86. Vesely MD, Kershaw MH, Schreiber RD, Smyth MJ. Natural Innate and Adaptive Immunity to Cancer. *Annual Review of Immunology*. 2011;29(1):235-271. doi:10.1146/annurev-immunol-031210-101324

87. Siu H, Vitetta ES, May RD, Uhr JW. Tumor dormancy. I. Regression of BCL1 tumor and induction of a dormant tumor state in mice chimeric at the major histocompatibility complex. *The Journal of Immunology*. 1986;137(4):1376-1382. doi:10.4049/jimmunol.137.4.1376

88. Weinhold KJ, Goldstein LT, Wheelock EF. Tumour-dormant states established with L5178Y lymphoma cells in immunised syngeneic murine hosts. *Nature*. 1977;270(5632):59-61. doi:10.1038/270059a0

89. Koebel CM, Vermi W, Swann JB, et al. Adaptive immunity maintains occult cancer in an equilibrium state. *Nature*. 2007;450(7171):903-907. doi:10.1038/nature06309

90. Schreiber RD, Old LJ, Smyth MJ. Cancer Immunoediting: Integrating Immunity's Roles in Cancer Suppression and Promotion. *Science*. 2011;331(6024):1565-1570. doi:10.1126/science.1203486

91. Wculek SK, Cueto FJ, Mujal AM, Melero I, Krummel MF, Sancho D. Dendritic cells in cancer immunology and immunotherapy. *Nat Rev Immunol*. 2020;20(1):7-24. doi:10.1038/s41577-019-0210-z

92. Broz ML, Binnewies M, Boldajipour B, et al. Dissecting the Tumor Myeloid Compartment Reveals Rare Activating Antigen-Presenting Cells Critical for T Cell Immunity. *Cancer Cell*. 2014;26(5):638-652. doi:10.1016/j.ccell.2014.09.007

93. Merad M, Sathe P, Helft J, Miller J, Mortha A. The Dendritic Cell Lineage: Ontogeny and Function of Dendritic Cells and Their Subsets in the Steady State and the Inflamed Setting. *Annual Review of Immunology*. 2013;31(1):563-604. doi:10.1146/annurev-immunol-020711-074950

94. Spranger S, Bao R, Gajewski TF. Melanoma-intrinsic β-catenin signalling prevents anti-tumour immunity. *Nature*. 2015;523(7559):231-235. doi:10.1038/nature14404

95. Spranger S, Dai D, Horton B, Gajewski TF. Tumor-Residing Batf3 Dendritic Cells Are Required for Effector T Cell Trafficking and Adoptive T Cell Therapy. *Cancer Cell*. 2017;31(5):711-723.e4. doi:10.1016/j.ccell.2017.04.003

96. Böttcher JP, Bonavita E, Chakravarty P, et al. NK Cells Stimulate Recruitment of cDC1 into the Tumor Microenvironment Promoting Cancer Immune Control. *Cell*. 2018;172(5):1022-1037.e14. doi:10.1016/j.cell.2018.01.004

97. Böttcher JP, Sousa CR e. The Role of Type 1 Conventional Dendritic Cells in Cancer Immunity. *Trends in Cancer*. 2018;4(11):784-792. doi:10.1016/j.trecan.2018.09.001

98. Maier B, Leader AM, Chen ST, et al. A conserved dendritic-cell regulatory program limits antitumour immunity. *Nature*. 2020;580(7802):257-262. doi:10.1038/s41586-020-2134-y

99. Rooney MS, Shukla SA, Wu CJ, Getz G, Hacohen N. Molecular and Genetic Properties of Tumors Associated with Local Immune Cytolytic Activity. Published online 2015. doi:10.1016/j.cell.2014.12.033

100. Turajlic S, Litchfield K, Xu H, et al. Insertion-and-deletion-derived tumour-specific neoantigens and the immunogenic phenotype: a pan-cancer analysis. *The Lancet Oncology*. 2017;18(8):1009-1021. doi:10.1016/S1470-2045(17)30516-8

101. Samstein RM, Lee CH, Shoushtari AN, et al. Tumor mutational load predicts survival after immunotherapy across multiple cancer types. *Nat Genet*. 2019;51(2):202-206. doi:10.1038/s41588-018-0312-8

102. Jardim DL, Goodman A, de Melo Gagliato D, Kurzrock R. The Challenges of Tumor Mutational Burden as an Immunotherapy Biomarker. *Cancer Cell*. 2021;39(2):154-173. doi:10.1016/j.ccell.2020.10.001

103. Ricciuti B, Wang X, Alessi JV, et al. Association of High Tumor Mutation Burden in Non–Small Cell Lung Cancers With Increased Immune Infiltration and Improved Clinical Outcomes of PD-L1 Blockade Across PD-L1 Expression Levels. *JAMA Oncology*. 2022;8(8):1160-1168. doi:10.1001/jamaoncol.2022.1981

104. Yarchoan M, Hopkins A, Jaffee EM. Tumor Mutational Burden and Response Rate to PD-1 Inhibition. *N Engl J Med*. 2017;377(25):2500-2501. doi:10.1056/NEJMc1713444

105. Subudhi SK, Vence L, Zhao H, et al. Neoantigen responses, immune correlates, and favorable outcomes after ipilimumab treatment of patients with prostate cancer. *Science Translational Medicine*. 2020;12(537):eaaz3577. doi:10.1126/scitranslmed.aaz3577

106. McGranahan N, Swanton C. Neoantigen quality, not quantity. *Science Translational Medicine*. 2019;11(506):eaax7918. doi:10.1126/scitranslmed.aax7918

107. Daud AI, Loo K, Pauli ML, et al. Tumor immune profiling predicts response to anti–PD-1 therapy in human melanoma. *J Clin Invest*. 2016;126(9):3447-3452. doi:10.1172/JCI87324

108. Ayers M, Lunceford J, Nebozhyn M, et al. IFN-γ-related mRNA profile predicts clinical response to PD-1 blockade. *Journal of Clinical Investigation*. 2017;127(8):2930-2940. doi:10.1172/JCI91190

109. Tumeh PC, Harview CL, Yearley JH, et al. PD-1 blockade induces responses by inhibiting adaptive immune resistance. *Nature*. 2014;515(7528):568-571. doi:10.1038/nature13954

110. Reschke R, Yu J, Flood BA, Higgs EF, Hatogai K, Gajewski TF. Immune cell and tumor cell-derived CXCL10 is indicative of immunotherapy response in metastatic melanoma. *J Immunother Cancer*. 2021;9(9):e003521. doi:10.1136/jitc-2021-003521

111. House IG, Savas P, Lai J, et al. Macrophage-Derived CXCL9 and CXCL10 Are Required for Antitumor Immune Responses Following Immune Checkpoint Blockade. *Clinical Cancer Research*. 2020;26(2):487-504. doi:10.1158/1078-0432.CCR-19-1868

112. Dangaj D, Bruand M, Grimm AJ, et al. Cooperation between Constitutive and Inducible Chemokines Enables T-cell Engraftment and Immune Attack in Solid Tumors. *Cancer Cell*. 2019;35(6):885-900.e10. doi:10.1016/j.ccell.2019.05.004

113. Chow MT, Ozga AJ, Servis RL, et al. Intratumoral Activity of the CXCR3 Chemokine System Is Required for the Efficacy of Anti-PD-1 Therapy. *Immunity*. 2019;50(6):1498-1512.e5. doi:10.1016/j.immuni.2019.04.010

114. Harlin H, Meng Y, Peterson AC, et al. Chemokine Expression in Melanoma Metastases Associated with CD8+ T-Cell Recruitment. *Cancer Res*. 2009;69(7):10.1158/0008-5472.CAN-08-2281. doi:10.1158/0008-5472.CAN-08-2281

115. Josefowicz SZ, Lu LF, Rudensky AY. Regulatory T Cells: Mechanisms of Differentiation and Function. *Annual Review of Immunology*. 2012;30(1):531-564. doi:10.1146/annurev.immunol.25.022106.141623

116. Qureshi OS, Zheng Y, Nakamura K, et al. Trans-endocytosis of CD80 and CD86: a molecular basis for the cell extrinsic function of CTLA-4. *Science*. 2011;332(6029):600-603. doi:10.1126/science.1202947

117. Zajac AJ, Blattman JN, Murali-Krishna K, et al. Viral Immune Evasion Due to Persistence of Activated T Cells Without Effector Function. *Journal of Experimental Medicine*. 1998;188(12):2205-2213. doi:10.1084/jem.188.12.2205

118. Lechner F, Wong DKH, Dunbar PR, et al. Analysis of Successful Immune Responses in Persons Infected with Hepatitis C Virus. *Journal of Experimental Medicine*. 2000;191(9):1499-1512. doi:10.1084/jem.191.9.1499

119. Reignat S, Webster GJM, Brown D, et al. Escaping High Viral Load Exhaustion : CD8 Cells with Altered Tetramer Binding in Chronic Hepatitis B Virus Infection. *Journal of Experimental Medicine*. 2002;195(9):1089-1101. doi:10.1084/jem.20011723

120. Shankar P, Russo M, Harnisch B, Patterson M, Skolnik P, Lieberman J. Impaired function of circulating HIV-specific CD8+ T cells in chronic human immunodeficiency virus infection. *Blood*. 2000;96(9):3094-3101. doi:10.1182/blood.V96.9.3094

121. Barber DL, Wherry EJ, Masopust D, et al. Restoring function in exhausted CD8 T cells during chronic viral infection. *Nature*. 2006;439(7077):682-687. doi:10.1038/nature04444

122. Hirano F, Kaneko K, Tamura H, et al. Blockade of B7-H1 and PD-1 by Monoclonal Antibodies Potentiates Cancer Therapeutic Immunity. *Cancer Research*. 2005;65(3):1089-1096. doi:10.1158/0008-5472.1089.65.3

123. Iwai Y, Ishida M, Tanaka Y, Okazaki T, Honjo T, Minato N. Involvement of PD-L1 on tumor cells in the escape from host immune system and tumor immunotherapy by PD-L1 blockade. *Proceedings of the National Academy of Sciences*. 2002;99(19):12293-12297. doi:10.1073/pnas.192461099

124. Pauken KE, Wherry EJ. Overcoming T cell exhaustion in infection and cancer. *Trends in Immunology*. 2015;36(4):265-276. doi:10.1016/j.it.2015.02.008

125. Pardoll DM. The blockade of immune checkpoints in cancer immunotherapy. *Nat Rev Cancer*. 2012;12(4):252-264. doi:10.1038/nrc3239

126. Sharma P, Allison JP. Dissecting the mechanisms of immune checkpoint therapy. *Nat Rev Immunol*. 2020;20(2):75-76. doi:10.1038/s41577-020-0275-8

127. Jenkins RW, Thummalapalli R, Carter J, Cañadas I, Barbie DA. Molecular and Genomic Determinants of Response to Immune Checkpoint Inhibition in Cancer. *Annual Review of Medicine*. 2018;69(1):333-347. doi:10.1146/annurev-med-060116-022926

128. Spranger S, Gajewski TF. Mechanisms of Tumor Cell–Intrinsic Immune Evasion. *Annual Review of Cancer Biology*. 2018;2(1):213-228. doi:10.1146/annurev-cancerbio-030617-050606

129. Oldenborg PA, Zheleznyak A, Fang YF, Lagenaur CF, Gresham HD, Lindberg FP. Role of CD47 as a Marker of Self on Red Blood Cells. *Science*. 2000;288(5473):2051-2054. doi:10.1126/science.288.5473.2051

130. Blazar BR, Lindberg FP, Ingulli E, et al. Cd47 (Integrin-Associated Protein) Engagement of Dendritic Cell and Macrophage Counterreceptors Is Required to Prevent the Clearance of Donor Lymphohematopoietic Cells. *Journal of Experimental Medicine*. 2001;194(4):541-550. doi:10.1084/jem.194.4.541

131. Tsai RK, Discher DE. Inhibition of "self" engulfment through deactivation of myosin-II at the phagocytic synapse between human cells. *Journal of Cell Biology*. 2008;180(5):989-1003. doi:10.1083/jcb.200708043

132. Veillette A, Thibaudeau E, Latour S. High Expression of Inhibitory Receptor SHPS-1 and Its Association with Protein-tyrosine Phosphatase SHP-1 in Macrophages *. *Journal of Biological Chemistry*. 1998;273(35):22719-22728. doi:10.1074/jbc.273.35.22719

133. Okazawa H, Motegi S ichiro, Ohyama N, et al. Negative Regulation of Phagocytosis in Macrophages by the CD47-SHPS-1 System. *The Journal of Immunology*. 2005;174(4):2004-2011. doi:10.4049/jimmunol.174.4.2004

134. Fujioka Y, Matozaki T, Noguchi T, et al. A novel membrane glycoprotein, SHPS-1, that binds the SH2-domain-containing protein tyrosine phosphatase SHP-2 in response to mitogens and cell adhesion. *Molecular and Cellular Biology*. 1996;16(12):6887-6899. doi:10.1128/MCB.16.12.6887

135. Morrissey MA, Kern N, Vale RD. CD47 Ligation Repositions the Inhibitory Receptor SIRPA to Suppress Integrin Activation and Phagocytosis. *Immunity*. 2020;53(2):290-302.e6. doi:10.1016/j.immuni.2020.07.008

136. Kharitonenkov A, Chen Z, Sures I, Wang H, Schilling J, Ullrich A. A family of proteins that inhibit signalling through tyrosine kinase receptors. *Nature*. 1997;386(6621):181-186. doi:10.1038/386181a0

137. Barclay AN, Brown MH. The SIRP family of receptors and immune regulation. *Nat Rev Immunol*. 2006;6(6):457-464. doi:10.1038/nri1859

138. Majeti R, Chao MP, Alizadeh AA, et al. CD47 Is an Adverse Prognostic Factor and Therapeutic Antibody Target on Human Acute Myeloid Leukemia Stem Cells. *Cell*. 2009;138(2):286-299. doi:10.1016/j.cell.2009.05.045

139. Jaiswal S, Jamieson CHM, Pang WW, et al. CD47 Is Upregulated on Circulating Hematopoietic Stem Cells and Leukemia Cells to Avoid Phagocytosis. *Cell*. 2009;138(2):271-285. doi:10.1016/j.cell.2009.05.046

140. Betancur PA, Abraham BJ, Yiu YY, et al. A CD47-associated super-enhancer links pro-inflammatory signalling to CD47 upregulation in breast cancer. *Nat Commun*. 2017;8(1):14802. doi:10.1038/ncomms14802

141. Lo J, Lau EYT, Ching RHH, et al. Nuclear factor kappa B–mediated CD47 up-regulation promotes sorafenib resistance and its blockade synergizes the effect of sorafenib in hepatocellular carcinoma in mice. *Hepatology*. 2015;62(2):534-545. doi:10.1002/hep.27859

142. Zhang X, Wang Y, Fan J, et al. Blocking CD47 efficiently potentiated therapeutic effects of anti-angiogenic therapy in non-small cell lung cancer. *Journal for ImmunoTherapy of Cancer*. 2019;7(1):346. doi:10.1186/s40425-019-0812-9

143. Casey SC, Tong L, Li Y, et al. MYC regulates the antitumor immune response through CD47 and PD-L1. *Science*. 2016;352(6282):227-231. doi:10.1126/science.aac9935

144. Chen J, Zheng DX, Yu XJ, et al. Macrophages induce CD47 upregulation via IL-6 and correlate with poor survival in hepatocellular carcinoma patients. *OncoImmunology*. 2019;8(11):e1652540. doi:10.1080/2162402X.2019.1652540

145. Barkal AA, Brewer RE, Markovic M, et al. CD24 signalling through macrophage Siglec-10 is a target for cancer immunotherapy. *Nature*. 2019;572(7769):392-396. doi:10.1038/s41586-019-1456-0

146. Mateo V, Lagneaux L, Bron D, et al. CD47 ligation induces caspase-independent cell death in chronic lymphocytic leukemia. *Nat Med*. 1999;5(11):1277-1284. doi:10.1038/15233

147. Advani R, Flinn I, Popplewell L, et al. CD47 Blockade by Hu5F9-G4 and Rituximab in Non-Hodgkin's Lymphoma. *N Engl J Med*. 2018;379(18):1711-1721. doi:10.1056/NEJMoa1807315

148. Zelenay S, van der Veen AG, Böttcher JP, et al. Cyclooxygenase-Dependent Tumor Growth through Evasion of Immunity. *Cell*. 2015;162(6):1257-1270. doi:10.1016/j.cell.2015.08.015

149. Shen Q, Cohen B, Zheng W, et al. Notch Shapes the Innate Immunophenotype in Breast Cancer. *Cancer Discovery*. 2017;7(11):1320-1335. doi:10.1158/2159-8290.CD-17-0037

150. Topper MJ, Vaz M, Chiappinelli KB, et al. Epigenetic Therapy Ties MYC Depletion to Reversing Immune Evasion and Treating Lung Cancer. *Cell*. 2017;171(6):1284-1300.e21. doi:10.1016/j.cell.2017.10.022

151. Kortlever RM, Sodir NM, Wilson CH, et al. Myc Cooperates with Ras by Programming Inflammation and Immune Suppression. *Cell*. 2017;171(6):1301-1315.e14. doi:10.1016/j.cell.2017.11.013

152. Gettinger S, Choi J, Hastings K, et al. Impaired HLA Class I Antigen Processing and Presentation as a Mechanism of Acquired Resistance to Immune Checkpoint Inhibitors in Lung Cancer. *Cancer Discovery*. 2017;7(12):1420-1435. doi:10.1158/2159-8290.CD-17-0593

153. Shukla SA, Rooney MS, Rajasagi M, et al. Comprehensive analysis of cancer-associated somatic mutations in class I HLA genes. *Nat Biotechnol*. 2015;33(11):1152-1158. doi:10.1038/nbt.3344

154. McGranahan N, Rosenthal R, Hiley CT, et al. Allele-Specific HLA Loss and Immune Escape in Lung Cancer Evolution. *Cell*. 2017;171(6):1259-1271.e11. doi:10.1016/j.cell.2017.10.001

155. Hicklin DJ, Wang Z, Arienti F, Rivoltini L, Parmiani G, Ferrone S. beta2-Microglobulin mutations, HLA class I antigen loss, and tumor progression in melanoma. *J Clin Invest*. 1998;101(12):2720-2729. doi:10.1172/JCI498

156. Gao J, Shi LZ, Zhao H, et al. Loss of IFN-γ Pathway Genes in Tumor Cells as a Mechanism of Resistance to Anti-CTLA-4 Therapy. *Cell*. 2016;167(2):397-404.e9. doi:10.1016/j.cell.2016.08.069

157. Manguso RT, Pope HW, Zimmer MD, et al. In vivo CRISPR screening identifies Ptpn2 as a cancer immunotherapy target. *Nature*. 2017;547(7664):413-418. doi:10.1038/nature23270

158. Pan D, Kobayashi A, Jiang P, et al. A major chromatin regulator determines resistance of tumor cells to T cell–mediated killing. *Science*. 2018;359(6377):770-775. doi:10.1126/science.aao1710

159. Zaretsky JM, Garcia-Diaz A, Shin DS, et al. Mutations Associated with Acquired Resistance to PD-1 Blockade in Melanoma. *New England Journal of Medicine*. 2016;375(9):819-829. doi:10.1056/NEJMoa1604958

160. Lawson KA, Sousa CM, Zhang X, et al. Functional genomic landscape of cancer-intrinsic evasion of killing by T cells. *Nature*. 2020;586(7827):120-126. doi:10.1038/s41586-020-2746-2

161. Patel SJ, Sanjana NE, Kishton RJ, et al. Identification of essential genes for cancer immunotherapy. *Nature*. 2017;548(7669):537-542. doi:10.1038/nature23477

162. Hugo W, Zaretsky JM, Sun L, et al. Genomic and Transcriptomic Features of Response to Anti-PD-1 Therapy in Metastatic Melanoma. *Cell*. 2016;165(1):35-44. doi:10.1016/j.cell.2016.02.065

163. Dersh D, Phelan JD, Gumina ME, et al. Genome-wide Screens Identify Lineage- and Tumor-Specific Genes Modulating MHC-I- and MHC-II-Restricted Immunosurveillance of Human Lymphomas. *Immunity*. 2021;54(1):116-131.e10. doi:10.1016/j.immuni.2020.11.002

164. Peng D, Kryczek I, Nagarsheth N, et al. Epigenetic silencing of TH1-type chemokines shapes tumour immunity and immunotherapy. *Nature*. 2015;527(7577):249-253. doi:10.1038/nature15520

165. Zingg D, Arenas-Ramirez N, Sahin D, et al. The Histone Methyltransferase Ezh2 Controls Mechanisms of Adaptive Resistance to Tumor Immunotherapy. *Cell Reports*. 2017;20(4):854-867. doi:10.1016/j.celrep.2017.07.007

166. Wee ZN, Li Z, Lee PL, Lee ST, Lim YP, Yu Q. EZH2-Mediated Inactivation of IFN-γ-JAK-STAT1 Signaling Is an Effective Therapeutic Target in MYC-Driven Prostate Cancer. *Cell Reports*. 2014;8(1):204-216. doi:10.1016/J.CELREP.2014.05.045

167. Ennishi D, Takata K, Béguelin W, et al. Molecular and genetic characterization of MHC deficiency identifies ezh2 as therapeutic target for enhancing immune recognition. *Cancer Discovery*. 2019;9(4):546-563. doi:10.1158/2159-8290.CD-18-1090

168. Spranger S, Spaapen RM, Zha Y, et al. Up-Regulation of PD-L1, IDO, and Tregs in the Melanoma Tumor Microenvironment Is Driven by CD8+ T Cells. *Science Translational Medicine*. 2013;5(200):200ra116-200ra116. doi:10.1126/scitranslmed.3006504

169. Ribas A. Adaptive Immune Resistance: How Cancer Protects from Immune Attack. *Cancer Discovery*. 2015;5(9):915-919. doi:10.1158/2159-8290.CD-15-0563

170. Taube JM, Anders RA, Young GD, et al. Colocalization of Inflammatory Response with B7-H1 Expression in Human Melanocytic Lesions Supports an Adaptive Resistance Mechanism of Immune Escape. *Science Translational Medicine*. 2012;4(127):127ra37-127ra37. doi:10.1126/scitranslmed.3003689

171. Green MR, Monti S, Rodig SJ, et al. Integrative analysis reveals selective 9p24.1 amplification, increased PD-1 ligand expression, and further induction via JAK2 in nodular sclerosing Hodgkin lymphoma and primary mediastinal large B-cell lymphoma. *Blood*. 2010;116(17):3268-3277. doi:10.1182/blood-2010-05-282780

172. Roemer MGM, Advani RH, Ligon AH, et al. PD-L1 and PD-L2 genetic alterations define classical hodgkin lymphoma and predict outcome. *Journal of Clinical Oncology*. 2016;34(23):2690-2697. doi:10.1200/JCO.2016.66.4482

173. Georgiou K, Chen L, Berglund M, et al. Genetic basis of *PD-L1* overexpression in diffuse large B-cell lymphomas. *Blood*. 2016;127(24):3026-3034. doi:10.1182/blood-2015-12-686550

174. Twa DDW, Chan FC, Ben-Neriah S, et al. Genomic rearrangements involving programmed death ligands are recurrent in primary mediastinal large B-cell lymphoma. *Blood*. 2014;123(13):2062-2065. doi:10.1182/blood-2013-10-535443

175. Twa DDW, Chan FC, Ben-Neriah S, et al. Genomic rearrangements involving programmed death ligands are recurrent in primary mediastinal large B-cell lymphoma. *Blood*. 2014;123(13):2062-2065. doi:10.1182/blood-2013-10-535443

176. Kataoka K, Shiraishi Y, Takeda Y, et al. Aberrant PD-L1 expression through 3′-UTR disruption in multiple cancers. *Nature*. 2016;534(7607):402-406. doi:10.1038/nature18294

177. Hanahan D, Weinberg RA. Hallmarks of Cancer: The Next Generation. *Cell*. 2011;144(5):646-674. doi:10.1016/j.cell.2011.02.013

178. Jaiswal S, Chao MP, Majeti R, Weissman IL. Macrophages as mediators of tumor immunosurveillance. *Trends in Immunology*. 2010;31(6):212-219. doi:10.1016/j.it.2010.04.001

179. Chao MP, Alizadeh AA, Tang C, et al. Anti-CD47 antibody synergizes with rituximab to promote phagocytosis and eradicate non-Hodgkin lymphoma. *Cell*. 2010;142(5):699-713. doi:10.1016/j.cell.2010.07.044

180. Jaiswal S, Jamieson CHM, Pang WW, et al. CD47 Is Upregulated on Circulating Hematopoietic Stem Cells and Leukemia Cells to Avoid Phagocytosis. *Cell*. 2009;138(2):271-285. doi:10.1016/j.cell.2009.05.046

181. Advani RH, Flinn I, Popplewell L, et al. Activity and tolerabilty of the first-in-class anti-CD47 antibody Hu5F9-G4 with rituximab tolerated in relapsed/refractory non-Hodgkin lymphoma: Initial phase 1b/2 results. *ASCO Annual Meeting*. 2018;36, suppl;

182. Advani R, Flinn I, Popplewell L, et al. CD47 Blockade by Hu5F9-G4 and Rituximab in Non-Hodgkin's Lymphoma. *https://doi.org/101056/NEJMoa1807315*. 2018;379(18):1711-1721. doi:10.1056/NEJMOA1807315

183. Liu X, Pu Y, Cron K, et al. CD47 blockade triggers T cell-mediated destruction of immunogenic tumors. *Nat Med*. 2015;21(10):1209-1215. doi:10.1038/nm.3931

184. Barkal AA, Weiskopf K, Kao KS, et al. Engagement of MHC class I by the inhibitory receptor LILRB1 suppresses macrophages and is a target of cancer immunotherapy. *Nat Immunol*. 2018;19(1):76-84. doi:10.1038/s41590-017-0004-z

185. Ennishi D, Healy S, Bashashati A, et al. TMEM30A loss-of-function mutations drive lymphomagenesis and confer therapeutically exploitable vulnerability in B-cell lymphoma. *Nature Medicine*. 2020;26(4):577-588. doi:10.1038/s41591-020-0757-z

186. Kaneda MM, Messer KS, Ralainirina N, et al. PI3Kγ is a molecular switch that controls immune suppression. *Nature*. 2016;539(7629):437-442. doi:10.1038/nature19834

187. Green JM, Noel PJ, Sperling AI, et al. Absence of B7-dependent responses in CD28-deficient mice. *Immunity*. 1994;1(6):501-508. doi:10.1016/1074-7613(94)90092-2

188. Linsley PS, Brady W, Urnes M, Grosmaire LS, Damle NK, Ledbetter JA. CTLA-4 is a second receptor for the B cell activation antigen B7. *Journal of Experimental Medicine*. 1991;174(3):561-569. doi:10.1084/jem.174.3.561

189. Walunas TL, Lenschow DJ, Bakker CY, et al. CTLA-4 can function as a negative regulator of T cell activation. *Immunity*. 1994;1(5):405-413. doi:10.1016/1074-7613(94)90071-X

190. Tivol EA, Borriello F, Schweitzer AN, Lynch WP, Bluestone JA, Sharpe AH. Loss of CTLA-4 leads to massive lymphoproliferation and fatal multiorgan tissue destruction, revealing a critical negative regulatory role of CTLA-4. *Immunity*. 1995;3(5):541-547. doi:10.1016/1074-7613(95)90125-6

191. Krummel MF, Allison JP. CD28 and CTLA-4 have opposing effects on the response of T cells to stimulation. *Journal of Experimental Medicine*. 1995;182(2):459-465. doi:10.1084/jem.182.2.459

192. Leach DR, Krummel MF, Allison JP. Enhancement of Antitumor Immunity by CTLA-4 Blockade. *Science*. 1996;271(5256):1734-1736. doi:10.1126/science.271.5256.1734

193. Weber J, Thompson JA, Hamid O, et al. A Randomized, Double-Blind, Placebo-Controlled, Phase II Study Comparing the Tolerability and Efficacy of Ipilimumab Administered with or without Prophylactic Budesonide in Patients with Unresectable Stage III or IV Melanoma. *Clinical Cancer Research*. 2009;15(17):5591-5598. doi:10.1158/1078-0432.CCR-09-1024

194. Wolchok JD, Neyns B, Linette G, et al. Ipilimumab monotherapy in patients with pretreated advanced melanoma: a randomised, double-blind, multicentre, phase 2, dose-ranging study. *The Lancet Oncology*. 2010;11(2):155-164. doi:10.1016/S1470-2045(09)70334-1

195. O'Day SJ, Maio M, Chiarion-Sileni V, et al. Efficacy and safety of ipilimumab monotherapy in patients with pretreated advanced melanoma: a multicenter single-arm phase II study. *Annals of Oncology*. 2010;21(8):1712-1717. doi:10.1093/annonc/mdq013

196. Hodi FS, O'Day SJ, McDermott DF, et al. Improved Survival with Ipilimumab in Patients with Metastatic Melanoma. *New England Journal of Medicine*. 2010;363(8):711-723. doi:10.1056/NEJMoa1003466

197. Wang J, Yoshida T, Nakaki F, Hiai H, Okazaki T, Honjo T. Establishment of NOD-Pdcd1-/- mice as an efficient animal model of type I diabetes. *Proceedings of the National Academy of Sciences*. 2005;102(33):11823-11828. doi:10.1073/pnas.0505497102

198. Nishimura H, Minato N, Nakano T, Honjo T. Immunological studies on PD-1 deficient mice: implication of PD-1 as a negative regulator for B cell responses. *International Immunology*. 1998;10(10):1563-1572. doi:10.1093/intimm/10.10.1563

199. Nishimura H, Okazaki T, Tanaka Y, et al. Autoimmune Dilated Cardiomyopathy in PD-1 Receptor-Deficient Mice. *Science*. 2001;291(5502):319-322. doi:10.1126/science.291.5502.319

200. Nishimura H, Nose M, Hiai H, Minato N, Honjo T. Development of Lupus-like Autoimmune Diseases by Disruption of the PD-1 Gene Encoding an ITIM Motif-Carrying Immunoreceptor. *Immunity*. 1999;11(2):141-151. doi:10.1016/S1074-7613(00)80089-8

201. Freeman GJ, Long AJ, Iwai Y, et al. Engagement of the Pd-1 Immunoinhibitory Receptor by a Novel B7 Family Member Leads to Negative Regulation of Lymphocyte Activation. *Journal of Experimental Medicine*. 2000;192(7):1027-1034. doi:10.1084/jem.192.7.1027

202. Barber DL, Wherry EJ, Masopust D, et al. Restoring function in exhausted CD8 T cells during chronic viral infection. *Nature*. 2006;439(7077):682-687. doi:10.1038/nature04444

203. Brahmer JR, Drake CG, Wollner I, et al. Phase I Study of Single-Agent Anti–Programmed Death-1 (MDX-1106) in Refractory Solid Tumors: Safety, Clinical Activity, Pharmacodynamics, and Immunologic Correlates. *J Clin Oncol*. 2010;28(19):3167-3175. doi:10.1200/JCO.2009.26.7609

204. Weber JS, D'Angelo SP, Minor D, et al. Nivolumab versus chemotherapy in patients with advanced melanoma who progressed after anti-CTLA-4 treatment (CheckMate 037): a randomised, controlled, open-label, phase 3 trial. *The Lancet Oncology*. 2015;16(4):375-384. doi:10.1016/S1470-2045(15)70076-8

205. Weber J, Mandala M, Del Vecchio M, et al. Adjuvant Nivolumab versus Ipilimumab in Resected Stage III or IV Melanoma. *N Engl J Med*. 2017;377(19):1824-1835. doi:10.1056/NEJMoa1709030

206. Robert C, Long GV, Brady B, et al. Nivolumab in Previously Untreated Melanoma without BRAF Mutation. *N Engl J Med*. 2015;372(4):320-330. doi:10.1056/NEJMoa1412082

207. Chen R, Zinzani PL, Lee HJ, et al. Pembrolizumab in relapsed or refractory Hodgkin lymphoma: 2-year follow-up of KEYNOTE-087. *Blood*. 2019;134(14):1144-1153. doi:10.1182/blood.2019000324

208. Moskowitz CH, Zinzani PL, Fanale MA, et al. Pembrolizumab in Relapsed/Refractory Classical Hodgkin Lymphoma: Primary End Point Analysis of the Phase 2 Keynote-087 Study. *Blood*. 2016;128(22):1107. doi:10.1182/blood.V128.22.1107.1107

209. Ansell SM, Lesokhin AM, Borrello I, et al. PD-1 Blockade with Nivolumab in Relapsed or Refractory Hodgkin's Lymphoma. *N Engl J Med*. 2015;372(4):311-319. doi:10.1056/NEJMoa1411087

210. Armand P, Rodig S, Melnichenko V, et al. Pembrolizumab in Relapsed or Refractory Primary Mediastinal Large B-Cell Lymphoma. *JCO*. 2019;37(34):3291-3299. doi:10.1200/JCO.19.01389

211. Sharma P, Retz M, Siefker-Radtke A, et al. Nivolumab in metastatic urothelial carcinoma after platinum therapy (CheckMate 275): a multicentre, single-arm, phase 2 trial. *The Lancet Oncology*. 2017;18(3):312-322. doi:10.1016/S1470-2045(17)30065-7

212. Vuky J, Balar AV, Castellano D, et al. Long-Term Outcomes in KEYNOTE-052: Phase II Study Investigating First-Line Pembrolizumab in Cisplatin-Ineligible Patients With Locally Advanced or Metastatic Urothelial Cancer. *JCO*. 2020;38(23):2658-2666. doi:10.1200/JCO.19.01213

213. Seiwert TY, Burtness B, Mehra R, et al. Safety and clinical activity of pembrolizumab for treatment of recurrent or metastatic squamous cell carcinoma of the head and neck (KEYNOTE-012): an open-label, multicentre, phase 1b trial. *The Lancet Oncology*. 2016;17(7):956-965. doi:10.1016/S1470-2045(16)30066-3

214. Mehra R, Seiwert TY, Gupta S, et al. Efficacy and safety of pembrolizumab in recurrent/metastatic head and neck squamous cell carcinoma: pooled analyses after long-term follow-up in KEYNOTE-012. *Br J Cancer*. 2018;119(2):153-159. doi:10.1038/s41416-018-0131-9

215. Langer CJ, Gadgeel SM, Borghaei H, et al. Carboplatin and pemetrexed with or without pembrolizumab for advanced, non-squamous non-small-cell lung cancer: a randomised, phase 2 cohort of the open-label KEYNOTE-021 study. *The Lancet Oncology*. 2016;17(11):1497-1508. doi:10.1016/S1470-2045(16)30498-3

216. Reck M, Rodríguez–Abreu D, Robinson AG, et al. Updated Analysis of KEYNOTE-024: Pembrolizumab Versus Platinum-Based Chemotherapy for Advanced Non–Small-Cell Lung Cancer With PD-L1 Tumor Proportion Score of 50% or Greater. *JCO*. 2019;37(7):537-546. doi:10.1200/JCO.18.00149

217. Reck M, Rodríguez-Abreu D, Robinson AG, et al. Pembrolizumab versus Chemotherapy for PD-L1–Positive Non–Small-Cell Lung Cancer. *New England Journal of Medicine*. 2016;375(19):1823-1833. doi:10.1056/NEJMoa1606774

218. Leighl NB, Hellmann MD, Hui R, et al. Pembrolizumab in patients with advanced non-small-cell lung cancer (KEYNOTE-001): 3-year results from an open-label, phase 1 study. *The Lancet Respiratory Medicine*. 2019;7(4):347-357. doi:10.1016/S2213-2600(18)30500-9

219. Rizvi NA, Mazières J, Planchard D, et al. Activity and safety of nivolumab, an anti-PD-1 immune checkpoint inhibitor, for patients with advanced, refractory squamous non-small-cell lung cancer (CheckMate 063): a phase 2, single-arm trial. *The Lancet Oncology*. 2015;16(3):257-265. doi:10.1016/S1470-2045(15)70054-9

220. Le DT, Durham JN, Smith KN, et al. Mismatch repair deficiency predicts response of solid tumors to PD-1 blockade. *Science*. 2017;357(6349):409-413. doi:10.1126/science.aan6733

221. Le DT, Uram JN, Wang H, et al. PD-1 Blockade in Tumors with Mismatch-Repair Deficiency. *N Engl J Med*. 2015;372(26):2509-2520. doi:10.1056/NEJMoa1500596

222. Lenz HJ, Van Cutsem E, Luisa Limon M, et al. First-Line Nivolumab Plus Low-Dose Ipilimumab for Microsatellite Instability-High/Mismatch Repair-Deficient Metastatic Colorectal Cancer: The Phase II CheckMate 142 Study. *JCO*. 2022;40(2):161-170. doi:10.1200/JCO.21.01015

223. Rudin CM, Liu SV, Lu S, et al. SKYSCRAPER-02: Primary results of a phase III, randomized, double-blind, placebo-controlled study of atezolizumab (atezo) + carboplatin + etoposide (CE) with or without tiragolumab (tira) in patients (pts) with untreated extensive-stage small cell lung cancer (ES-SCLC). *JCO*. 2022;40(17_suppl):LBA8507-LBA8507. doi:10.1200/JCO.2022.40.17_suppl.LBA8507

224. Cho BC, Abreu DR, Hussein M, et al. Tiragolumab plus atezolizumab versus placebo plus atezolizumab as a first-line treatment for PD-L1-selected non-small-cell lung cancer (CITYSCAPE): primary and follow-up analyses of a randomised, double-blind, phase 2 study. *The Lancet Oncology*. 2022;23(6):781-792. doi:10.1016/S1470-2045(22)00226-1

225. Harding JJ, Moreno V, Bang YJ, et al. Blocking TIM-3 in Treatment-refractory Advanced Solid Tumors: A Phase Ia/b Study of LY3321367 with or without an Anti-PD-L1 Antibody. *Clinical Cancer Research*. 2021;27(8):2168-2178. doi:10.1158/1078-0432.CCR-20-4405

226. Hellmann MD, Bivi N, Calderon B, et al. Safety and Immunogenicity of LY3415244, a Bispecific Antibody Against TIM-3 and PD-L1, in Patients With Advanced Solid Tumors. *Clinical Cancer Research*. 2021;27(10):2773-2781. doi:10.1158/1078-0432.CCR-20-3716

227. Legat A, Maby-El Hajjami H, Baumgaertner P, et al. Vaccination with LAG-3Ig (IMP321) and Peptides Induces Specific CD4 and CD8 T-Cell Responses in Metastatic Melanoma

Patients—Report of a Phase I/IIa Clinical Trial. *Clinical Cancer Research*. 2016;22(6):1330-1340. doi:10.1158/1078-0432.CCR-15-1212

228. Tawbi HA, Schadendorf D, Lipson EJ, et al. Relatlimab and Nivolumab versus Nivolumab in Untreated Advanced Melanoma. *New England Journal of Medicine*. 2022;386(1):24-34. doi:10.1056/NEJMoa2109970

229. Curti BD, Kovacsovics-Bankowski M, Morris N, et al. OX40 Is a Potent Immune-Stimulating Target in Late-Stage Cancer Patients. *Cancer Research*. 2013;73(24):7189-7198. doi:10.1158/0008-5472.CAN-12-4174

230. Glisson BS, Leidner RS, Ferris RL, et al. Safety and Clinical Activity of MEDI0562, a Humanized OX40 Agonist Monoclonal Antibody, in Adult Patients with Advanced Solid Tumors. *Clinical Cancer Research*. 2020;26(20):5358-5367. doi:10.1158/1078-0432.CCR-19-3070

231. Gopal AK, Levy R, Houot R, et al. First-in-Human Study of Utomilumab, a 4-1BB/CD137 Agonist, in Combination with Rituximab in Patients with Follicular and Other CD20+ Non-Hodgkin Lymphomas. *Clinical Cancer Research*. 2020;26(11):2524-2534. doi:10.1158/1078-0432.CCR-19-2973

232. Ullenhag GJ, Yachnin J, Carneiro A, et al. A first-in-human, multicenter, open-label, phase 1 study of ATOR-1017, a 4-1BB antibody, in patients with advanced solid malignancies. *JCO*. 2021;39(15_suppl):2646-2646. doi:10.1200/JCO.2021.39.15_suppl.2646

233. Akce M, Hu-Lieskovan S, Reilley M, et al. A phase 1 multiple-ascending dose study to evaluate the safety and tolerability of XmAb23104 (PD-1 x ICOS) in subjects with selected advanced solid tumors (DUET-3). *JCO*. 2022;40(16_suppl):2604-2604. doi:10.1200/JCO.2022.40.16_suppl.2604

234. Hansen AR, Stanton TS, Hong MH, et al. INDUCE-3: A randomized, double-blind study of GSK3359609 (GSK609), an inducible T-cell co-stimulatory (ICOS) agonist antibody, plus pembrolizumab (PE) versus placebo (PL) plus PE for first-line treatment of PD-L1-positive recurrent/metastatic head and neck squamous cell carcinoma (R/M HNSCC). *JCO*. 2020;38(15_suppl):TPS6591-TPS6591. doi:10.1200/JCO.2020.38.15_suppl.TPS6591

235. Roemer MGM, Redd RA, Cader FZ, et al. Major Histocompatibility Complex Class II and Programmed Death Ligand 1 Expression Predict Outcome After Programmed Death 1 Blockade in Classic Hodgkin Lymphoma. *JCO*. 2018;36(10):942-950. doi:10.1200/JCO.2017.77.3994

236. Labanieh L, Mackall CL. CAR immune cells: design principles, resistance and the next generation. *Nature*. 2023;614(7949):635-648. doi:10.1038/s41586-023-05707-3

237. Scholler N, Perbost R, Locke FL, et al. Tumor immune contexture is a determinant of anti-CD19 CAR T cell efficacy in large B cell lymphoma. *Nat Med*. 2022;28(9):1872-1882. doi:10.1038/s41591-022-01916-x

238. Falchi L, Vardhana SA, Salles GA. Bispecific antibodies for the treatment of B-cell lymphoma: promises, unknowns, and opportunities. *Blood*. 2023;141(5):467-480. doi:10.1182/blood.2021011994

239. Locatelli F, Zugmaier G, Rizzari C, et al. Effect of Blinatumomab vs Chemotherapy on Event-Free Survival Among Children With High-risk First-Relapse B-Cell Acute Lymphoblastic Leukemia: A Randomized Clinical Trial. *JAMA*. 2021;325(9):843-854. doi:10.1001/jama.2021.0987

240. Brown PA, Ji L, Xu X, et al. Effect of Postreinduction Therapy Consolidation With Blinatumomab vs Chemotherapy on Disease-Free Survival in Children, Adolescents, and Young Adults With First Relapse of B-Cell Acute Lymphoblastic Leukemia: A Randomized Clinical Trial. *JAMA*. 2021;325(9):833-842. doi:10.1001/jama.2021.0669

241. Viardot A, Goebeler ME, Hess G, et al. Phase 2 study of the bispecific T-cell engager (BiTE) antibody blinatumomab in relapsed/refractory diffuse large B-cell lymphoma. *Blood*. 2016;127(11):1410-1416. doi:10.1182/blood-2015-06-651380

242. Sun LL, Ellerman D, Mathieu M, et al. Anti-CD20/CD3 T cell–dependent bispecific antibody for the treatment of B cell malignancies. *Science Translational Medicine*. 2015;7(287):287ra70-287ra70. doi:10.1126/scitranslmed.aaa4802

243. Gentles AJ, Newman AM, Liu CL, et al. The prognostic landscape of genes and infiltrating immune cells across human cancers. *Nat Med*. 2015;21(8):938-945. doi:10.1038/nm.3909

244. Thorsson V, Gibbs DL, Brown SD, et al. The Immune Landscape of Cancer. *Immunity*. 2018;48(4):812-830.e14. doi:10.1016/j.immuni.2018.03.023

245. Bröske AME, Korfi K, Belousov A, et al. Pharmacodynamics and molecular correlates of response to glofitamab in relapsed/refractory non-Hodgkin lymphoma. *Blood Advances*. 2022;6(3):1025-1037. doi:10.1182/bloodadvances.2021005954

246. Kotlov N, Bagaev A, Revuelta MV, et al. Clinical and Biological Subtypes of B-cell Lymphoma Revealed by Microenvironmental Signatures. *Cancer Discovery*. 2021;11(6):1468-1489. doi:10.1158/2159-8290.CD-20-0839

247. Van Roosbroeck K, Ferreiro JF, Tousseyn T, et al. Genomic alterations of the JAK2 and PDL loci occur in a broad spectrum of lymphoid malignancies. *Genes Chromosomes Cancer*. 2016;55(5):428-441. doi:10.1002/gcc.22345

248. Chapuy B, Stewart C, Dunford AJ, et al. Genomic analyses of PMBL reveal new drivers and mechanisms of sensitivity to PD-1 blockade. *Blood*. 2019;134(26):2369-2382. doi:10.1182/blood.2019002067

249. Godfrey J, Tumuluru S, Bao R, et al. PD-L1 gene alterations identify a subset of diffuse large B-cell lymphoma harboring a T-cell–inflamed phenotype. *Blood*. 2019;133(21):2279-2290. doi:10.1182/blood-2018-10-879015

250. Dufva O, Pölönen P, Brück O, et al. Immunogenomic Landscape of Hematological Malignancies. *Cancer Cell*. 2020;38(3):380-399.e13. doi:10.1016/j.ccell.2020.06.002

251. Charoentong P, Finotello F, Angelova M, et al. Pan-cancer Immunogenomic Analyses Reveal Genotype-Immunophenotype Relationships and Predictors of Response to Checkpoint Blockade. *Cell Reports*. 2017;18(1):248-262. doi:10.1016/j.celrep.2016.12.019

252. Charoentong P, Finotello F, Angelova M, et al. Pan-cancer Immunogenomic Analyses Reveal Genotype-Immunophenotype Relationships and Predictors of Response to Checkpoint Blockade. *Cell Reports*. 2017;18(1):248-262. doi:10.1016/j.celrep.2016.12.019

253. Aran D, Hu Z, Butte AJ. xCell: Digitally portraying the tissue cellular heterogeneity landscape. *Genome Biology*. 2017;18(1). doi:10.1186/s13059-017-1349-1

254. Wright G, Tan B, Rosenwald A, Hurt EH, Wiestner A, Staudt LM. A gene expression-based method to diagnose clinically distinct subgroups of diffuse large B cell lymphoma. *Proceedings of the National Academy of Sciences of the United States of America*. 2003;100(17):9991-9996. doi:10.1073/pnas.1732008100

255. Ranuncolo SM, Polo JM, Dierov J, et al. Bcl-6 mediates the germinal center B cell phenotype and lymphomagenesis through transcriptional repression of the DNA-damage sensor ATR. *Nat Immunol*. 2007;8(7):705-714. doi:10.1038/ni1478

256. Deregulated BCL6 expression recapitulates the pathogenesis of human diffuse large B cell lymphomas in mice - ScienceDirect. Accessed February 20, 2023. https://www.sciencedirect.com/science/article/pii/S1535610805001261?via%3Dihub

257. Phan RT, Saito M, Basso K, Niu H, Dalla-Favera R. BCL6 interacts with the transcription factor Miz-1 to suppress the cyclin-dependent kinase inhibitor p21 and cell cycle arrest in germinal center B cells. *Nat Immunol*. 2005;6(10):1054-1060. doi:10.1038/ni1245

258. Phan RT, Dalla-Favera R. The BCL6 proto-oncogene suppresses p53 expression in germinal-centre B cells. *Nature*. 2004;432(7017):635-639. doi:10.1038/nature03147

259. Niu H, Cattoretti G, Dalla-Favera R. BCL6 Controls the Expression of the B7-1/CD80 Costimulatory Receptor in Germinal Center B Cells. *Journal of Experimental Medicine*. 2003;198(2):211-221. doi:10.1084/jem.20021395

260. Shaffer AL, Yu X, He Y, Boldrick J, Chan EP, Staudt LM. BCL-6 Represses Genes that Function in Lymphocyte Differentiation, Inflammation, and Cell Cycle Control. *Immunity*. 2000;13(2):199-212. doi:10.1016/S1074-7613(00)00020-0

261. Schmitz R, Wright GW, Huang DW, et al. Genetics and Pathogenesis of Diffuse Large B-Cell Lymphoma. *N Engl J Med*. 2018;378(15):1396-1407. doi:10.1056/NEJMoa1801445

262. Hänzelmann S, Castelo R, Guinney J. GSVA: gene set variation analysis for microarray and RNA-Seq data. *BMC Bioinformatics*. 2013;14(1):7. doi:10.1186/1471-2105-14-7

263. Reddy A, Zhang J, Davis NS, et al. Genetic and Functional Drivers of Diffuse Large B Cell Lymphoma. *Cell*. 2017;171(2):481-494.e15. doi:10.1016/j.cell.2017.09.027

264. Chapuy B, Stewart C, Dunford AJ, et al. Molecular subtypes of diffuse large B cell lymphoma are associated with distinct pathogenic mechanisms and outcomes. *Nat Med*. 2018;24(5):679-690. doi:10.1038/s41591-018-0016-8

265. Susanibar-Adaniya S, Barta SK. 2021 Update on Diffuse large B cell lymphoma: A review of current data and potential applications on risk stratification and management. *Am J Hematol*. 2021;96(5):617-629. doi:10.1002/ajh.26151

266. Langerbeins P, Busch R, Anheier N, et al. Poor efficacy and tolerability of R-CHOP in relapsed/refractory chronic lymphocytic leukemia and Richter transformation. *Am J Hematol*. 2014;89(12):E239-43. doi:10.1002/ajh.23841

267. Sharma P, Allison JP. The future of immune checkpoint therapy. *Science*. 2015;348(6230):56-61. doi:10.1126/science.aaa8172

268. Galon J, Costes A, Sanchez-Cabo F, et al. Type, Density, and Location of Immune Cells Within Human Colorectal Tumors Predict Clinical Outcome. *Science*. 2006;313(5795):1960-1964. doi:10.1126/science.1129139

269. Bindea G, Mlecnik B, Tosolini M, et al. Spatiotemporal Dynamics of Intratumoral Immune Cells Reveal the Immune Landscape in Human Cancer. *Immunity*. 2013;39(4):782-795. doi:10.1016/j.immuni.2013.10.003

270. Dufva O, Pölönen P, Brück O, et al. Immunogenomic Landscape of Hematological Malignancies. *Cancer Cell*. 2020;38(3):380-399.e13. doi:10.1016/j.ccell.2020.06.002

271. Ennishi D, Jiang A, Boyle M, et al. Double-Hit Gene Expression Signature Defines a Distinct Subgroup of Germinal Center B-Cell-Like Diffuse Large B-Cell Lymphoma. *JCO*. 2019;37(3):190-201. doi:10.1200/JCO.18.01583

272. Duns G, Viganò E, Ennishi D, et al. Characterization of DLBCL with a PMBL gene expression signature. *Blood*. 2021;138(2):136-148. doi:10.1182/BLOOD.2020007683

273. Lacy SE, Barrans SL, Beer PA, et al. Targeted sequencing in DLBCL, molecular subtypes, and outcomes: a Haematological Malignancy Research Network report. *Blood*. 2020;135(20):1759-1771. doi:10.1182/blood.2019003535

274. Tiacci E, Döring C, Brune V, et al. Analyzing primary Hodgkin and Reed-Sternberg cells to capture the molecular and cellular pathogenesis of classical Hodgkin lymphoma. *Blood*. 2012;120(23):4609-4620. doi:10.1182/blood-2012-05-428896

275. Staudt LM, Dave S. The Biology of Human Lymphoid Malignancies Revealed by Gene Expression Profiling. *Adv Immunol*. 2005;87:163-208. doi:10.1016/S0065-2776(05)87005-1

276. Greaves P, Clear A, Owen A, et al. Defining characteristics of classical Hodgkin lymphoma microenvironment T-helper cells. *Blood*. 2013;122(16):2856-2863. doi:10.1182/blood-2013-06-508044

277. Liu WR, Shipp MA. Signaling pathways and immune evasion mechanisms in classical Hodgkin lymphoma. *Blood*. 2017;130(21):2265-2270. doi:10.1182/blood-2017-06-781989

278. Aoki T, Chong LC, Takata K, et al. Single-cell transcriptome analysis reveals disease-defining t-cell subsets in the tumor microenvironment of classic hodgkin lymphoma. *Cancer Discovery*. 2020;10(3):406-421. doi:10.1158/2159-8290.CD-19-0680

279. Ott G, Rosenwald A, Campo E. Understanding MYC-driven aggressive B-cell lymphomas: pathogenesis and classification. *Blood*. 2013;122(24):3884-3891. doi:10.1182/blood-2013-05-498329

280. Grimm KE, O'Malley DP. Aggressive B cell lymphomas in the 2017 revised WHO classification of tumors of hematopoietic and lymphoid tissues. *Annals of Diagnostic Pathology*. 2019;38:6-10. doi:10.1016/j.anndiagpath.2018.09.014

281. Riedell PA, Smith SM. Double hit and double expressors in lymphoma: Definition and treatment. *Cancer*. 2018;124(24):4622-4632. doi:10.1002/cncr.31646

282. Olszewski AJ, Kurt H, Evens AM. Defining and treating high-grade B-cell lymphoma, NOS. *Blood*. 2022;140(9):943-954. doi:10.1182/blood.2020008374

283. Sha C, Barrans S, Cucco F, et al. Molecular High-Grade B-Cell Lymphoma: Defining a Poor-Risk Group That Requires Different Approaches to Therapy. *Journal of clinical oncology : official journal of the American Society of Clinical Oncology*. 2019;37(3):202-212. doi:10.1200/JCO.18.01314

284. Kamizono S. The SOCS box of SOCS-1 accelerates ubiquitin-dependent proteolysis of TEL-JAK2. *J Biol Chem*. 2001;276(16):12530-12538. doi:10.1074/jbc.m010074200

285. Liau NPD, Laktyushin A, Lucet IS, et al. The molecular basis of JAK/STAT inhibition by SOCS1. *Nature Communications 2018 9:1*. 2018;9(1):1-14. doi:10.1038/s41467-018-04013-1

286. Alexander WS, Starr R, Fenner JE, et al. SOCS1 is a critical inhibitor of interferon γ signaling and prevents the potentially fatal neonatal actions of this cytokine. *Cell*. 1999;98(5):597-608. doi:10.1016/S0092-8674(00)80047-1

287. Reichel J, Chadburn A, Rubinstein PG, et al. Flow sorting and exome sequencing reveal the oncogenome of primary Hodgkin and Reed-Sternberg cells. *Blood*. 2015;125(7):1061-1072. doi:10.1182/blood-2014-11-610436

288. Wienand K, Chapuy B, Stewart C, et al. Genomic analyses of flow-sorted Hodgkin Reed-Sternberg cells reveal complementary mechanisms of immune evasion. *Blood Advances*. 2019;3(23):4065-4080. doi:10.1182/bloodadvances.2019001012

289. Mottok A, Hung SS, Chavez EA, et al. Integrative genomic analysis identifies key pathogenic mechanisms in primary mediastinal large B-cell lymphoma. *Blood*. 2019;134(10):802-813. doi:10.1182/blood.2019001126

290. Cader FZ, Schackmann RCJ, Hu X, et al. Mass cytometry of Hodgkin lymphoma reveals a CD4+ regulatory T-cell–rich and exhausted T-effector microenvironment. *Blood*. 2018;132(8):825-836. doi:10.1182/blood-2018-04-843714

291. Steidl C, Connors JM, Gascoyne RD. Molecular Pathogenesis of Hodgkin's Lymphoma: Increasing Evidence of the Importance of the Microenvironment. *JCO*. 2011;29(14):1812-1826. doi:10.1200/JCO.2010.32.8401

292. Galon J, Bruni D. Tumor Immunology and Tumor Evolution: Intertwined Histories. *Immunity*. 2020;52(1):55-81. doi:10.1016/j.immuni.2019.12.018

293. Teng MWL, Galon J, Fridman WH, Smyth MJ. From mice to humans: developments in cancer immunoediting. *J Clin Invest*. 2015;125(9):3338-3346. doi:10.1172/JCI80004

294. Peng W, Chen JQ, Liu C, et al. Loss of PTEN Promotes Resistance to T Cell–Mediated Immunotherapy. *Cancer Discovery*. 2016;6(2):202-216. doi:10.1158/2159-8290.CD-15-0283

295. Wellenstein MD, de Visser KE. Cancer-Cell-Intrinsic Mechanisms Shaping the Tumor Immune Landscape. *Immunity*. 2018;48(3):399-416. doi:10.1016/j.immuni.2018.03.004

296. Salmon H, Remark R, Gnjatic S, Merad M. Host tissue determinants of tumour immunity. *Nat Rev Cancer*. 2019;19(4):215-227. doi:10.1038/s41568-019-0125-9

297. Steen CB, Luca BA, Esfahani MS, et al. The landscape of tumor cell states and ecosystems in diffuse large B cell lymphoma. *Cancer Cell*. 2021;39(10):1422-1437.e10. doi:10.1016/j.ccell.2021.08.011

298. Foeng J, Comerford I, McColl SR. Harnessing the chemokine system to home CAR-T cells into solid tumors. *Cell Rep Med*. 2022;3(3):100543. doi:10.1016/j.xcrm.2022.100543

299. Ruffell B, Chang-Strachan D, Chan V, et al. Macrophage IL-10 Blocks CD8+ T Cell-Dependent Responses to Chemotherapy by Suppressing IL-12 Expression in Intratumoral Dendritic Cells. *Cancer Cell*. 2014;26(5):623-637. doi:10.1016/j.ccell.2014.09.006

300. Ma Z, Li W, Yoshiya S, et al. Augmentation of Immune Checkpoint Cancer Immunotherapy with IL18. *Clinical Cancer Research*. 2016;22(12):2969-2980. doi:10.1158/1078-0432.CCR-15-1655

301. Hu B, Ren J, Luo Y, et al. Augmentation of Antitumor Immunity by Human and Mouse CAR T Cells Secreting IL-18. *Cell Rep*. 2017;20(13):3025-3033. doi:10.1016/j.celrep.2017.09.002

302. Guo L, Junttila IS, Paul WE. Cytokine-induced cytokine production by conventional and innate lymphoid cells. *Trends in Immunology*. 2012;33(12):598-606. doi:10.1016/j.it.2012.07.006

303. Chen PH, Lipschitz M, Weirather JL, et al. Activation of CAR and non-CAR T cells within the tumor microenvironment following CAR T cell therapy. *JCI Insight*. 2020;5(12). doi:10.1172/jci.insight.134612

304. Wei J, Montalvo-Ortiz W, Yu L, et al. CD22-targeted CD28 bispecific antibody enhances antitumor efficacy of odronextamab in refractory diffuse large B cell lymphoma models. *Science Translational Medicine*. 2022;14(670):eabn1082. doi:10.1126/scitranslmed.abn1082

305. Stavnezer J, Guikema JEJ, Schrader CE. Mechanism and Regulation of Class Switch Recombination. *Annu Rev Immunol*. 2008;26:261-292. doi:10.1146/annurev.immunol.26.021607.090248

306. Stavnezer J. Immunoglobulin class switching. *Current Opinion in Immunology*. 1996;8(2):199-205. doi:10.1016/S0952-7915(96)80058-6

307. Luo W, Weisel F, Shlomchik MJ. B cell receptor and CD40 Signaling are Rewired for Synergistic induction of the c-Myc transcription factor in Germinal Center B cells. *Immunity*. 2018;48(2):313-326.e5. doi:10.1016/j.immuni.2018.01.008

308. Wu YL, Rada C. Molecular fine-tuning of affinity maturation in germinal centers. *J Clin Invest*. 2016;126(1):32-34. doi:10.1172/JCI85627

309. Finkin S, Hartweger H, Oliveira TY, Kara EE, Nussenzweig MC. Protein Amounts of the MYC Transcription Factor Determine Germinal Center B Cell Division Capacity. *Immunity*. 2019;51(2):324-336.e5. doi:10.1016/j.immuni.2019.06.013

310. Dominguez-Sola D, Victora GD, Ying CY, et al. The proto-oncogene MYC is required for selection in the germinal center and cyclic reentry. *Nat Immunol*. 2012;13(11):1083-1091. doi:10.1038/ni.2428

311. God JM, Cameron C, Figueroa J, et al. Elevation of c-MYC Disrupts HLA Class II–Mediated Immune Recognition of Human B Cell Tumors. *The Journal of Immunology*. 2015;194(4):1434-1445. doi:10.4049/jimmunol.1402382

312. Inghirami G, Grignani F, Sternas L, Lombardi L, Knowles DM, Dalla-Favera R. Down-regulation of LFA-1 Adhesion Receptors by C-myc Oncogene in Human B Lymphoblastoid Cells. *Science*. 1990;250(4981):682-686. doi:10.1126/science.2237417

313. Chang CH, Qiu J, O'Sullivan D, et al. Metabolic Competition in the Tumor Microenvironment Is a Driver of Cancer Progression. *Cell*. 2015;162(6):1229-1241. doi:10.1016/j.cell.2015.08.016

314. Gao P, Tchernyshyov I, Chang TC, et al. c-Myc suppression of miR-23a/b enhances mitochondrial glutaminase expression and glutamine metabolism. *Nature*. 2009;458(7239):762-765. doi:10.1038/nature07823

315. Mushtaq M, Darekar S, Klein G, Kashuba E. Different Mechanisms of Regulation of the Warburg Effect in Lymphoblastoid and Burkitt Lymphoma Cells. *PLOS ONE*. 2015;10(8):e0136142. doi:10.1371/journal.pone.0136142

316. Le A, Lane AN, Hamaker M, et al. Glucose-Independent Glutamine Metabolism via TCA Cycling for Proliferation and Survival in B Cells. *Cell Metabolism*. 2012;15(1):110-121. doi:10.1016/j.cmet.2011.12.009